VOL. 7 NO. 2 FEBRUARY 1964

Journal of

ELECTROANALYTICAL CHEMISTRY

International Journal Dealing with all Aspects of Electroanalytical Chemistry, Including Fundamental Electrochemistry

ELSEVIER

GENERAL INFORMATION

See also Suggestions and Instructions to Authors which will be sent free, on request to the Publishers.

Types of contributions

(a) Original research work not previously published in other periodicals.
(b) Reviews on recent developments in various fields.
(c) Short communications.
(d) Bibliographical notes and book reviews.

Languages

Papers will be published in English, French or German.

Submission of papers

Papers should be sent to one of the following Editors:

Professor J. O'M. BOCKRIS, John Harrison Laboratory of Chemistry, University of Pennsylvania, Philadelphia 4, Pa., U.S.A.
Dr. R. PARSONS, Department of Chemistry, The University, Bristol 8, England.
Professor C. N. REILLEY, Department of Chemistry, University of North Carolina, Chapel Hill, N.C., U.S.A.

Authors should preferably submit two copies in double-spaced typing on pages of uniform size. Legends for figures should be typed on a separate page. The figures should be in a form suitable for reproduction, drawn in Indian ink on drawing paper or tracing paper, with lettering etc. in thin pencil. The sheets of drawing or tracing paper should preferably be of the same dimensions as those on which the article is typed. Photographs should be submitted as clear black and white prints on glossy paper.
All references should be given at the end of the paper. They should be numbered and the numbers should appear in the text at the appropriate places.
A summary of 50 to 200 words should be included.

Reprints

Twenty-five reprints will be supplied free of charge. Additional reprints can be ordered at quoted prices. They must be ordered on order forms which are sent together with the proofs.

Publication

The *Journal of Electroanalytical Chemistry* appears monthly and has six issues per volume and two volumes per year, each of approx. 500 pages.

Subscription price (post free): £ 10.15.0 or $ 30.00 or Dfl. 108.00 per year; £ 5.7.6 or $ 15.00 or Dfl. 54.00 per volume.
Additional cost for copies by air mail available on request.
For advertising rates apply to the publishers.

Subscriptions

Subscriptions should be sent to:

ELSEVIER PUBLISHING COMPANY, P.O. Box 211, Amsterdam, The Netherlands.

SUMMARIES OF PAPERS PUBLISHED IN JOURNAL OF ELECTROANALYTICAL CHEMISTRY

Vol. 7, No. 2, February 1964

EXALTATION OF THE FIRST OXYGEN WAVE AT THE DROPPING MERCURY ELECTRODE

When hydrogen peroxide formed on the first reduction wave of oxygen reacts rapidly with a constituent in the solution with the formation of a compound which is reduced at the same potentials as, or at more positive potentials than those at which oxygen yields its first reduction wave, an exaltation of this wave is observed. Molybdate in a phosphate buffer of pH 7, or in weakly acid buffers produces such an exaltation. The effect is small in a neutral salt and does not occur in alkaline solution. An exaltation by vinyl acetate is also observed in unbuffered solutions of neutral salts. Apparently, a hydroperoxide is formed and this is responsible for the exaltation.

When the reaction product with hydrogen peroxide is reduced at more positive potentials than the peroxide, the second oxygen wave is displaced to more positive potentials. Tetraethylammonium hydroxide solutions contain a highly volatile impurity. When this impurity is present in unbuffered solutions of neutral salts, a wave is observed immediately after the first oxygen wave, while the total diffusion current (4-electron reduction) remains unchanged. The effect of pH on this additional wave in solutions containing oxygen in the absence and presence of hydrogen peroxide has been studied. The additional wave is well-defined and its height is more than 20% of that of the total reduction wave in mixtures containing 6×10^{-4} *M* hydrogen peroxide and very small amounts of oxygen (about 1 to 2×10^{-5} *M*).

I. M. KOLTHOFF AND K. IZUTSU,

J. Electroanal. Chem., 7 (1964) 85–93

CHRONOPOTENTIOMETRIC STUDY OF THE REDOX CHARACTERISTICS OF $PtCl_6^{2-}$ AND $PtCl_4^{2-}$ AT A PLATINUM ELECTRODE

A solution of $PtCl_6^{2-}$ in 1 *M* hydrochloric acid does not show a chronopotentiometric reduction wave at a platinum cathode whose surface has been cleaned with *aqua regia*. When the electrode has previously been coated with a small quantity of platinum black a well-developed reduction wave is observed. Under the latter condition the transition time is diffusion-controlled, and corresponds to reduction of +4 Pt to the +3 state.

A solution of +2 Pt ($PtCl_4^{2-}$) in 1 *M* hydrochloric acid shows both anodic and cathodic chronopotentiometric waves with a platinum electrode. The anodic and cathodic transition times are approximately equal, and correspond respectively to the oxidation of +2 Pt to the +4 state and reduction to metallic platinum.

J. J. LINGANE,

J. Electroanal. Chem., 7 (1964) 94–101

RAPID SCAN VOLTAMMETRY AND CHRONOPOTENTIOMETRIC STUDIES OF IRON IN MOLTEN FLUORIDES

FABRICATION AND USE OF A PYROLYTIC GRAPHITE INDICATOR ELECTRODE

Voltammetric and chronopotentiometric studies of iron(II) in molten LiF–NaF–KF and LiF–BeF_2 were conducted. The current–voltage curves were recorded by means of a controlled-potential polarograph capable of measuring cell currents up to 5 mA and providing scan-rates from 50 mV/min to 10 V/min. At faster scan-rates ($\sim$ 1 V/min and greater) peak-shaped curves resulted which indicated that the transport process to the electrode was diffusion-controlled. The diffusion coefficient was calculated to be approximately $1 \cdot 10^{-6}$ cm^2/sec and $5 \cdot 10^{-6}$ cm^2/sec in molten LiF–NaF–KF and LiF–BeF_2, respectively. The diffusion coefficient of iron(II) in molten LiF–BeF_2, calculated from chronopotentiometric data, was too large. This was later found to be due to an alternate current path within the cell. Pyrolytic graphite electrodes prepared from commercially available plates, when properly oriented and insulated in boron nitride, appear to be well suited for electrochemical measurements in corrosive melts.

D. L. MANNING AND G. MAMANTOV,

J. Electroanal. Chem., 7 (1964) 102–108

DIRECT DIFFERENTIAL GALVANOSTATIC METHOD FOR INVESTIGATION OF ELECTRODE ADSORPTION CAPACITANCE

A method for obtaining directly the adsorption pseudocapacity associated with adsorbed intermediates in electrode reactions as a function of electrode potential is described. The procedure is based on fast electronic differentiation of charging or discharging curves using an operational amplifier. Theoretical advantages over a chronopotentiometric differential capacity method are discussed.

H. ANGERSTEIN-KOZLOWSKA AND B. E. CONWAY,

J. Electroanal. Chem., 7 (1964) 109–115

VOLTAMMETRY OF Ce(IV), Mn(VII), Cr(VI) AND V(V) WITH THE PYROLYTIC GRAPHITE ELECTRODE

Voltammetry of Ce(IV), Cr(VI) and V(V) in either sulfuric acid or sulfuric acid–phosphoric acid medium is feasible with the pyrolytic graphite electrode (P.G.E.). In these media, the usable potential range extends to +1.5 V *vs.* S.C.E. Data taken from repetitive current–voltage curves are reproducible, the relative standard deviation ranges from 4–8%. No intervening treatment of the electrode is required. The Ce(IV)–Ce(III) electrode reaction at the P.G.E. is reversible. Results of the voltammetry of Mn(VII) are not reproducible.

F. J. MILLER AND H. E. ZITTEL,

J. Electroanal. Chem., 7 (1964) 116–122

VERSATILE AUTOMATIC TITRATOR

An electrochemical titrator is described which is suitable for automatic potentiometric, amperometric and coulometric analyses. Its two most prominent features are versatility for various kinds of electrochemical analyses, and the ability to reveal false end-points arising from slowness of the analytical reaction near the end-point. The revealing of these false end-points has been obtained by introducing special timing circuits to put the apparatus in a waiting position between the apparent end of the analytical reaction and the reading signal. The results which have been obtained with this apparatus are shown in several diagrams and tables.

G. MILAZZO,

J. Electroanal. Chem., 7 (1964) 123–135

THE DESCRIPTION OF ADSORPTION AT ELECTRODES

A number of different isotherms has been used to describe the adsorption of ions and molecules at metal electrodes. These are discussed critically with the object of assessing their usefulness for this purpose. The problem of the electrical variable is discussed and it is concluded that isotherms at constant charge provide parameters with the simpler interpretation.

Methods of fitting isotherms to experimental results are considered. While the surface pressure–concentration curve combines reliability of the experimental results with simplicity of interpretation, it is much less sensitive than the capacity to the detailed nature of the isotherms; in particular it is doubtful whether the distinction between localized and non-localized adsorption can be made using the results in this form. On the other hand, the capacity is more difficult to interpret because it is a more complicated function of the isotherm and of the standard free energy of adsorption. The most promising technique appears to be the analysis of capacity–concentration curves at constant charge. Analysis of experimental results in this way suggests that adsorption on mercury is probably non-localized. An isotherm developed from the equation of state of a two-dimensional hard sphere gas is suggested which should be of wide applicability. The predictions of this isotherm are compared with those of previously used equations.

R. PARSONS,

J. Electroanal. Chem., 7 (1964) 136–152

A NOTE ON THE PAPER "THE DESCRIPTION OF ADSORPTION AT ELECTRODES" BY R. PARSONS

A. N. FRUMKIN,

J. Electroanal. Chem., 7 (1964) 152–155

DISCUSSION ON THE CHOICE OF THE ELECTRICAL VARIABLE IN THE STUDY OF THE ADSORPTION ISOTHERMS OF ORGANIC COMPOUNDS AND ON THE FORM OF THE ADSORPTION ISOTHERM

B. B. DAMASKIN,

J. Electroanal. Chem., 7 (1964) 155–159

EXALTATION OF THE FIRST OXYGEN WAVE AT THE DROPPING MERCURY ELECTRODE

I. M. KOLTHOFF AND K. IZUTSU

School of Chemistry, University of Minnesota, Minneapolis, Minn. (U.S.A.)

(Received November 1st, 1963)

Recently we have shown[1] that there is no exaltation of the first oxygen wave at the dropping mercury electrode in solutions of ordinary inorganic supporting electrolytes and pure tetraalkylammonium salts provided (i) a correction is made for the contribution to the current of hydrogen peroxide formed during the first reduction and (ii) stirring of the liquid around the growing mercury drop is eliminated by a trace of polyacrylamide. A genuine exaltation of the first oxygen wave is observed in the presence of catalase[2]. The hydrogen peroxide formed on the first reduction wave of oxygen is catalytically decomposed to oxygen and water and the increase in the current is kinetically controlled. An exaltation of the first wave can also be expected when the hydrogen peroxide formed at the electrode rapidly reacts with a constituent of the solution with the formation of a reaction product which is reduced at the same potential as oxygen or more positive potential than oxygen. This paper shows that such conditions exist in the reduction of oxygen in the presence of molybdate at a suitable pH. Molybdate rapidly reacts with hydrogen peroxide with formation of permolybdate which is reduced at a more positive potential than oxygen[3].

$$O_2 + 2\,H^+ + 2\,e \rightarrow H_2O_2 \qquad (1)$$

$$H_2O_2 + MoO_4^{2-} \rightarrow H_2O + MoO_5^{2-} \qquad (2)$$

$$MoO_5^{2-} + 2H^+ + 2\,e \rightarrow MoO_4^{2-} + H_2O \qquad (3)$$

At given molybdate and hydrogen ion concentrations the exaltation is determined by the rate of reaction (2).

The effect of molybdate on the first oxygen wave is similar to that of hemin protein enzymes, except that the reaction of hemin with hydrogen peroxide yields a wave at potentials intermediate between those of the first and second oxygen waves[4].

An unusually large exaltation of the first oxygen wave in 0.1 *M* tetraethyl- and 0.01 *M* tetrapropylammonium chloride has been reported by CORNELISSEN AND GIERST[5]. It is shown in this paper that this exaltation does not occur in solutions of pure tetraalkyl salts, but is observed in solutions prepared by neutralization of tetraalkylammonium hydroxide. The compound responsible for this exaltation is highly volatile and is easily removed by passing nitrogen through the solution at room temperature. No exaltation is observed after volatilization of this compound.

It has been reported[6] that solutions of tetraethylammonium hydroxide decompose with formation of compounds such as ethylene and triethylamine. Experiments in which the impurity formed in tetraethylammonium hydroxide was collected by volatilization followed by condensation in liquid nitrogen are described in this paper. When added to an air-saturated solution of a neutral supporting electrolyte the impurity gave rise to the exaltation of the first oxygen wave. No effort has been made to identify the highly volatile impurity. Instead, the effect on the first oxygen wave of certain compounds containing the ethylene linkage — vinylacetate, acrylonitrile and allyl acetate — has been investigated.

KOLTHOFF AND JORDAN[7] observed an oxygen-induced electro-reduction of hydrogen peroxide at pre-cathodized rotated platinum and gold electrodes. It is now well known[8,9] that the characteristics of oxygen waves at such electrodes are highly dependent upon the pre-treatment of these electrodes. We have not been able to reproduce the results of KOLTHOFF AND JORDAN, although we submitted our electrodes to a great variety of pre-treatments. In the present work we have investigated the effect of small concentrations of platinum(IV) on the first oxygen wave at the dropping mercury electrode. Platinum(IV) forms a film of platinum on the electrode at potentials which are much more positive than that at which oxygen reduction starts.

EXPERIMENTAL

The experimental technique and most of the chemicals used have been described in a previous paper[1]. Solutions 0.1 *M* in tetraethylammonium chloride were prepared in two ways: (a) from the recrystallized Eastman Organic Chemicals product; (b) by neutralizing the hydroxide with hydrochloric acid to a given pH using the Beckman glass electrode (Model G) as indicator electrode. Two grades of tetraethylammonium hydroxide were used. One was a polarographic grade commercial product from the South-eastern Analytical Chemists. The other was prepared by shaking a solution of recrystallized tetraethylammonium bromide with silver oxide and removing silver bromide by filtration.

Vinyl acetate, acrylonitrile and allyl acetate were freshly distilled before use. Other chemicals were of analytical grade and used without further purification.

RESULTS AND DISCUSSION

Effect of sodium molybdate

Experiments were carried out in a buffer solution of pH 7, prepared from potassium monohydrogen and potassium dihydrogen phosphate, the total phosphate concentration being 0.05 *M*. It can be seen from the curves in Fig. 1 that molybdate gives rise to an exaltation of the first oxygen wave, the height of the total 4-electron reduction wave not being affected by molybdate. The effects is also observed in 0.1 *M* molybdate in the absence of the buffer (Fig. 1, curve 4). An exaltation of about the same extent as in the phosphate buffer of pH 7 (Fig. 1, curve 2) was observed in an air-saturated solution of 0.1 *M* potassium dihydrogen phosphate which was 0.01 *M* in molybdate. In this solution the reduction of Mo(VI) starts at −0.4 V *vs.* S.C.E. and the second oxygen wave cannot be measured. In neutral 0.1 *M* sodium perchlorate, 0.01 *M* molybdate caused an increase of the first current from 3.19 to 3.50 μA, while in phosphate buffer the wave increased to 4.50 μA. The difference is due

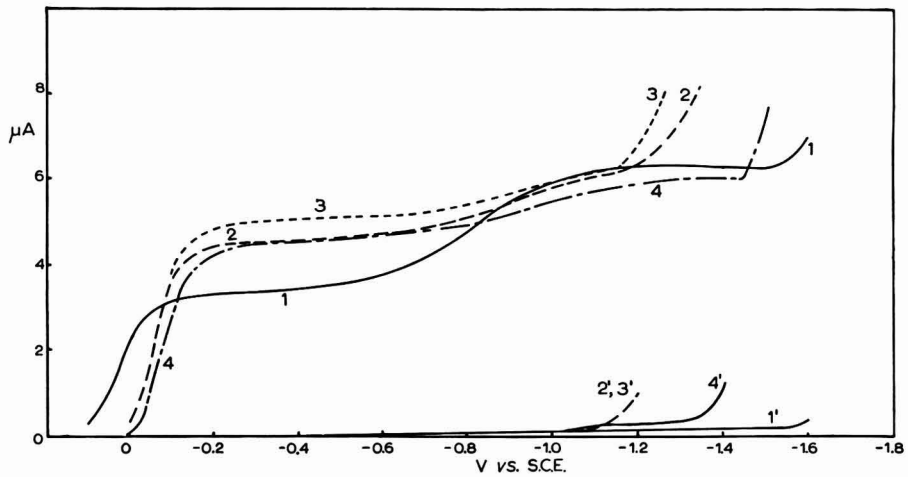

Fig. 1. Effect of molybdate on first oxygen wave in air-saturated phosphate buffer, pH 7.0. (1), no Mo(VI); (2), + $1 \cdot 10^{-2}$ *M* Mo(VI); (3), + $2 \cdot 10^{-2}$ *M* Mo(VI); (4), in 0.1 *M* Na_2MoO_4, (no phosphate; (1'), (2'), (3'), (4'), air-free solutions.

to the effect of hydroxyl ions produced during the first reduction of oxygen in sodium perchlorate. No exaltation occurs in sodium perchlorate in dilute alkali hydroxide solutions. In acetate buffers of pH lower than 5, the reduction current of molybdate started before the limiting current of the first oxygen wave was attained.

Effect of the impurity formed in tetraethylammonium hydroxide solutions

In air-saturated 0.1 *M* solutions of pure tetramethyl- or tetraethylammonium chloride, no exaltation of the first oxygen wave was observed, the polarogram being practically identical with that in the phosphate buffer of pH 7.0. On the other hand

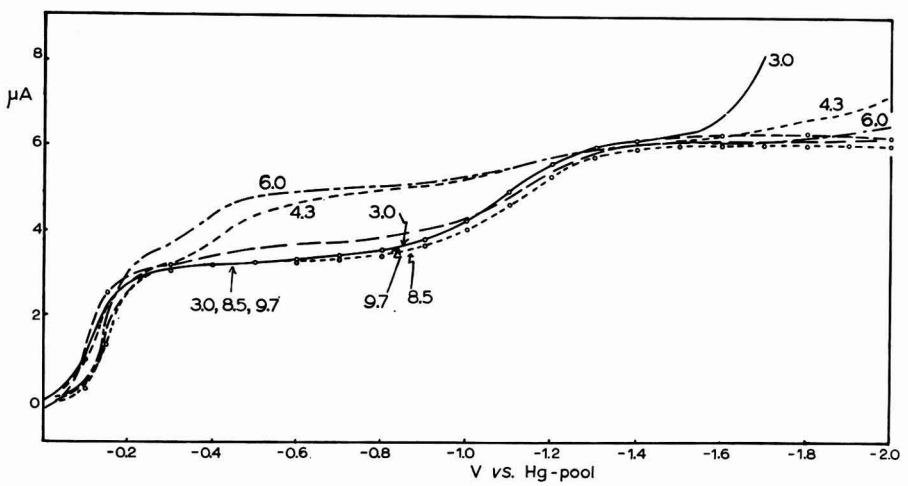

Fig. 2. Effect of pH on the "exaltation" of the first oxygen wave in impure 0.1 *M* $(Et)_4NCl$; (i_{max} is plotted). Numbers on curves indicate pH.

a pronounced apparent exaltation was found in solutions obtained by neutralizing tetraethylammonium hydroxide with hydrochloric acid. Qualitatively the effect was the same in neutralized solutions of the commercial hydroxide as in those obtained from the hydroxide prepared from pure tetraethylammonium bromide silver oxide. It is evident from the curves in Fig. 2 that the extent of the increase of the first wave depends upon the pH of the neutralized unbuffered solutions. Under our experimental conditions the effect is small at pH 7.5, maximal at pH 6, decreases at pH 4 and is not observed when the solutions are neutralized to pH 9.7, 8.5 and 3 respectively. A closer observation of the curves at pH 4.3 and 6.0 reveals that we are not dealing with a true exaltation, as the increase of current starts just at the potential where the first limiting current of oxygen is obtained. It can also be seen that the total (4-electron reduction) wave of oxygen is not affected by the "impurity" formed in the hydroxide solution. Qualitatively the effect of the impurity is the same as that of hemin[4]. Apparently, at the appropriate pH the impurity reacts rapidly with hydrogen peroxide with formation of a compound which is reduced at a much more positive potential than hydrogen peroxide. Since hydroxyl ions are formed in the reduction of oxygen, it would appear that the effect is observed only when the hydroxyl ion concentration at the electrode in the unbuffered solution is of the order of 10^{-4} M. It may be that at widely different alkalinity the rate of reaction between the impurity and hydrogen peroxide is too small to give rise to the additional wave which occurs immediately after the first oxygen wave. No effect of the "impurity" in the tetraalkyl salt was observed in the presence of acetate buffer pH 4.7, phosphate buffer pH 7.0, borate buffer pH 9.2 and carbonate buffer pH 10.6. Upon the addition of 0.02 M potassium thiocyanate to the neutralized "impure" tetraethylammonium

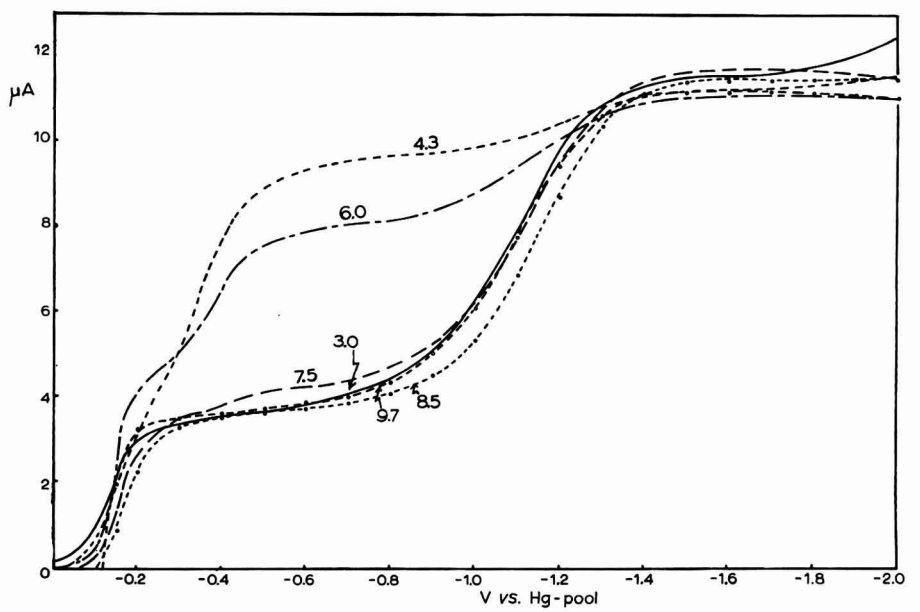

Fig. 3. Effect of pH on polarograms of $5 \cdot 10^{-4}$ M H_2O_2 and oxygen in air-saturated solutions of impure 0.1 M $(Et)_4NCl$; (i_{max} was measured). Numbers on curves indicate pH.

chloride solution the effect was observed, both the first and additional wave being shifted to somewhat more negative potentials. The addition of 0.005% polyacrylamide did not eliminate the effect, although the additional wave became more distorted.

In an air-saturated 0.1 *M* solution of "impure" tetraethylammonium chloride which was also $5 \cdot 10^{-4}$ *M* in hydrogen peroxide, no additional wave was observed immediately after the first oxygen wave when the pH of the unbuffered solution was 9.7, 8.5 or 3. It can be seen in Fig. 3 that a small additional wave appears at pH 7.5, a much larger one at pH 6.0 and the largest at a pH of 4.3 in the bulk of the solution. Considering that the limiting current of the first oxygen wave was 3.5 μA and that of the additional wave was $(9.5-3.5) = 6$ μA, it is quite clear that at pH 4.3 under our experimental conditions a considerable fraction of the hydrogen peroxide added to the solution reacts with the impurity at the surface of the electrode with formation of a compound which is reduced on the additional wave. When the pH of the solution was equal to 3 no additional wave was observed (Fig. 3). The reason is that the hydrogen ion concentration at the surface of the electrode is in excess of that needed to neutralize the hydroxyl ions formed during the reduction of oxygen and hydrogen peroxide. Under these conditions the product formed by reaction of the impurity with hydrogen peroxide does not seem to be formed. When nitrogen was passed for 5 min or longer through the solutions used in Figs. 2 and 3, followed by saturation with air, no "additional" wave was observed at any pH. The impurity had been volatilized. Because of the great volatility of the impurity it was not possible to investigate its effect on the hydrogen peroxide reduction at various hydroxyl ion concentrations in the complete absence of oxygen. In the following experiment it was possible to reduce the oxygen concentration from 2.5×10^{-4} *M* to about 1.5×10^{-5} *M* at 25°. A solution of commercial tetraethylammonium hydroxide was neutralized with air-free hydrochloric acid and diluted with air-free

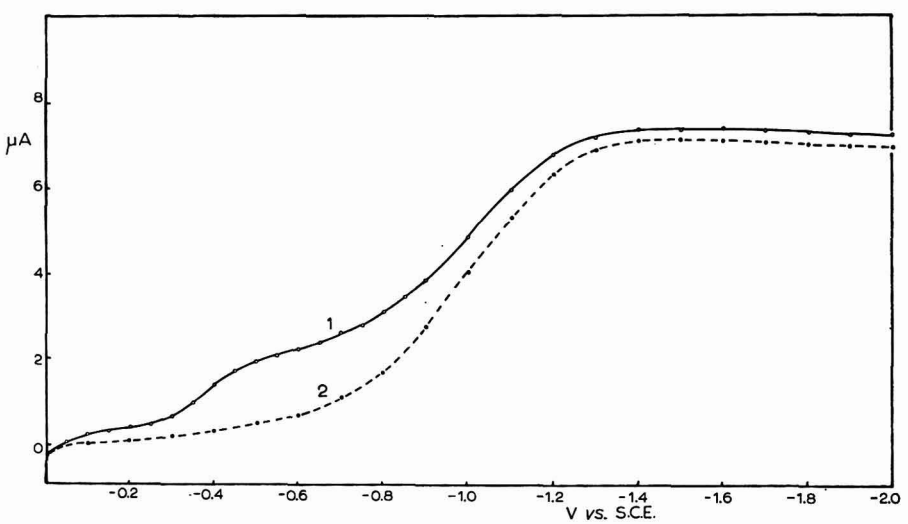

Fig. 4. Polarograms of 6.4×10^{-4} *M* H_2O_2. (1), in 0.1 *M* impure $(Et)_4NCl$, oxygen concn. about 1.5×10^{-5} *M*; (2), after removal of impurity and oxygen.

water to yield a 1 M solution of the chloride of pH 5.5. 45 ml of a $7 \cdot 10^{-4}$ M solution of hydrogen peroxide in water was introduced into the electrolysis cell. Oxygen was removed with nitrogen and then 5 ml of the 1 M tetraalkyl solution was added and a polarogram run immediately (Fig. 4, curve 1). The impurity and oxygen were then removed with nitrogen and curve 2 was recorded. The first diffusion current of oxygen on curve 1 was only 0.15 μA. The additional wave was very pronounced with a height of 1.5 μA at —0.6 V, more than 20% of the total hydrogen peroxide wave. When the experiment corresponding to curve 1 in Fig. 4 was repeated in an air-saturated solution, the increase of the additional wave brought about by 6.4×10^{-4} M peroxide was 2 μA at —0.6 V. Since the height of the additional wave varies with the hydroxyl ion concentration at the surface of the electrode, no definite conclusion as to the effect of oxygen concentration on the wave height can be drawn from the above experiments.

No indication was obtained that the impurity reacts with hydrogen peroxide in the bulk of the solutions. A 0.1 M solutions of "impure" tetraethylammonium chloride was made $5 \cdot 10^{-4}$ M in hydrogen peroxide and the pH adjusted to 4.3, 6.0, 7.5, 8.9, 9.7 and 10.6 respectively. After a reaction time of 20 min, nitrogen was passed through the solution for 20 min. Only the normal hydrogen peroxide wave could be observed (with no pre-wave) after volatilization of the impurity from the solutions of various pH.

By passing nitrogen through solutions of "impure" tetraethylammonium chloride the impurity could be condensed in a trap immersed in liquid nitrogen. Upon dissolving this condensate in an air-saturated 0.1 M solution of pure tetraethylammonium chloride the additional wave appeared, its height being dependent on pH, as illustrated in Fig. 2.

Attempts of condense the impurity in a trap surrounded by a dry ice–ethanol mixture at —70° instead of liquid nitrogen, were unsuccessful. Because of the great volatility of the impurity, further studies of its reactivity with hydrogen peroxide under different conditions were discontinued.

Effect of vinyl acetate

The experiments in Fig. 5 were carried out in 0.1 M sodium perchlorate as supporting electrolyte. A comparison of curves 2 and 3 in Fig. 5 reveals an exaltation of the first oxygen wave in the presence of 0.05 M vinyl acetate, the total oxygen wave at —1.4 V being about 5% smaller in the presence of the acetate than in its absence. The exaltation of the first oxygen wave was already noticeable at a concentration of 0.005 M vinyl acetate and reached a maximum in 0.03–0.05 M solutions. The exaltation also occurred in unbuffered solutions of potassium chloride, potassium thiocyanate and pure tetraethylammonium perchlorate and chloride. No exaltation was observed in 0.1 M solutions of a strong acid, in acetate buffer pH 4.7, phosphate buffer pH 7.0 and borate buffer pH 9.2. In 0.1 M sodium hydroxide the first oxygen wave in the presence of 0.05 M vinyl acetate was distorted by the reduction of acetaldehyde produced by the hydrolysis of vinyl acetate.

In oxygen-free solutions of hydrogen peroxide in 0.1 M sodium perchlorate the presence of vinyl acetate shifts the peroxide wave by about 0.13 V to more positive potentials (Fig. 5, curves 4 and 5), the diffusion current being decreased by about 7%. A large exaltation of the first oxygen wave is observed in a mixture of oxygen

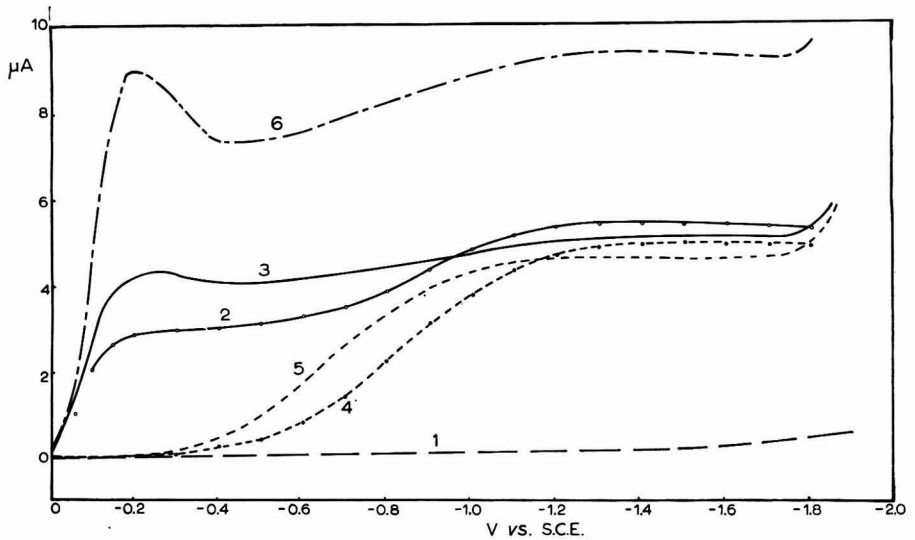

Fig. 5. Effect of vinyl acetate (V.A.) on oxygen and H_2O_2 waves in 0.1 *M* $NaClO_4$ (no SAS; i_{av} was recorded). (1), residual current in presence of 0.05 *M* V.A.; (2), air-saturated, no V.A.; (3), air-saturated + 0.05 *M* V.A.; (4), $5 \cdot 10^{-4}$ *M* H_2O_2, no V.A.; (5), $5 \cdot 10^{-4}$ *M* H_2O_2 + 0.05 *M* V.A.; (6), air-saturated + $5 \cdot 10^{-4}$ *M* H_2O_2 + 0.05 *M* V.A.

(air-saturated) and $5 \cdot 10^{-4}$ *M* hydrogen peroxide in the presence of 0.05 *M* vinyl acetate (Fig. 5, curve 6). The additional wave after the first oxygen wave in the presence of the "impurity" in tetraethylammonium chloride was observed only in unbuffered solutions when the hydroxyl ion concentration in the solution around the electrode during the electrolysis was of the order of 10^{-4} *M*. A similar situation prevails as far as the exaltation by vinyl acetate is concerned. In air-saturated neutral supporting electrolytes, *e.g.*, sodium perchlorate or potassium chloride, the exaltation was eliminated by the addition of 2.5×10^{-4} *M* hydrochloric acid. Since hydrogen ions diffuse much faster than oxygen it can be easily shown that a hydrogen ion concentration of 2.5×10^{-4} *M* is sufficient to neutralize the hydroxyl ions formed at the surface of the electrode at potentials where the first limiting current of oxygen is attained in air-saturated solutions.

In order to investigate further the cause of the exaltation, current–potential curves were run on oxygen-free mixtures of hydrogen peroxide ($5 \cdot 10^{-4}$ *M*) and vinyl acetate (0.01 *M*) in very dilute solutions of sodium hydroxide. The results are presented in Fig. 6. It is clear that traces of alkali displace the hydrogen peroxide wave to much more positive potentials. The effect of 1.5×10^{-4} *M* hydroxide is already very pronounced (Fig. 6, curve 2), while a maximum effect is observed in $5 \cdot 10^{-4}$ *M* hydroxide (curve 3). The polarograms in $5 \cdot 10^{-4}$ *M* hydroxide exhibit a very pronounced maximum at −0.2 V *vs.* S.C.E.

It is not hydrogen peroxide which is reduced at these positive potentials but a reaction product, probably a hydroperoxide, formed by reaction between hydrogen peroxide and vinyl acetate in the presence of traces of alkali hydroxide. When the mixture, which was $5 \cdot 10^{-4}$ *M* in hydrogen peroxide, 0.01 *M* in vinyl acetate and

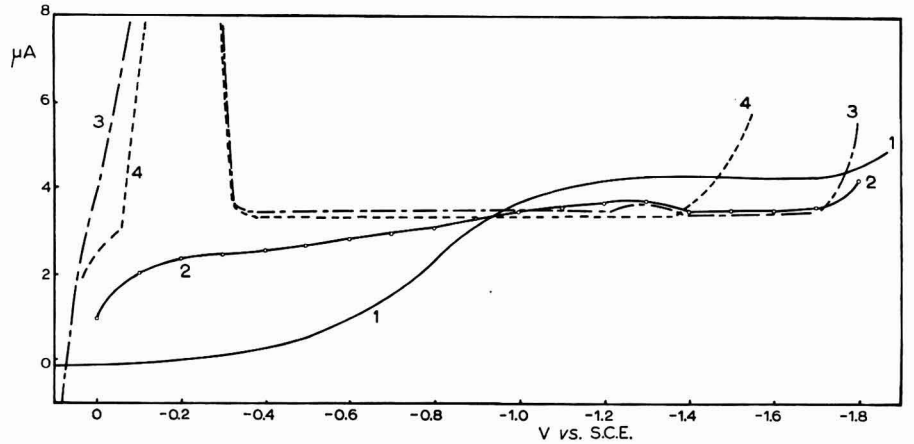

Fig. 6. Effect of vinyl acetate on H_2O_2 wave. (1), $5 \cdot 10^{-4}$ *M* H_2O_2 + 0.01 *M* V.A. + 0.1 *M* KCl, pH 5.0; (2), as (1) in 1.5×10^{-4} *M* NaOH; (3) as (1) in $5 \cdot 10^{-4}$ *M* NaOH; (4), after recording curve (3), the solution was acidified with HCl to pH 3.3.

$5 \cdot 10^{-4}$ *M* in sodium hydroxide (curve 3) was acidified to a pH of about 3 the polarogram (Fig. 6, curve 4) was practically the same as in curve 3. On the other hand, the polarogram obtained in a mixture of hydrogen peroxide ($5 \cdot 10^{-4}$ *M*) and vinyl acetate (0.01 *M*) to which no alkali hydroxide but hydrochloric acid has been added to pH 3.3, was the same as that of hydrogen peroxide in the absence of acid (Fig. 6, curve 1).

From the above experiments it can be concluded that the exaltation of the first oxygen wave by vinyl acetate is due to a reaction product, formed at the surface of the electrode in neutral unbuffered solutions, between hydrogen peroxide and vinyl acetate. This reaction product is reduced at more positive potentials than oxygen (compare curves 3 and 4 in Fig. 6 with oxygen curves at pH 3.0, 8.5 or 9.7 in Fig. 2).

Acrylonitrile and *allyl acetate* did not affect the oxygen wave in air-saturated solutions of neutral salts. Preliminary experiments were carried out in saturated solutions of styrene. This vinyl compound exerts some effect on oxygen and hydrogen peroxide waves. The effects are not easily accounted for and are the subject of further study.

Effect of platinum(IV)

Experiments were carried out in air-saturated solutions 0.1 *M* in sodium perchlorate and 4.5×10^{-5} *M* or $9 \cdot 10^{-5}$ *M* in platinum(IV). The current–potential curves were abnormal and the drop times extremely large until a potential of −0.35 V was attained. The same observations were made in the absence of oxygen. Upon subtraction of the blanks obtained in the absence of oxygen but in the presence of platinum(IV), the three current–potential curves overlapped. Hence, a platinum film formed on the surface of the dropping mercury does not give rise to an exaltation of the first oxygen wave. The same result was obtained in 0.1 *M* perchloric acid or 0.1 *M* potassium hydroxide.

SUMMARY

When hydrogen peroxide formed on the first reduction wave of oxygen reacts rapidly with a constituent in the solution with the formation of a compound which is reduced at the same potentials as, or at more positive potentials than those at which oxygen yields its first reduction wave, an exaltation of this wave is observed. Molybdate in a phosphate buffer of pH 7, or in weakly acid buffers produces such an exaltation. The effect is small in a neutral salt and does not occur in alkaline solution. An exaltation by vinyl acetate is also observed in unbuffered solutions of neutral salts. Apparently, a hydroperoxide is formed and this is responsible for the exaltation.

When the reaction product with hydrogen peroxide is reduced at more positive potentials than the peroxide, the second oxygen wave is displaced to more positive potentials. Tetraethylammonium hydroxide solutions contain a highly volatile impurity. When this impurity is present in unbuffered solutions of neutral salts, a wave is observed immediately after the first oxygen wave, while the total diffusion current (4-electron reduction) remains unchanged. The effect of pH on this additional wave in solutions containing oxygen in the absence and presence of hydrogen peroxide has been studied. The additional wave is well-defined and its height is more than 20% of that of the total reduction wave in mixtures containing 6×10^{-4} M hydrogen peroxide and very small amounts of oxygen (about 1 to 2×10^{-5} M).

ACKNOWLEDGEMENT

Financial support by the U.S. Public Health Service is gratefully acknowledged.

REFERENCES

1 I. M. KOLTHOFF AND K. IZUTSU, in press.
2 R. BRDIČKA, K. WIESNER AND K. SCHAFERNA, *Naturwissenschaften*, 31 (1943) 390; see also M. BŘEZINA AND P. ZUMAN, *Polarography in Medicine, Biochemistry and Pharmacy*, Interscience Publishers Inc., New York, 1958, p. 690.
3 I. M. KOLTHOFF AND E. P. PARRY, *J. Am. Chem. Soc.*, 73 (1951) 5315.
4 R. BRDIČKA AND C. TROPP, *Biochem. Z.*, 289 (1937) 301; R. BRDIČKA AND K. WIESNER, *Collection Czech. Chem. Commun.*, 12 (1947) 39; *Naturwissenschaften*, 31 (1943) 247.
5 R. CORNELISSEN AND L. GIERST, *J. Electroanal. Chem.*, 3 (1962) 219.
6 A. W. HOFMANN, *Ann. Chem.*, 78 (1951) 263; see *e.g.*, L. FIESER AND M. FIESER, *Advanced Organic Chemistry*, Reinhold Publishing Corp., London, 1961.
7 I. M. KOLTHOFF AND J. JORDAN, *J. Am. Chem. Soc.*, 74 (1952) 4801.
8 J. J. LINGANE, *J. Electroanal. Chem.*, 2 (1961) 296.
9 D. T. SAWYER AND L. V. INTERRANTE, *ibid.*, 2 (1961) 310.

CHRONOPOTENTIOMETRIC STUDY OF THE REDOX CHARACTERISTICS OF $PtCl_6^{2-}$ AND $PtCl_4^{2-}$ AT A PLATINUM ELECTRODE

JAMES J. LINGANE

Department of Chemistry, Harvard University, Cambridge 38, Mass. (U.S.A.)

(Received 5th November, 1963)

In connection with other studies in progress in this laboratory the need arose for more information than is available in the literature[1,2], about the processes involved in the reduction of +4 Pt, and in the oxidation and reduction of +2 Pt at a platinum electrode in chloride medium. In the present investigation a start has been made towards obtaining this information.

EXPERIMENTAL TECHNIQUE

The electrode used in this study was authentically pure platinum wire (0.050 cm diameter) sealed into the end of a soft glass tube to leave an exposed area of 0.268 cm^2. The electrode was positioned vertically in the chronopotentiometric cell shown in Fig. 2 on p. 380 of the *Journal of Electroanalytical Chemistry*, Vol. 1, 1960.

The electrical circuit and the technique of the chronopotentiometric measurements were the same as described by LINGANE[3]. Dissolved air was displaced from the test solutions with high purity nitrogen. The chronopotentiograms were recorded with a strip-chart potentiometer recorder (full scale response time of 1.8 sec); the examples reproduced herein are not tracings but the original recorded curves.

A solution of +4 Pt ($PtCl_6^{2-}$) was prepared by dissolving pure platinum in *aqua regia*, evoporating repeatedly to dryness on the steam bath to remove nitrogen compounds, and finally dissolving and diluting to a known volume in 1 *M* hydrochloric acid. The original source of +2 Pt was Fisher "purified" K_2PtCl_4. This salt was further purified by preparing a saturated solution in very dilute hydrochloric acid, filtering off the insoluble matter through a sintered glass filter, and evaporating to crystallization in a vacuum desiccator at room temperature. The resulting ruby red crystals of K_2PtCl_4 were separated from the mother liquor and dried in a vacuum desiccator. Solutions of K_2PtCl_4 were prepared by dissolving weighed samples of the salt in a known volume of 1 *M* hydrochloric acid.

It should be noted that the procedure recommended in *Inorganic Synthesis*[4] for purifying K_2PtCl_4 by recrystallization from *hot* dilute hydrochloric acid is unsatisfactory. It was found that *hot*, nearly saturated solutions of K_2PtCl_4 in very dilute hydrochloric acid undergo disproportionation rather rapidly with precipitation of yellow K_2PtCl_6. Recrystallization of K_2PtCl_4 must be performed at room temperature.

CHARACTERISTICS OF $PtCl_6^{2-}$ REDUCTION

Typical chronopotentiograms of $PtCl_6^{2-}$ in oxygen-free 1 *M* hydrochloric acid are shown in Fig. 1. Before this series of trials was started the electrode had been cleaned with warm *aqua regia*, followed by thorough washing with hot, dilute hydrochloric acid, and finally with water. This treatment left an etched surface, free of finely divided platinum, which hereinafter is referred to as a "clean" surface. Between each trial the solution was stirred for 2–3 min with a rapid stream of nitrogen, after which a period of at least one min was allowed for the solution to become quiescent before recording the chronopotentiogram.

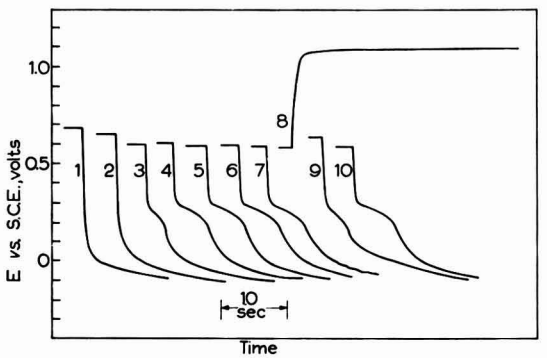

Fig. 1. Chronopotentiograms of 0.0134 *M* $PtCl_6^{2-}$ in air-free 1 *M* HCl at 25° with the platinum wire electrode. The electrode had initially been cleaned in warm *aqua regia*. In all cases the current was 278 μA, and the projected area of the electrode was 0.268 cm^2.

With a "clean" electrode surface (Fig. 1, curve 1) there is no indication of a reduction wave for $PtCl_6^{2-}$. However, the final potential attained by Curve 1 (as well as all the others) is seen to be only −0.10 V *vs.* S.C.E. (+0.14 V *vs.* N.H.E.), and thus about 0.14 V above the potential of hydrogen at 1 atm pressure. Evidently, when this final potential is reached, reduction of $PtCl_6^{2-}$ is occurring, but there is enough simultaneous reduction of hydrogen ion(to hydrogen at a partial pressure far below 1 atm) to prevent the appearance of a discrete "wave". After the cathodic trials are repeated a few times, a reduction wave does appear (Curve 3), and its transition time grows quickly to a constant value (curves 5, 6 and 7). The number of preceding cathodic trials required for the appearance of the wave becomes fewer the greater the current, and the longer the electrode is held at the final potential in each trial. When the wave appears, a visible coating of "platinum black" is observable on the electrode. Evidently the presence of finely divided platinum on the electrode is necessary in order for the reduction of $PtCl_6^{2-}$ to be fast enough to produce a diffusion-controlled wave.

After Curve 7 in Fig. 1 was recorded, the electrode was subjected to the anodic polarization represented by Curve 8, during which the potential was held for a fairly long time at the potential (+1.1 V *vs.* S.C.E.) of chlorine evolution and the solution was unstirred. Following this, the solution was stirred with a rapid stream of nitrogen for 10 min, and then cathodic Curve 9 was recorded. This pre-anodization causes a

significant decrease in the transition time for the $PtCl_6^{2-}$ wave (Curve 9), presumably because the anodization removes part (but not all) of the finely divided platinum from the electrode surface. (A recent study by PETERS AND LINGANE[5] has demonstrated that anodization of a platinum electrode under these conditions produces a film of $PtCl_2$ on the electrode surface which dissolves quite readily in 1 *M* hydrochloric acid.) In the second cathodic trial after the anodization (Curve 10) the transition was restored to the same values as in Curves 5, 6 and 7.

By employing the following pre-treatment of the electrode it was possible to reproduce transition times for the reduction of $PtCl_6^{2-}$ to about $\pm 5\%$. Any prior deposit of platinum black was first removed by immersing the electrode in warm *aqua regia* for a few minutes. The electrode was then washed thoroughly with water and placed in the test solution in the cell from which air had been displaced by nitrogen. With the solution unstirred, the electrode was polarized anodically for 50 sec with a current of 278 μA (current density close to 1 mA/cm^2). The solution was then stirred with a rapid stream of nitrogen for one min, after which, with the solution unstirred, the electrode was polarized cathodically for 50 sec with a current of 278 μA. This treatment produced a visible deposit of finely divided platinum on the electrode surface. Finally the solution was stirred with nitrogen for 5 min. The cathodic chronopotentiogram was then recorded three to four times in succession; between each trial the solution was stirred with nitrogen for a minute or two and at least one minute was allowed for it to become quiescent. The satisfactory reproducibility of the successive chronopotentiograms after this pre-treatment is shown by the typical example in Fig. 2.

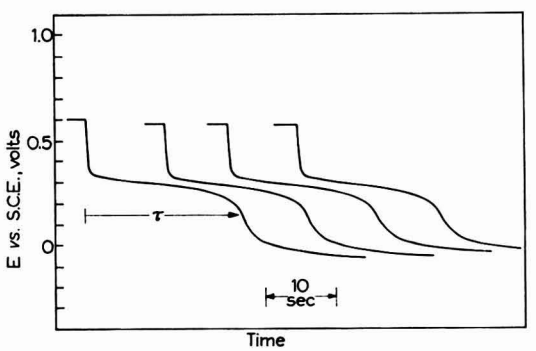

Fig. 2. Cathodic chronopotentiograms of 0.0134 *M* $PtCl_6^{2-}$ in air-free 1 *M* hydrochloric acid, after pre-treating the platinum wire electrode by anodization and cathodization as described in the text. The current was 186 μA. The average of the four transition times is 21.0 $\pm$ 0.8 sec.

Data obtained in this manner at seven different current values, with 0.0134 *M* $PtCl_6^{2-}$ in 1 *M* hydrochloric acid at 25°, are plotted in Fig. 3. At each value of the current the entire pre-treatment procedure described above was employed.

The theoretical relation between $i\tau^{\frac{1}{2}}/AC$ and τ for a symmetrically cylindrical diffusion field when diffusion is the controlling factor is[6]

$$\frac{i\tau^{\frac{1}{2}}}{AC} = \frac{\pi^{\frac{1}{2}} FnD^{\frac{1}{2}}}{\left(1 - \frac{\pi^{\frac{1}{2}} D^{\frac{1}{2}} \tau^{\frac{1}{2}}}{4r} + \frac{D\tau}{4r^2} - \frac{3\pi^{\frac{1}{2}} D^{\frac{1}{2}} \tau^{\frac{1}{2}}}{32r^2} + \ldots\right)} \quad (1)$$

where τ is the transition time (sec), i the constant current (A), A the area of the wire electrode (cm^2), r its radius (cm), C the concentration (moles/cm^3) of the electroactive substance in the body of the solution, D the diffusion coefficient (cm^2/sec) of the electroactive substance, n the number of Faradays per molar unit of the electrode reaction, F the faraday constant (96,493 C), and π is equal to 3.1417.

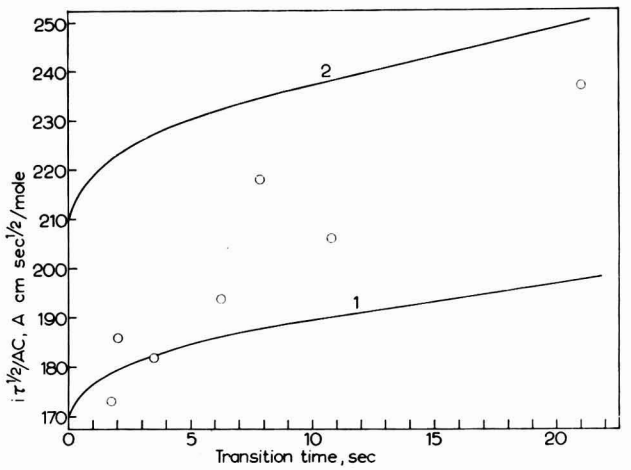

Fig. 3. Influence of the transition time(current density) on $i\tau^{\frac{1}{2}}/AC$ for the reduction of $PtCl_6^{2-}$ in 1 M hydrochloric acid at 25°. Before each measurement the platinum wire electrode (area 0.268 cm^2) was pre-treated as described in the text. The solid lines are the theoretical curves according to eqn. (1) for assumed values of D of 0.4×10^{-5} (curve 1), and 0.6×10^{-5} cm^2/sec (curve 2), and for $n = 1$.

To identify the n-value of the electrode reaction, a knowledge of the diffusion coefficient is required, but no experimental value for D for the $PtCl_6^{2-}$ ion in 1 M hydrochloric acid could be found in the literature. However, D for $PtCl_6^{2-}$ must be about the same as that for $SnCl_6^{2-}$, $FeCl_4^-$, or $CuCl_4^{2-}$, the polarographically evaluated D-values of which are, respectively, 0.68×10^{-5}, 0.47×10^{-5} and 0.79×10^{-5} cm^2/sec at 25°. The two theoretical curves in Fig. 3 were drawn assuming values of D of 0.4×10^{-5} and 0.6×10^{-5} cm^2/sec *and also assuming* $n=1$.

In spite of the mediocre precision of the experimental points, it is immediately evident that the transition time is diffusion-controlled and that the n-value is indeed 1, *i.e.*, the $PtCl_6^{2-}$ ion is reduced only to the +3 oxidation state, rather than to the +2 state. If reduction did proceed to the +2 state ($n=2$) the value of D would have to be only one-fourth as large, or only about 0.1×10^{-5} cm^2/sec, which is much too small to be at all probable. Alternatively, for the expected D-value of about 0.5×10^{-5} cm^2/sec the value of $i\tau^{\frac{1}{2}}/AC$ would have to be twice as large as that observed if n were actually 2. There is, of course, the remote possibility that the transition

time actually is kinetically-controlled and that the rate constant of the controlling step just happens to have the right value to produce a transition time that corresponds to $n=1$ for diffusion-control. However, such a coincidence is much too improbable to be plausible.

The slope of the experimental points in Fig. 3 is somewhat larger than the slope of the theoretical curve. Most likely, this is caused by some disproportionation of the $+3$ Pt species produced at the electrode surface, into $PtCl_6^{2-}$ and $PtCl_4^{2-}$, the $PtCl_6^{2-}$ being immediately re-reduced. The net result is that the apparent n-value is increased somewhat above 1. The relative magnitude of this effect would be expected to increase (as observed) as the transition time is increased.

Several compounds of platinum in the $+3$ oxidation state are known, including green $PtCl_3$ and such complex salts as Cs_2PtCl_5. However, scarcely anything is known about the solution chemistry of this oxidation state of platinum, apart from the fact that it readily disproportionates into $+2$ and $+4$ Pt in chloride media. The present experiments constitute the first evidence for its formation by an electrolytic reaction.

The fact that reduction of $PtCl_6^{2-}$ occurs readily only when some finely divided platinum is present on the surface of the platinum electrode renders inescapable the conclusion that, whatever the detailed mechanism of the reduction may be, metallic platinum must participate in a far more specific way than merely serving as a relatively inert source of electrons. From similar observations in the reduction of oxygen at a platinum cathode, the writer has previously suggested[7] that the primary, rate-determining step in the reduction of any oxidant at a platinum cathode may very well be a "chemical" reduction of the oxidant by metallic platinum, and that the current-producing step is the subsequent, rapid reduction of the platinum species so formed.

In the present case the primary step may be

$$Pt^{4+} + Pt = Pt^{3+} + Pt^{+} \qquad (2)$$

and the subsequent current-producing reaction would then be

$$Pt^{+} + e = Pt \qquad (3)$$

where the superscripts denote only oxidation states and not actual ionic species. Reaction (3) would be expected to be very rapid, so that the rate of reaction (2) determines the extant concentration of $+1$ Pt at the electrode surface, and hence the instantaneous potential of the electrode. With a "clean" platinum electrode, and when the current is held constant, reaction (2) proceeds too slowly to produce $+1$ Pt as quickly as demanded by reaction (3). Consequently, the potential drops almost immediately to a value at which some other oxidant (*e.g.*, hydrogen ion) supplies the requisite $+1$ Pt, and no reduction wave for $PtCl_6^{2-}$ is observed (Fig. 1, Curves 1 and 2). When finely divided platinum is present on the electrode surface, reaction(2) is accelerated sufficiently to keep up with reaction (3). Under this condition the rate of supply of $+4$ Pt ($PtCl_6^{2-}$) to the electrode surface by diffusion becomes the limiting factor in reaction (2), and hence it governs the extant concentration of $+1$ Pt and the electrode potential. Whether the "catalytic" effect of finely divided platinum results merely from the large increase in the microscopic area of the electrode, or whether

some more fundamental property of the freshly deposited platinum is involved (such as enhancement of the relative proportion of crystal faces or "active sites" most favorable to reaction (2)) is a moot question.

A marked change in the reduction wave of $PtCl_6^{2-}$ was observed when the platinized electrode was kept for a long time in the solution. This "aging effect" is demonstrated by the chronopotentiograms in Fig. 4. Curve 1 was recorded after the electrode had

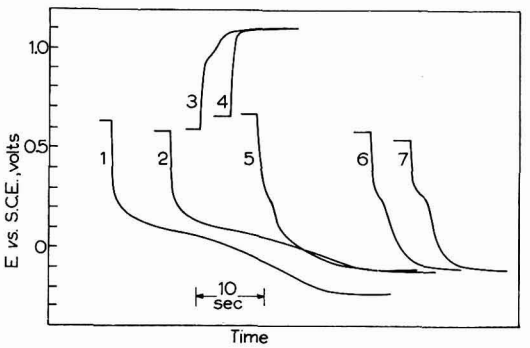

Fig. 4. Influence of "aging" of the platinized electrode surface on the chronopotentiogram of $PtCl_6^{2-}$ reduction in 0.0134 *M* $PtCl_6^{2-}$ in oxygen-free 1 *M* hydrochloric acid at 25°. In all cases the constant current was 462 μA, and the projected area of the platinum wire cathode was 0.268 cm^2.

been (i) pre-treated as described for the curves in Fig. 2, (ii) used to measure the point at 3.52 sec in Fig. 3, and then (iii) allowed to stand for 2 days in the test solution under nitrogen. It should be noted that the reduction wave of Curve 1 begins at about the same potential as with the freshly platinized electrode, but it is greatly attenuated, and the potential finally drops all the way to the value (−0.25 V *vs.* S.C.E.) of hydrogen ion reduction, instead of halting above this value as in Figs. 1 and 2. Repetition of the cathodic trial (Curve 2) causes a considerable decrease of the transition time, and the final potential returns to its "normal" value of about 0.14 V above the potential of hydrogen ion reduction. After the anodization depicted by Curves 3 and 4, the transition time is restored to a value corresponding to a 1-electron reduction (Curves 5, 6 and 7). The transition time of curve 1 is 28 $\pm$ 5 sec, corresponding to a value of $i\tau^{\frac{1}{2}}/AC$ of 680 $\pm$ 120 A sec$^{\frac{1}{2}}$cm/mole. This value is close to four times the value observed in Fig. 3 for a 1-electron reduction, and thus it corresponds to the 4-electron reduction of $PtCl_6^{2-}$ all the way to metallic platinum. Evidently, +3 Pt is much less stable when produced at an "aged" platinized surface than at a fresh one, but why this should be so is obscure.

CHARACTERISTICS OF $PtCl_4^{2-}$ (+ 2 Pt)

As shown in Fig. 5 both the oxidation and reduction of $PtCl_4^{2-}$ at the platinum electrode produce well-defined chronopotentiometric waves. The curves were recorded *seriatim*, and the electrode had previously been cleaned and etched in warm *aqua regia*.

The first anodic wave (Curve 1) is rather poorly delineated, but, after the subsequent cathodization represented by Curve 2, the succeeding anodic waves (Curves 3, 4, 5 and 6) display a more sharply-defined transition time. This apparent "improvement" probably results from the finely divided platinum which the electrode had acquired

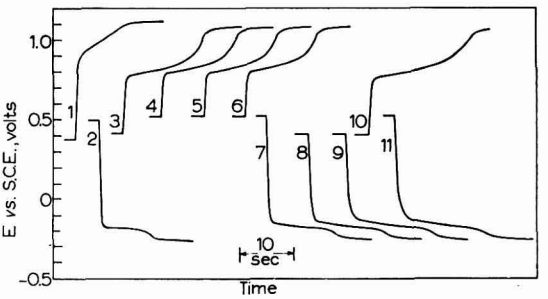

Fig. 5. Chronopotentiograms for the oxidation and reduction of +2 Pt in 0.0140 M $PtCl_4^{2-}$ in oxygen-free 1 M hydrochloric acid at 25°. The platinum wire electrode (area = 0.268 cm^2) had previously been cleaned and etched with warm *aqua regia*. In all cases the constant current was 694 μA.

during cathodic Curve 2. However, platinum itself is known to undergo oxidation at the potential of this anodic wave to a degree directly proportional to the surface area, and since this produces part of the current the total transition time is increased. The large increase in microscopic area caused by the finely divided platinum greatly magnifies this effect. This is demonstrated by Curve 10. Because of the preceding cathodic trials (Curves 7, 8 and 9) the quantity of finely divided platinum on the electrode when Curve 10 was recorded was about four times greater than during the recording of Curves 3–6, and this increased the transition time by nearly 40%. Consequently, the transition time of Curve 1 ought to be more nearly "correct" in the sense of agreement with eqn. (1), and this is substantiated by the following considerations.

The transition time of Curve 1 in Fig. 5 (measured at +1.05 V) is 7.5 sec. From this value $i\tau^{\frac{1}{2}}/AC$ is 507 $\pm$50 A $sec^{\frac{1}{2}}$ cm/mole. Because this is approximately twice as large as the value (200) observed for the 1-electron reduction of $PtCl_6^{2-}$ at the same transition time (see Fig. 3) it is immediately evident that the oxidation of $PtCl_4^{2-}$ must proceed all the way to $PtCl_6^{2-}$ ($n = 2$) rather than to +3 Pt. From the observed value of $i\tau^{\frac{1}{2}}/AC$ and eqn. (1), for $n=2$ and with appropriate allowance for the cylindricity correction term, the apparent diffusion coefficient of $PtCl_4^{2-}$ is calculated to be 0.7×10^{-5} cm^2/sec. This value, in the same neighborhood as the D values of $FeCl_4^-$, $CuCl_4^{2-}$ and $SnCl_6^{2-}$ (*vide supra*), is reasonable. On the other hand, when no correction is made for concomitant electrode oxidation, the transition time of Curves 3, 4, 5 and 6 (13.8 $\pm$ 0.6 sec) leads to an apparent value of D of 1.2×10^{-5} cm^2/sec, which is too large to be plausible. The still larger apparent D value from Curve 10 (1.7×10^{-5} cm^2/sec) is, of course, even more implausible.

The transition time (9.7 sec) of cathodic Curve 2 in Fig. 5 agrees well enough with that of anodic Curve 1 to leave no doubt that the reduction of $PtCl_4^{2-}$ also involves

2 electrons. However, as the cathodic trials are repeated (Curves 7, 8, 9 and 11) the transition time increases, until finally (Curve 11) it is nearly twice the original value. A possible cause of this enhancement is that as the amount of platinum black on the electrode increases the surface becomes so rough that the effective area, pertinent to eqn. (1), is increased. (This may also be a contributing factor to the progressive enhancement of the anodic transition time.) On this basis, since τ is approximately proportional to the area squared, the doubling of the transition time between Curves 2 and 11 corresponds to an increase of the effective area by a factor of $\sqrt{2}$ or 1.4. Another factor that probably contributes to the enhancement of the cathodic transition time in succeeding trials is concomitant reduction of hydrogen ion along with the reduction of $PtCl_4^{2-}$. The fraction of the constant total current resulting from hydrogen ion reduction would be expected to increase as more and more finely divided platinum accumulates on the electrode surface, and as a consequence the transition time should increase (as observed).

It is evident from the curves in Fig. 5 that neither the reduction nor the oxidation of $PtCl_4^{2-}$ proceeds reversibly. From the potentials at which the waves occur relative to the initial potentials, the cathodic overpotential is seen to be considerably larger than the anodic overpotential.

SUMMARY

A solution of $PtCl_6^{2-}$ in 1 *M* hydrochloric acid does not show a chronopotentiometric reduction wave at a platinum cathode whose surface has been cleaned with *aqua regia*. When the electrode has previously been coated with a small quantity of platinum black a well-developed reduction wave is observed. Under the latter condition the transition time is diffusion-controlled, and corresponds to reduction of +4 Pt to the +3 state.

A solution of +2 Pt ($PtCl_4^{2-}$) in 1 *M* hydrochloric acid shows both anodic and cathodic chronopotentiometric waves with a platinum electrode. The anodic and cathodic transition times are approximately equal, and correspond respectively to the oxidation of +2 Pt to the +4 state and reduction to metallic platinum.

REFERENCES

1 G. GRUBE AND H. REINHARDT, *Z. Elektrochem.*, 37 (1931) 307.
2 O. STELLING, *Z. Elektrochem.*, 37 (1931) 321.
3 J. J. LINGANE, *J. Electroanal. Chem.*, 1 (1960) 380.
4 *Inorganic Synthesis*, Vol. II, McGraw-Hill Co. Inc., New York, 1946, p. 247.
5 D. G. PETERS AND J. J. LINGANE, *J. Electroanal. Chem.*, 4 (1926) 193.
6 D. G. PETERS AND J. J. LINGANE, *J. Electroanal. Chem.*, 2 (1960) 1.
7 J. J. LINGANE, *J. Electroanal. Chem.*, 2 (1961) 296.

RAPID SCAN VOLTAMMETRY AND CHRONOPOTENTIOMETRIC STUDIES OF IRON IN MOLTEN FLUORIDES

FABRICATION AND USE OF A PYROLYTIC GRAPHITE INDICATOR ELECTRODE

D. L. MANNING[a] AND GLEB MAMANTOV[b]

[a] *Analytical Chemistry Division, Oak Ridge National Laboratory*, Oak Ridge, Tenn. (U.S.A.)*
[b] *Reactor Chemistry Division, Oak Ridge National Laboratory, Oak Ridge, Tenn. (U.S.A.), and Chemistry Department, University of Tennessee, Knoxville, Tenn. (U.S.A.)*

(Received November 19th, 1963)

In a previous study[1] on the voltammetry of iron in molten LiF–NaF–KF at relatively slow scan-rates, a value for the diffusion coefficient of iron(II) in the melt was not obtained because of the large contribution of convection to the mass transfer process during the duration of the polarogram. In this report, studies on rapid scan voltammetry of iron in molten fluorides are presented. Preliminary chronopotentiometric results are included.

In an effort to find more inert indicator electrodes for electrochemical measurements in molten fluorides, a pyrolytic graphite electrode was tested. MILLER[2] has shown that pyrolytic graphite electrodes prepared from commercially available plates, when properly oriented and sheathed in epoxy resin present an impervious surface to aqueous solutions, acting only as an electron acceptor and donor in the cases studied. The same should hold true in high temperature melts if the exposed layered edges of the "c" planes could be adequately insulated. For this purpose, hot-pressed boron nitride was chosen; YIM AND FEINLEIB[3] have demonstrated its compatibility with molten fluorides. Boron nitride is a non-conducting material, at least at temperatures used in this study. LAITINEN AND RHODES[4], using a specially prepared pyrolytic graphite electrode, demonstrated its usefulness in molten LiCl–KCl.

A controlled-potential polarograph[5], modified to produce rapid scan-rates and to measure cell currents as high as 5 mA, was used to record the current–voltage curves. A pyrolytic graphite electrode coupled with a platinum quasi-reference electrode[6] comprised the measuring system. A third platinum electrode which was isolated in a separate graphite compartment served as the counter electrode.

EXPERIMENTAL

The cell assembly and general procedure for handling molten LiF–NaF–KF and carrying out the electrochemical measurements, are the same as previously described[1].

* Operated by Union Carbide Corporation for the U. S. Atomic Energy Commission.

The molten $LiF-BeF_2$ was contained in a graphite vessel 4 in. in diam. and 5 in. long which was enclosed in a flanged nickel container. The electrodes, a platinum tube used for bubbling helium through the melt, and a platinum–platinum/rhodium (10%) thermocouple were introduced into the electrolytic cell by means of Teflon-insulated "Swagelock" fittings which were located at the upper ends of nickel risers welded to the upper nickel flange. A side-arm to one of the nickel risers provided a helium outlet and a vacuum connection. A three-electrode system was employed. The indicator electrode was a pyrolytic graphite electrode described below. Its potential was measured against a platinum quasi-reference electrode (a 1/8-in. platinum rod). The counter electrode, another platinum electrode, was located in a separate graphite compartment containing the same solvent as in the main vessel. This graphite tube was threaded into the main graphite vessel. A fourth electrode, a 1/8-in. platinum rod, was used as the cathode in the purification of the melt by electrolysis.

The eutectics LiF–NaF–KF (46.5–11.5–42 mole %) and $LiF-BeF_2$ (66–34 mole %) were prepared and purified by the Reactor Chemistry Division of the Oak Ridge National Laboratory. The general procedure is described elsewhere[7].

An ORNL Model Q-1988 controlled-potential polarograph was used to record the current–voltage curves. The polarograph was modified as follows. Electronically controlled scan-rates from 0.05–10 V/min were incorporated into the instrument. The current measuring range of the instrument was increased from 500 μA to 5 mA per full scale deflection of the recorder. The current–voltage curves were displayed on a Moseley Autograph X-Y recorder, Model 3S.

For the chronopotentiometric studies an instrument designed and built by the Analytical Instrumentation Group of the Oak Ridge National Laboratory was used[8]. This instrument is capable of producing up to 10 mA for cathodic studies and 4 mA for the anodic studies. The chronopotentiograms were recorded on the Moseley X–Y recorder, Model 4; for fast recording the Tektronix oscilloscope, Model 531 combined with a Polaroid camera was used.

The pyrolytic graphite electrode was prepared by brazing an 18-gauge platinum wire directly to pyrolytic graphite at high temperature under vacuum. The brazing was effected as follows. A small hole, slightly larger in diameter than the wire, was drilled into the graphite normal to its "a" plane (the plane parallel to the deposition surface). After inserting the wire, the brazing alloy (Ti(48%)–Cu(48%)–Be(4%)) in fine powder form was packed into the hole so as to surround the wire completely, and Nicrobraze cement was next applied to hold the braze. The graphite and wire were then placed in a zirconia tube and evacuated to $3 \cdot 10^{-4}$ p.s.i. following which the zirconia tube was placed in a tube furnace at 950° for 1 min. After cooling, the electrode assembly was removed, cooled, and machined to 1/8-in. diameter. The electrode was then sheathed in hot-pressed boron nitride (The Carborundum Company, Latrobe, Penn.). The measured areas of the electrodes were 8 and 9 mm^2 for LiF–NaF–KF and $LiF-BeF_2$ work, respectively. The boron nitride sheath, 1/4 in. in diam. and 1 in. long, or 3/8 in. in diam. and 4 in. long was pressed to fit around the graphite with tolerances as close as possible, by machining techniques. So far this arrangement seems adequate for exposing only the impervious surface of the graphite to the melt. The solvents employed do not wet graphite appreciably and creeping of the melt between the pyrolytic graphite and boron nitride does not apparently take place. To complete the electrode, the end of the platinum wire was gold-soldered to a 1/8 in.

nickel rod as previously described[1]. A typical electrode is shown in Fig. 1.

Once the electrode is inserted into the cell assembly and brought to thermal equilibrium it is not removed again unless absolutely necessary. Boron nitride tends to absorb moisture and should be kept in a dry environment at all times. When not in use, however, the electrode is raised out of the melt.

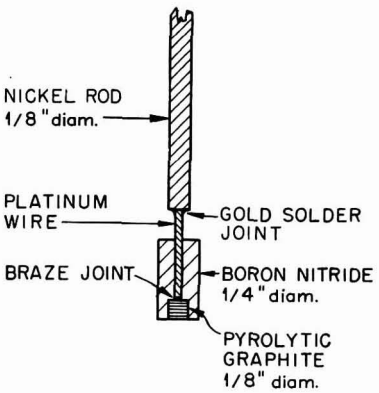

Fig. 1. Pyrolytic graphite indicator electrode.

RESULTS AND DISCUSSION

The effect of scan-rate on the current–voltage curves of iron(II) → iron(o) reduction is demonstrated in Fig. 2. At the slower scan-rates (< 0.5 V/min), the transport process is governed by both diffusion and convection and the curves are S-shaped. The effect of convection, however, is minimized at faster scan-rates and the electrode process appears to be controlled by diffusion as evidenced by the peak-shaped nature

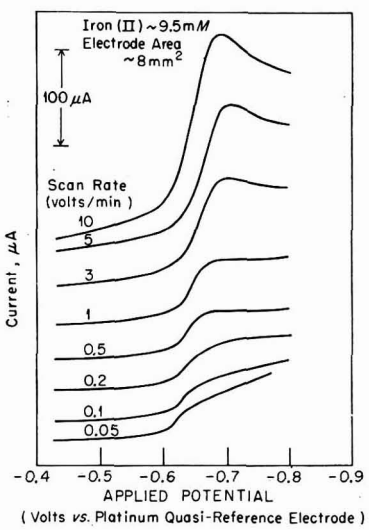

Fig. 2. Effect of scan-rate on the current–voltage curves of iron at pyrolytic graphite. LiF–NaF–KF (46.5–11.5–42.0 mole %); temp., 500°.

of the curves obtained. It is well known[9] that diffusion-controlled processes at solid micro-electrodes result in peak-shaped polarograms (such as obtained in oscillographic polarography). This fact has apparently been overlooked in much of the early voltammetric work in molten salts. Therefore, the values of the diffusion coefficients resulting from S-shaped polarographic waves obtained at solid electrodes are dependent upon the assumed thickness of the Nernst diffusion layer.

The relationship between peak current at 500° and scan-rate is given by the equation

$$i_p = 2.28 \times 10^5 n^{\frac{3}{2}} A D^{\frac{1}{2}} C v^{\frac{1}{2}} \quad (1)$$

where i_p = peak current (μA),
n = electron change,
C = concentration (mM),
A = electrode area (cm^2),
D = diffusion coefficient (cm^2/sec),
v = scan-rate (V/sec).

A plot of i_p *vs.* $v^{\frac{1}{2}}$ should result in a straight line and indeed this is the case as shown by Fig. 3. From the slope of the line, the diffusion coefficient of iron(II) in molten LiF–NaF–KF was calculated to be approximately $1 \cdot 10^{-6}$ cm^2/sec.

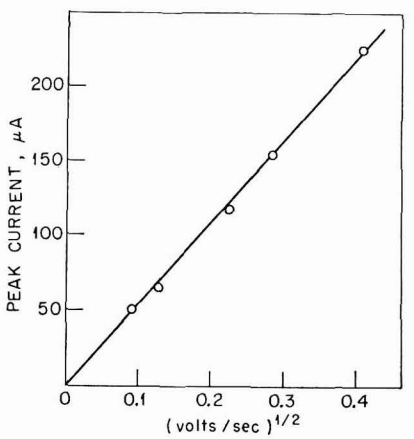

Fig. 3. Peak current *vs.* rate of voltage scanning.

In LiF–BeF_2 (66–34 mole %) the peak current (scan-rate = 5 V/min) was proportional to the molality of iron(II) in the approximate range $2–5 \cdot 10^{-3}$ molal. The relative average deviation for 54 runs was about 13% (the agreement between several consecutive runs was considerably better than this figure). Considerable scatter was observed in the $E_{p/2}$ values. It was found after the completion of this work that this phenomenon was caused mostly by an alternate high-resistance ($\sim$ 1000 Ω) current path (due to solidified LiF–BeF_2 between the electrodes above the solution level) and the resulting inability of the Q-1988 polarograph to control the potential of the

working electrode. This was accompanied by large residual currents. It is advisable therefore, to insulate the electrodes from the Teflon insulation in the Swagelock fitting to the melt level. The presence of an alternate current path was obviously quite deleterious in chronopotentiometry. A cathodic chronopotentiogram of Fe(II) in $LiF-BeF_2$ is shown in Fig. 4. From the Sand equation,

$$\tau^{\frac{1}{2}} = \frac{\pi^{\frac{1}{2}} nFAD^{\frac{1}{2}}C}{2i} \tag{2}$$

knowing τ and i, one can calculate the factor $AD^{\frac{1}{2}}C$. This factor was calculated from chronopotentiometry to be 6.9×10^{-9}. A calculation of $AD^{\frac{1}{2}}C$ from voltammetry, using eqn. (1) with $i_p = 409\ \mu A$ and $v^{\frac{1}{2}} = 0.289$ (V/sec)$^{\frac{1}{2}}$, gave a value of 2.5×10^{-9}.

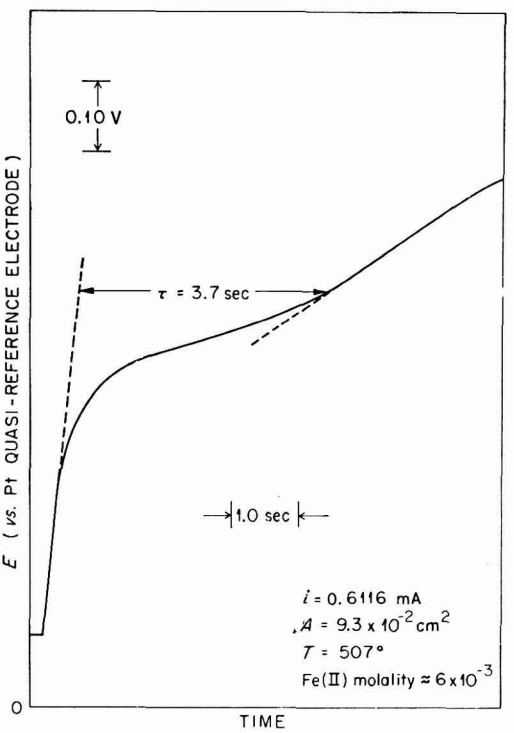

Fig. 4. Chronopotentiogram for the reduction of iron(II) to iron(o) on pyrolytic graphite. $LiF-BeF_2$ (66–34 mole %).

From this and other evidence it appears that the transition times obtained are too large (corresponding to smaller actual currents). It is planned, therefore, to repeat the chronopotentiometric experiments. From the value of $AD^{\frac{1}{2}}C$ obtained by voltammetry, and the knowledge of A (9.3×10^{-2} cm^2) and estimated C (5.9×10^{-3} molal $= 1.2 \times 10^{-2}$ M), the diffusion coefficient is $5 \cdot 10^{-6}$ cm^2/sec. This value is higher than the value of D for Fe(II) in LiF–NaF–KF, indicating that possibly smaller Fe(II) species are involved in $LiF-BeF_2$.

Good reproducibility can be obtained through the use of anodic stripping voltam-

metry. Figure 5 shows five consecutive anodic stripping polarograms of iron (plating time = 90 sec, initial potential = −1.10 V, area = 9.3×10^{-2} cm², temperature = 508°, molality $< 6 \cdot 10^{-3}$). The relative average deviation in i_p is 3.5%; thus, the reproducibility is much better than that obtained by cathodic voltammetry. Anodic stripping voltammetry is particularly suitable for the determination of trace quantities of metals[10].

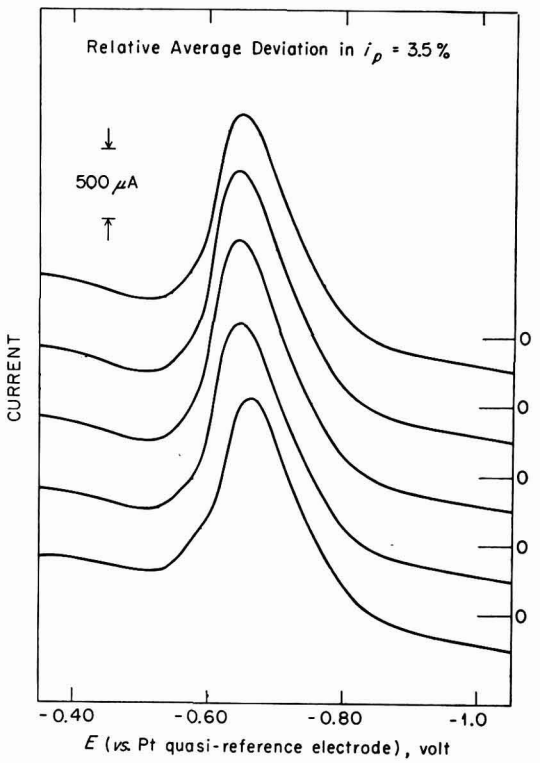

Fig. 5. Anodic stripping polarograms of iron from pyrolytic graphite. LiF–BeF_2 (66–34 mole %); temp., 507°.

On reverse scans, the stripping curve revealed no hesitation as it passed through zero-current; this is evidence that the electrode reaction at the pyrolytic graphite surface proceeds reversibly.

Generally speaking, the current–voltage curves were well-defined. The curves recorded at the pyrolytic graphite electrode, especially at faster scan-rates, were better defined than those recorded at platinum, silver and tungsten indicator electrodes. No difficulty was encountered in maintaining a reproducible electrode surface. The stock pyrolytic graphite was not pre-treated in any way. After each scan, the iron was removed from the electrode by anodic oxidation at zero volts *vs.* the platinum quasi-reference electrode.

An important advantage of rapid scan voltammetry over conventional techniques

as applied to high temperature melts is in achieving conditions where the transport process is more nearly diffusion-controlled. The increase in peak current with scan-rate appears to be analytically useful because of increased sensitivity.

SUMMARY

Voltammetric and chronopotentiometric studies of iron(II) in molten LiF–NaF–KF and LiF–BeF_2 were conducted. The current–voltage curves were recorded by means of a controlled-potential polarograph capable of measuring cell currents up to 5 mA and providing scan-rates from 50 mV/min to 10 V/min. At faster scan-rates ($\sim$ 1 V/min and greater) peak-shaped curves resulted which indicated that the transport process to the electrode was diffusion-controlled. The diffusion coefficient was calculated to be approximately $1 \cdot 10^{-6}$ cm^2/sec and $5 \cdot 10^{-6}$ cm^2/sec in molten LiF–NaF–KF and LiF–BeF_2, respectively. The diffusion coefficient of iron(II) in molten LiF–BeF_2, calculated from chronopotentiometric data, was too large. This was later found to be due to an alternate current path within the cell. Pyrolytic graphite electrodes prepared from commercially available plates, when properly oriented and insulated in boron nitride, appear to be well suited for electrochemical measurements in corrosive melts.

REFERENCES

1 D. L. MANNING, *J. Electroanal. Chem.*, 6 (1963) 227.
2 F. J. MILLER AND H. E. ZITTEL, *Anal. Chem.*, 35 (1963) 1866.
3 E. W. YIM AND MORRIS FEINLEIB, *J. Electrochem. Soc.*, 104 (1957) 622.
4 H. A. LAITINEN AND D. R. RHODES, *J. Electrochem. Soc.*, 109 (1962) 413.
5 M. T. KELLEY, H. C. JONES AND D. J. FISHER, *Anal. Chem.*, 31 (1959) 1475.
6 M. T. KELLEY, *et al.*, *Controlled Potential and Derivative Polarography, Advances in Polarography*, Vol. 1 (edited by I. S. LONGMUIR), Pergamon Press, New York, 1960, pp. 158–182.
7 W. R. GRIMES, D. R. CUNEO, F. F. BLANKENSHIP, G. W. KEILHOLTZ, H. F. POPPENDICK AND M. T. ROBINSON, *Chemical Aspects of Molten Fluoride–Salt Reactor Fuels, Fluid Fuel Reactors*, edited by J. A. LANE, H. G. MACPHERSON and FRANK MOSLAN, Addison-Wesley, Reading, Mass., 1958, p. 584.
8 W. L. MADDOX AND D. J. FISHER, *Anal. Chem. Ann. Prog. Rep.*, ORNL-3060, (1960), p. 4.
9 PAUL DELAHAY, *New Instrumental Methods in Electrochemistry*, Interscience Publishers, Inc., New York, 1954, pp. 115–146.
10 J. G. NIKELLY AND W. D. COOKE, *Anal. Chem.*, 29 (1957) 933.

DIRECT DIFFERENTIAL GALVANOSTATIC METHOD FOR INVESTIGATION OF ELECTRODE ADSORPTION CAPACITANCE

H. ANGERSTEIN-KOZLOWSKA* AND B. E. CONWAY

Department of Chemistry, University of Ottawa (Canada)

(Received October 10th, 1963)

INTRODUCTION

The importance of studies of adsorption pseudocapacitance associated with the potential dependence of coverage of electrode surfaces by chemisorbed intermediates, which are either produced or removed in some Faradaic charge-transfer step, has been realized for a number of years[1,2,18,19,20]. The variation of adsorption pseudo-capacitance with potential and coverage can be treated theoretically in a quantitative manner in terms of the form of the isotherms for the intermediates adsorbed at the electrode interface[3,4,5,19] and in terms of the degree to which equilibrium in a pre-rate-determining ion discharge step is disturbed in a series of consecutive electrochemical reactions, when one of these steps is rate-controlling[6,7]. The relationship of coverage behaviour to reaction mechanism has been studied by DEVANATHAN, BOCKRIS AND MEHL[20] for the hydrogen evolution reaction, by BOCKRIS, *et al.*[19,21,22] for intermediate adions in metal deposition and by GILEADI AND CONWAY[6,7] with regard to the adsorption pseudocapacitance arising in several other reactions.

The quantitative examination of adsorption pseudocapacitance behaviour is hence an important complementary approach to that involving steady-state current–potential relationships[8].

Hitherto, methods for determining the capacity–potential relationship have been based on (a) geometrical differentiation of d.c. galvanostatic charging curves obtained for example by the double-charging method[20] and open-circuit e.m.f. decay curves[5,9,10,11], and (b) direct a.c. capacitance studies[2,12]. The interpretation of results from the latter method is complicated by the large frequency dependence of the capacity which is still observed down to very low frequencies and over a wide frequency range, thus implying a wide range of rate constants for the radical producing or ionising step, associated with intrinsic heterogeneity[4] of the electrode surface. The former methods rely on rather unsatisfactory manual procedures for differentiation *e.g.*, by the prism and set square method, and cannot give the form of the capacity profile with the degree of detail required for quantitative theoretical analysis[4–7].

Attempts to display the electrostatic *ionic* double-layer capacity curve for mercury have been discussed by LOVELAND AND ELVING[13] and the difficulties of this method

* On leave of absence from the *Technical University of Warsaw (Poland)*.

have been examined by PARRY[14] in a thesis; the basis of this method is the measurement of the time-dependent charging current which results from the polarization by the linear voltage-time ("chronopotentiometric") sweep. Also, a slow differentiating apparatus for electro-analytical purposes has been described by IWAMOTO[15]. For studies of the potential-dependence of adsorption pseudocapacity, a fast d.c. method is desirable. In the present paper we describe a direct electronic method based on the use of an operational amplifier, which gives the capacity–potential profile in a single transient.

REQUIREMENTS AND METHOD

The method involved makes use of the fact that a galvanostatic potential (V)–time (t) trace is also equivalent to a potential–charge (q) trace if the current is known and satisfactorily maintained constant by appropriate resistors in the external circuit. The differential coefficient of such a trace is therefore $\mathrm{d}V/\mathrm{d}t$ which is equivalent to a trace of $\mathrm{d}V/\mathrm{d}q$ as a function of time or charge passed. The quantity $\mathrm{d}V/\mathrm{d}q$ is the reciprocal of the electrode capacitance, which can hence be obtained as a function of time or charge passed. Since the latter can be referred to potential on a simultaneously recorded direct galvanostatic charging or discharging curve, the capacitance can be obtained as a function of electrode potential over the range of electrode potentials identical with that covered in the charging curve itself.

For a galvanostatic transient taken by discharge at a current i_d from a previous polarization at a certain polarizing current density i_p it is necessary that

$$i_d \gg -i_p$$

since otherwise the self-discharge current i, which is normally equal[9,10] to i_p at the moment of cessation of polarization, will be comparable with i_d over a range of about 0.05–0.1 V (depending on the Tafel slope for the process involved) from the starting potential corresponding to the current density i_p. For polarizations to the moderate current densities required for the study of intermediates formed, for example, in the hydrogen evolution reaction[1] and in the formate discharge[5,10] reaction, this implies that the discharge current densities must be as high as about 10^{-2}–10^{-1} A cm^{-2} and the rise, or descent time in the transient and its differential coefficient must be of the order of 50–1000 μsec. In the case of open-circuit studies[9,10,11] and in general if reference electrodes having low exchange currents (*e.g.*, in some non-aqueous media),

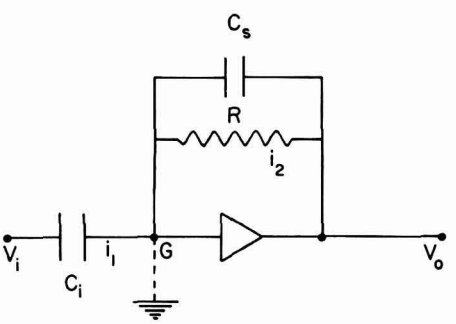

Fig. 1. Differentiating circuit of operational amplifier unit.

are employed, it is necessary to use a d.c. high impedance electrometer input stage to most electro-mechanical recorders and oscilloscopes. Electrometers such as the Keithley and General Radio types have rise times in such applications of only about 5 m sec and are hence suitable only for slow transients. The Tektronix operational amplifier, Type o, can be used simultaneously both as a high impedance unity gain amplifier with a high degree of feed-back giving a fast rise, and as a differentiating unit. This combination of operations is ideal for the present problem.

The differentiating circuit shown in Fig. 1 is used, with a known variable input capacitance C_i in series with an ohmic feed-back linkage R which is itself arranged in parallel between the input and output of the amplifier unit. A small noise suppression capacitor C_s (0.01 μF) is also in parallel with the feed-back resistor R but does not significantly influence the performance of the amplifier in this configuration.

The amplifier is used with negative grid at virtual ground, G. Under these conditions[16], the input current i_1 is related to C_i and the input potential V_i by

$$i_1 = C_i \mathrm{d}V_i/\mathrm{d}t,$$

the output potential V_o is that across the feed-back resistor R so that (see Fig. 1)

$$V_o = i_2 R.$$

Also, since $i_1 + i_2 = 0$, when G is a virtual ground,

$$V_o = RC_i \mathrm{d}V_i/\mathrm{d}t,$$

which gives a signal voltage proportional to the time differential coefficient of the electrode potential V_i taken as the input signal. The sensitivity is obviously determined by the time constant RC_i.

RESULTS

The accuracy of the method was examined by using a variable linear saw-tooth input signal, the slope of which could be measured directly from oscilloscope photographs. The saw-tooth signal was fed to one channel of a dual-beam Tektronix oscilloscope

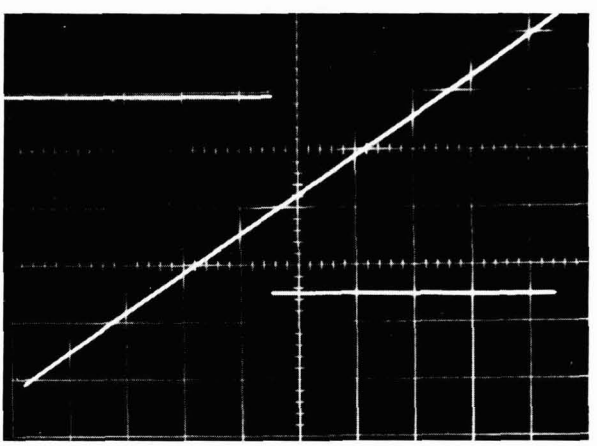

Fig. 2. Saw-tooth calibration (20 V cm^{-1}, 2 sec cm^{-1} time base) and differentiated saw-tooth record (1 V cm^{-1}; R = 0.5 MΩ; C_i = 1 μF).

and the differentiated signal obtained from the circuit shown in Fig. 1 was fed simultaneously to the second beam. The linear and the differentiated signals were photographed simultaneously. A typical record is shown in Fig. 2. The differential signal was switched in during the course of a single saw-tooth transient and the

TABLE 1

CALIBRATION DATA FOR THE DIFFERENTIAL GALVANOSTATIC METHOD

Saw tooth input signal *Voltage sweep rate* $\left(\frac{dV_t}{dt}\ V\ sec^{-1}\right)$	*Differential curve*				$\frac{dV_t}{dt} = \frac{V_o}{RC_t}$
	R (Ω)	C_t (*F*)	*Vertical sensitivity* ($V\ cm^{-1}$)	*Vertical deflection* (*cm*)	($V\ sec^{-1}$)
6.9	$5 \cdot 10^5$	$1 \cdot 10^{-6}$	1	3.4	6.8
6.9	$5 \cdot 10^5$	$1 \cdot 10^{-6}$	1	3.4	6.8
6.9	$5 \cdot 10^5$	$1 \cdot 10^{-6}$	1	3.45	6.9
$2.7 \cdot 10^1$	$1 \cdot 10^6$	$1 \cdot 10^{-6}$	5	5.4	$2.7 \cdot 10^1$
$2.7 \cdot 10^1$	$1 \cdot 10^6$	$1 \cdot 10^{-7}$	0.5	5.45	$2.7 \cdot 10^1$
$2.7 \cdot 10^2$	$1 \cdot 10^6$	$1 \cdot 10^{-8}$	0.5	5.5	$2.75 \cdot 10^2$
$2.7 \cdot 10^2$	$1 \cdot 10^6$	$1 \cdot 10^{-9}$	0.1	2.8	$2.8 \cdot 10^2$
$2.7 \cdot 10^2$	$1 \cdot 10^5$	$1 \cdot 10^{-9}$	$1 \cdot 10^{-2}$	2.8	$2.8 \cdot 10^2$
$2.7 \cdot 10^3$	$1 \cdot 10^5$	$1 \cdot 10^{-9}$	0.1	2.8	$2.8 \cdot 10^3$
$2.7 \cdot 10^4$	$1 \cdot 10^4$	$1 \cdot 10^{-10}$	$1 \cdot 10^{-2}$	2.8	$2.8 \cdot 10^4$
$2.7 \cdot 10^4$	$1 \cdot 10^4$	$1 \cdot 10^{-11}$	$2 \cdot 10^{-3}$	1.4	$2.8 \cdot 10^4$

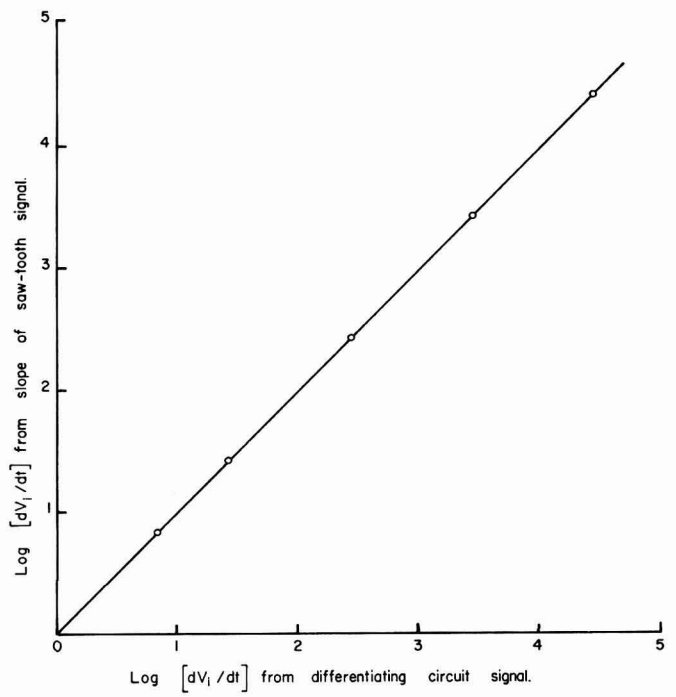

Fig. 3. Linear relation between calibration dV_t/dt and dV_t/dt calculated from C_t and R from the differentiated voltage signal (log scales).

magnitude of the differential coefficient is proportional to the height of the discontinuity exhibited by the second beam trace. Calibration data are shown in Table 1 for a range of voltage sweep rates from 6.9 V sec^{-1} to 2.7 $\times$ 10^4 V sec^{-1}. Corresponding differentiated signal magnitudes were calculated from the voltage sensitivity setting of the oscilloscope and the values of C_i and R chosen, and are shown in the last column of the table. Agreement to within 3% is obtained between the known signal voltage sweep rate and the differentiated signal for all the sweep rates examined. No systematic error with decreasing rise-time is indicated up to the minimum value of 30 μsec V^{-1} used, as shown by the linear relationship in Fig. 3. The apparatus and circuit is hence satisfactory for most moderately fast galvanostatic transients and will be satisfactory for obtaining the detailed forms of pseudocapacity–potential relations which are necessary for the quantitative evaluation of adsorption and kinetic parameters by the theoretical approaches we have proposed elsewhere[4-7].

Typical dual traces of transients [V as $f(t)$] are shown in Figs. 4a–4c. In Fig. 4a, a galvanostatic charging curve is shown for the formate–formic acid system at a platinum anode (6°) with the corresponding differential charging curve exhibiting the minimum and maximum. The initial arrest in this curve corresponds to ionization of adsorbed H and the main arrest to deposition of HCOO species[5,10] at higher anodic potentials. The capacity maximum estimated from the charging curve is 3300 μF cm^{-2} while that derived from the differential curve is 3400 μF cm^{-2}. The magnitude of the differential signal is, of course, proportional to the *reciprocal* of the adsorption pseudocapacitance. The minimum in the differential curve thus corresponds to the maximum capacitance which arises in the arrest region of the galvanostatic charging curve or the open-circuit decay[5] curve.

Potentials corresponding to various values of the adsorption capacitance can be read off with good precision from the direct discharge curve for given times across the sweep, since the differential and direct signals are "in phase" as can be checked by an a.c. reference signal in the input.

In Figs. 4b and 4c are shown open-circuit e.m.f. decay curves and the corresponding differential plots giving dV/dt as a function of time or potential. From Fig. 4b $dV/dt = -0.48$ V sec^{-1} from the decay curve, while the differential curve gives -0.48 V sec^{-1} calculated from the signal minimum and the values of $R = 0.5$ MΩ and $C_i = 1$ μF. Similarly, for Fig. 4c which shows two inflections, the values estimated from the decay curve are $dV/dt = -0.31$ and -0.40 V sec^{-1}, while the differential curve data give -0.32 and -0.40 V sec^{-1}, respectively. All data were obtained from magnified photographs. (Noise level on original trace is < 1 mV).

Applications of the method to a number of reactions involving adsorbed intermediates are in progress. The method is also applicable to evaluation of capacitance from rates of open-circuit e.m.f. decay dV/dt, by the procedure we have described elsewhere[5,10] provided a fast rise electrometer input stage is used. The method, used galvanostatically, can also be adapted to give a repetitive display of the differentiated charging curve, by use of an interrupter in the polarizing circuit. The present galvanostatic method for differential adsorption capacitance, offers some theoretical advantage over the voltage sweep method where the charging current is measured as a function of time. For the purpose of interpreting frequency effects in a.c. capacitance measurements[12] and dependence of capacitance on rise-time[17] in d.c. measurements, it is desirable to have the capacity–potential data obtained as a function of

various constant values of the charging current. The capacitance can then be worked out in terms of the steady-current kinetics[7] and the rise-time dependence or equivalent-frequency dependence of the capacitance can be examined quantitatively. In the voltage sweep method the charging current and potential are never constant and steady-current kinetics cannot be applied.

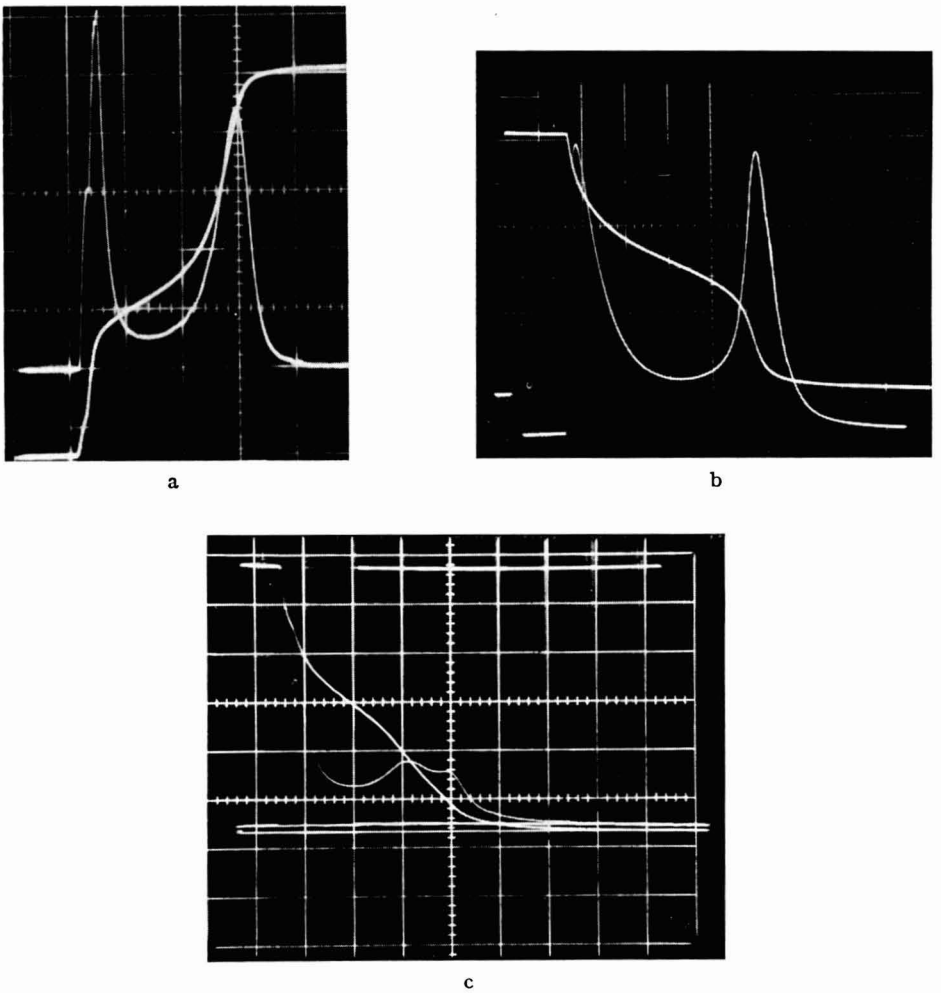

Fig. 4. Direct galvanostatic charging and open-circuit decay curves, and differential pseudo-capacity (humped line) for the anodic oxidation of formate in pure formic acid (1 *M* HCOOK in HCOOH at 6°), as a function of potential. Minimum on differential signal curve corresponds to maximum in capacity, and *vice-versa*.

(a) Galvanostatic charging and differential capacity curve: initial potential $E_H = +0.100$ V; anodic charging current density 7.4×10^{-4} A cm^{-2} (scales: 0.5 sec cm^{-1}; 200 mV cm^{-1} ordinate); $R = 0.5$ MΩ; $C_t = 1$ μF.

(b) Open-circuit decay and dV/dt curves: initial potential $E_H = +1.5$ V; initial current 2.0×10^{-3} A cm^{-2} (scales: 0.2 sec cm^{-1}, 200 mV cm^{-1} ordinate); $R = 0.5$ MΩ; $C_t = 1$ μF.

(c) Open-circuit decay and dV/dt curves: initial potential $E_H = +1.4$ V; initial current 2.9×10^{-4} A cm^{-2} (scales: 0.5 sec cm^{-1}; 200 mV cm^{-1} ordinate); $R = 0.5$ MΩ; $C_t = 1$μF.

ACKNOWLEDGEMENT

Grateful acknowledgement is made to the Defence Research Board, Department of National Defence, for support of this work on Grant No. 5412-01.

SUMMARY

A method for obtaining directly the adsorption pseudocapacity associated with adsorbed intermediates in electrode reactions, as a function of electrode potential is described. The procedure is based on fast electronic differentiation of charging or discharging curves using an operational amplifier. Theoretical advantages over a chronopotentiometric differential capacity method are discussed.

REFERENCES

1 A. N. FRUMKIN AND A. SLYGIN, *Acta Physicochim. U.R.S.S.*, 4 (1936) 991.
2 A. EUCKEN AND B. WEBLUS, *Z. Elektrochem.*, 55 (1951) 114.
3 M. I. TEMKIN, *Zh. Fiz. Khim.*, 15 (1941) 296.
4 B. E. CONWAY AND E. GILEADI, *Trans. Faraday Soc.*, 58 (1962) 2493.
5 B. E. CONWAY, E. GILEADI AND M. DZIECIUCH, *Electrochim. Acta*, 8 (1963) 143.
6 B. E. CONWAY AND E. GILEADI, *Can. J. Chem.*, in press (January, 1964).
7 E. GILEADI AND B. E. CONWAY, *J. Chem. Phys.*, in press (December, 1963).
8 For example, see J. O'M. BOCKRIS, *Modern Aspects of Electrochemistry*, Vol. I, Academic Press, New York, 1954 Chapter IV.
9 H. B. MORLEY AND F. E. W. WETMORE, *Can. J. Chem.*, 34 (1956) 359.
10 B. E. CONWAY AND M. DZIECIUCH, *Can. J. Chem.*, 41 (1963) 55.
11 V. I. PAST AND Z. A. IOFA, *J. Phys. Chem. U.R.S.S.*, 33 (1959) 913, 1230.
12 M. BREITER, *Trans. Symposium on Electrode Processes, the Electrochemical Society, 1958*, John Wiley and Son, New York, 1959.
13 J. W. LOVELAND AND P. ELVING, *J. Phys. Chem.*, 56 (1952) 250; *ibid.*, 255.
14 J. M. PARRY, Ph.D. Thesis, Bristol University, (1960).
15 R. T. IWAMOTO, *Anal. Chem.*, 31 (1959) 1062.
16 G. W. GRAY, *Electronic Instruments*, M.I.T. Radiation Laboratories Series, Vol. XXI, McGraw Hill, New York, 1948.
17 B. E. CONWAY, H. A. KOZLOWSKA AND E. GILEADI, in course of publication.
18 P. DOLIN AND B. V. ERSHLER, *Acta Physicochim. U.R.S.S.*, 13 (1940) 747; see also P. ROITAR, M. JUZA AND J. POLUYAN, *ibid.*, 10 (1939) 389, 845.
19 J. O'M. BOCKRIS AND H. KITA, *J. Electrochem. Soc.*, 108 (1961) 676.
20 M. A. V. DEVANATHAN, J. O'M. BOCKRIS AND W. MEHL, *J. Electroanal. Chem.*, 1 (1959/60) 143; see also M. A. V. DEVANATHAN AND L. SELVARATNAM, *Trans. Faraday Soc.*, 56 (1960) 1820.
21 H. KITA, M. ENYO AND J. O'M. BOCKRIS, *Can. J. Chem.*, 39 (1961) 1670.
22 W. MEHL AND J. O'M. BOCKRIS, *Can. J. Chem.*, 37 (1959) 190.

VOLTAMMETRY OF Ce(IV), Mn(VII), Cr(VI) AND V(V) WITH THE PYROLYTIC GRAPHITE ELECTRODE

F. J. MILLER AND H. E. ZITTEL

Analytical Chemistry Division, Oak Ridge National Laboratory, Oak Ridge, Tenn. (U.S.A.)

(Received November 7th, 1963)

The study of the pyrolytic graphite electrode (P.G.E.) for use with ions of high positive potential resulted from the difficulty of voltammetry of these ions with noble-metal electrodes. In the presence of strong oxidants, noble-metal electrodes become coated with either an oxide or hydroxide; thus, they can no longer be considered to be truly *inert* electrodes. The mechanism of charge transfer through the layer, a subject of controversy, is discussed both by LAITINEN[1] and LINGANE[2]. The poor definition of voltammetric waves of ions that have a high positive potential is attributed to the action of the layers of mixed oxides on the surface of the noble-metal electrodes. The article by DESIDERI[3] on the determination of Ce(IV) with a platinum electrode illustrates some of the difficulties encountered.

EXPERIMENTAL

Apparatus

Polarograph. ORNL Model Q-1673; Current–voltage curves were obtained using this instrument[4].

Pyrolytic graphite electrode. This electrode has been described previously[5].

Reference electrode. A saturated calomel electrode (S.C.E.) prepared in the usual manner was used as a reference electrode. The S.C.E. was connected to the cell by a bridge that contained a saturated solution of KNO_3. The bridge was terminated by an unfired Vycor tube in the cell.

Reagents

All solutions were prepared from reagent-grade chemicals and were standardized, when necessary, by generally accepted procedures.

Procedure

After the test solutions were de-aerated with argon, current–voltage curves were obtained by means of the ORNL Model Q-1673 polarograph. The scan rate was fixed at 0.1 V/min.

RESULTS AND DISCUSSION

Well-defined and reproducible cathodic current–voltage curves were obtained for Ce(IV), Cr(VI), and V(V). With a new or thoroughly cleaned electrode, curves of excellent form were obtained for Mn(VII) also, but the precision of data taken from them was poor. Typical curves are shown in Fig. 1; data obtained successively are given in Table 1. The values of the i_d/C ratios and the $E_{\frac{1}{4}}$ values are relatively constant for all the ions studied except Mn(VII).

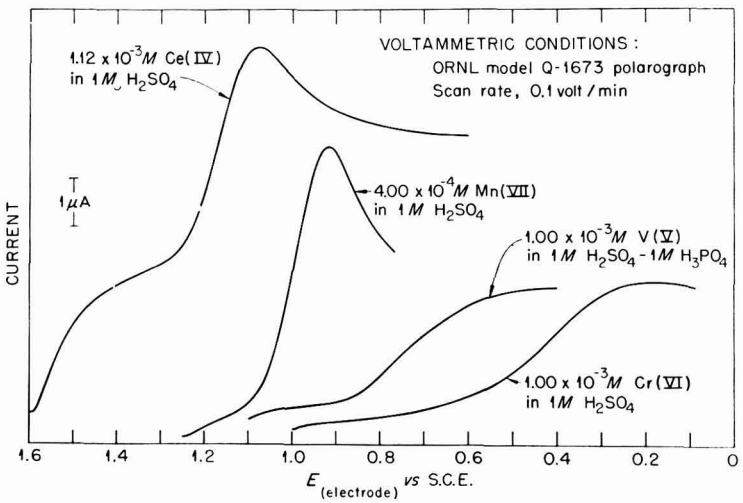

Fig. 1. Composite plot of typical voltammetric curves with the pyrolytic graphite electrode.

TABLE 1

RESULTS OF VOLTAMMETRY OF Ce(IV), Mn(VII), Cr(VI) AND V(V) WITH THE PYROLYTIC GRAPHITE ELECTRODE

Polarograph, ORNL Model Q-1673; indicator electrode, pyrolytic graphite (0.28-cm² area); reference electrode, S.C.E.; scan rate, 0.1 V/min.

Concn. of ion ($M \cdot 10^4$)	i_d (μA)	i_d/C ($\mu A/mM/l$)	$E_{\frac{1}{4}}$ (*V vs. S.C.E.*)
	Ce(IV) in 1 M H_2SO_4		
0.56	1.73	3.10	+1.16
	1.70	3.04	+1.15
1.12	3.68	3.29	+1.17
	3.67	3.29	+1.14
	3.85	3.44	+1.15
	3.63	3.25	+1.15
2.23	7.04	3.15	+1.15
	7.04	3.15	+1.16
Standard deviation = 4.0%			

TABLE 1 (continued)

Concn. of ion ($M \cdot 10^4$)	i_d (μA)	i_d/C ($\mu A/mM/l$)	$E_{\frac{1}{4}}$ (*V vs. S.C.E.*)
	Mn(VII) in 1 *M* H_2SO_4		
1.00	6.75	6.75	+0.94
	6.50	6.50	+1.00
	8.25	8.25	+0.98
2.00	22.30	11.10	+0.94
	18.00	9.00	+0.96
	18.50	9.30	+0.94
3.00	34.00	11.30	+0.93
	20.00	6.60	+0.94
	51.50	17.20	+0.93
	31.50	10.50	+0.96
4.00	41.00	10.20	+0.95
	36.50	9.10	+0.96
	43.30	10.80	+0.96
	46.50	11.80	+0.95
	32.50	8.10	+0.96
5.00	60.00	12.00	+0.96
	38.00	7.60	+0.94
	Cr(VI) in 1 *M* H_2SO_4		
1.00	23.50	23.50	+0.33
	22.40	22.40	+0.31
2.00	42.00	21.00	+0.38
	40.00	20.00	+0.40
	41.00	20.50	+0.43
3.00	61.00	20.33	+0.43
	60.00	20.00	+0.46
4.00	87.00	21.70	+0.44
	76.00	19.00	+0.46
	80.00	20.00	+0.46
5.00	106.20	21.20	+0.45
	103.20	20.64	+0.45
	103.00	20.60	+0.46
	107.60	21.52	+0.46
Standard deviation = 5.5%			
	V(V) in 1 *M* H_2SO_4–1 *M* H_2SO_4		
2.00	0.74	0.37	+0.66
	0.69	0.35	+0.66
4.00	1.14	0.28	+0.68
5.00	1.45	0.29	+0.68
6.00	1.51	0.25	+0.70
8.00	1.94	0.24	+0.73
	2.16	0.27	+0.70
	2.05	0.26	+0.69
10.00	2.34	0.23	+0.71
	2.32	0.23	+0.72
Standard deviation = 8.1%			

The Ce(IV)–Ce(III) electrode reaction in 1 M H_2SO_4 is reversible at the P.G.E. Analysis of the wave by plotting log $[(i_d - i)/i]$ *vs.* $E_{P.G.E.}$ gives a line of slope 0.062, which is in good agreement with the value 0.059 that is indicative of a 1-electron change. The $E_{\frac{1}{2}}$ for the cathodic wave of Ce(IV) is 1.20 V *vs.* S.C.E. and that for the anodic wave of Ce(III) is 1.15 V. The near coincidence of these $E_{\frac{1}{2}}$ values is further evidence that the reaction is reversible. Figure 2 shows that the current–voltage

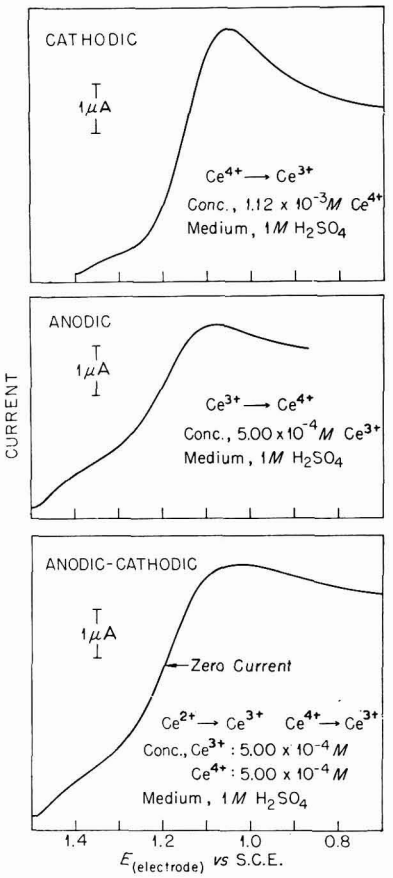

Fig. 2. Anodic–cathodic current–voltage curves for Ce(III)–Ce(IV).

curve for a solution that is equimolar in Ce(III) and Ce(IV) is smooth and passes through the zero-current point. An additional criterion for reversibility is that the electrode potential of the anodic–cathodic curve at the zero-current point should coincide with the standard redox potential of the redox system. The potential of the Ce(III)–Ce(IV) system at the zero-current point was found to be 1.46 V *vs.* N.H.E., which is in reasonable agreement with the standard redox potential of 1.44 V *vs.* N.H.E. in 1 M H_2SO_4. For a solution of Ce(IV), the peak current was calculated

according to the following equation given by DELAHAY[6], which is valid only for a reversible reaction:

$$i_p = (2.72 \times 10^5)\, n^{\frac{3}{2}} A D^{\frac{1}{2}} C^{\circ} v^{\frac{1}{2}}$$

where i_p = peak current (A),
A = area of the electrode (cm^2),
C° = concentration of electroactive species (moles cm^{-3}),
D = diffusion coefficient (cm^2 sec^{-1}),
v = voltage scan rate (V sec^{-1}),
n = electron change.

The conditions were: electrode area, 0.28 cm^2; Ce(IV) concentration, 1.117×10^{-6} moles/cm^3; scan rate, 0.1 V/min and diffusion coefficient, 0.6×10^{-5} cm^2/sec. The calculated value for i_p was 2.47 μA; the measured value was 3.00 μA. The i_p for an anodic wave of Ce(III) at a concentration of $5 \cdot 10^{-4}$ M was calculated from eqn. (1) to be 1.22 μA; the measured peak current was 1.30 μA. For both the reduction of Ce(IV) and the oxidation of Ce(III), the agreement between the calculated and measured i_p values is reasonably good and is additional evidence that the Ce(IV)–Ce(III) electrode reaction in 1 M H_2SO_4 is reversible at the P.G.E.

The electrode reactions of Mn(VII), Cr(VI) and V(V) ions do not approximate reversibility. The formation of unstable intermediates apparently militates against reversible behaviour of these ions at the electrode.

For Mn(VII), well-defined curves are obtained only with new or freshly cleaned electrodes. The poor reproducibility of the data for Mn(VII) is attributed to the formation of MnO_2 in the reduction process and the subsequent adsorption of the MnO_2 on the electrode. To achieve even minimal reproducibility, it was necessary to clean the electrode thoroughly by washing it alternately with chromic acid and ammonia water following each reduction of Mn(VII). The fluctuation in current is caused possibly by variations in the thickness of the MnO_2 layer on the surface of the electrode. The changing current cannot be attributed to oxidation of the electrode surface by Mn(VII) since Ce(IV), at a higher positive potential, behaves reproducibly without any treatment of the electrode.

Cathodic current–voltage curves for Cr(VI) and V(V) can be reproduced without cleaning of the electrode. The data are reasonably precise as shown in Table 1.

The log–function plots, log $[(i_d - i)/i]$ *vs.* $E_{S.C.E.}$, provide information that is difficult to assess. The slopes of the lines are: Mn(VII), 0.059; Cr(VI), 0.224 and V(V), approximately 0.159. These results do not correlate with any other data. However, some useful information can be obtained from the plots. The point of intersection of the line with the abscissa should define an $E_{\frac{1}{4}}$ that is more nearly correct than the $E_{\frac{1}{4}}$ measured from the current–voltage curve. A comparison (Table 2) of the $E_{\frac{1}{4}}$ values measured from the curves, with those taken from the log–function plots, shows that in the case of V(V) there is a large difference between the two values. The difference is caused by the complexity of the V(V) wave, which is a double wave.

The $E_{\frac{1}{4}}$ values of the ions studied fall in the same sequence as their standard potentials *vs.* N.H.E., except for Cr(VI) and V(V), where the positions are switched (Table 3). It is possible that the interchange of the normal order for these two ions is caused by the difference in the supporting electrolyte. In the case of V(V), the supporting electrolyte was a mixture of sulfuric and phosphoric acids, in the case

TABLE 2

COMPARISON OF MEASURED AND GRAPHICAL $E_{\frac{1}{4}}$ VALUES

Ion	$E_{\frac{1}{4}}$ *vs. S.C.E. (V)*	
	Measured	*Graphical*
Ce(IV)	+1.15	+1.15
Mn(VII)	+0.95	+0.97
V(V)	+0.70	+0.48
Cr(VI)	+0.41	+0.44

TABLE 3

COMPARISON OF THE ORDER OF STANDARD POTENTIALS WITH THE ORDER OF $E_{\frac{1}{4}}$ VALUES

Ion	*Potential (V)*	
	Standard[4]	$E_{\frac{1}{4}}$[b]
Ce(IV)	+1.44[a]	+1.41
Mn(VII)	+1.51	+1.15
Cr(VI)	+1.32	+0.67
V(V)	+1.00	+0.96

[a] In 0.5 *M* H_2SO_4 [4].
[b] Corrected to N.H.E.

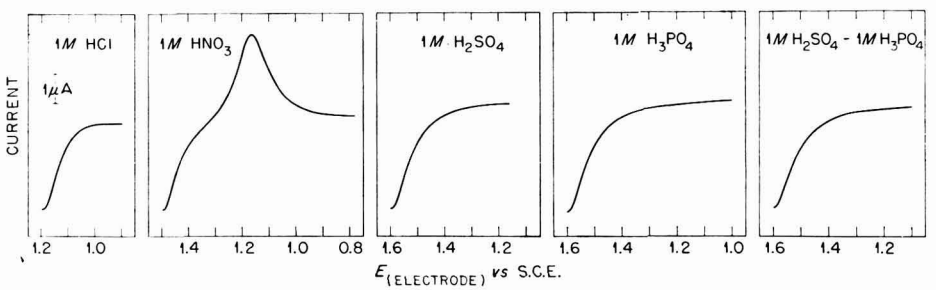

Fig. 3. Positive potential range of various acids. Scan rate, 0.1 V/min.

of Cr(VI), it was sulfuric acid only. The difference in the supporting electrolyte, however, should not have changed the sequence; if V(V) complexes with phosphate ion, the potential would be shifted in the negative direction.

The choice of sulfuric and phosphoric acids as supporting electrolytes was dictated by the necessity to extend the usable range of potential for the aqueous medium, in the positive direction. With either sulfuric acid or sulfuric acid–phosphoric acid, the range of the P.G.E. is extended to +1.5 V *vs.* S.C.E. Figure 3 shows that with other acids the range is more limited.

There has been no indication that the surface of the P.G.E. is oxidized by contact with ions of high positive potential. If an oxide layer does exist on the electrode, it does not interfere with the successful voltammetry of strongly oxidizing ions.

The merit of the pyrolytic graphite electrode as an indicator electrode in amperometric titrations with both Ce(IV)[7] and Cr(VI)[8] has been demonstrated. The work presented here shows that direct voltammetry of certain ions of highly positive potentials is possible in both sulfuric acid and sulfuric acid–phosphoric acid media.

SUMMARY

Voltammetry of Ce(IV), Cr(VI) and V(V) in either sulfuric acid or sulfuric acid–phosphoric acid medium is feasible with the pyrolytic graphite electrode (P.G.E.). In these media, the usable potential range extends to +1.5 V *vs.* S.C.E. Data taken from repetitive current–voltage curves are reproducible, the relative standard deviation ranges from 4–8%. No intervening treatment of the electrode is required. The Ce(IV)–Ce(III) electrode reaction at the P.G.E. is reversible. Results of the voltammetry of Mn(VII) are not reproducible.

REFERENCES

1 H. A. LAITINEN, *Chemical Analysis*, McGraw-Hill, New York, 1960, p. 334.
2 J. J. LINGANE, *Electroanalytical Chemistry*, Interscience Publishers Inc., New York, 1960, p. 129.
3 P. G. DESIDERI, *J. Electroanal. Chem.*, 2 (1961) 39.
4 D. J. FISHER, *Polarograph, ORNL model Q-1673, High-Sensitivity Diode Filter, Derivative, Recording*, Method Nos. 1-003042 and 9-003042 (2-13-57), *ORNL Master Analytical Manual*, U.S. At. Energy Comm. Rept. TID-7015, Sec. 1, April, 1958.
5 F. J. MILLER AND H. E. ZITTEL, *Anal. Chem.*, 35 (1963).
6 P. DELAHAY, *New Instrumental Methods in Electrochemistry*, Interscience Publishers Inc., New York, 1954, p. 119.
7 H. E. ZITTEL AND F. J. MILLER, *Anal. Chem.*, 36 (1964) in press.
8 R. F. APPLE AND H. E. ZITTEL, Analytical Chemistry Division, Oak Ridge National Laboratory, Oak Ridge, Tenn. (U.S.A.), private communication, 1963.

VERSATILE AUTOMATIC TITRATOR

GIULIO MILAZZO

Istituto Superiore di Sanità, Rome (Italy)

Dedicated to Prof. D. MONNIER on his 60th birthday.

(Received 16th November, 1963)

Many quantitative determinations are performed by volumetric analysis, *i.e.* by titration with a suitable reactant of known concentration, the end point of the reaction being detected by the instrumental measurement of a characteristic quantity, the behaviour of which as a function of the volume of reactant shows at the end of the analytical reaction as a crucial point: inflection, interception between two straight segments, zero-value, etc.

Electrochemical methods are widely used because of their many well known advantages. The ease with which they can be adapted to the automatic[1] control of analytical operations is of particular interest when a certain analysis has to be repeated many times (control of production, of quality, etc.).

Automatic analysis has several advantages over manual analysis. It gives results, in respect of precision and accuracy, as good as those obtained by a very good, well-trained and alert operator using the same analytical set-up and it enables a less qualified operator to maintain the same standards of precision and accuracy, thus leading to a worthwhile economy. It avoids individual errors in the detection of the end point in each single analysis (these errors become of course, statistically larger at the end of the working day as a consequence of operator fatigue) and finally it is time-saving.

The name *automatic titrator* can be used for two types of instrument: (i) an instrument recording a complete titration diagram, beyond the equivalence point, or (ii) an instrument stopping the flow of reactant at the equivalence point. In the first case, the exact volume of reactant necessary to complete the analytical reaction is read from the titration diagram after identification of the point corresponding to the end of the analytical reaction; in the second case it is read directly on the burette of the apparatus.

Bearing in mind the characteristics of the usual volumetric analysis, as performed manually by an analyst, it seems more logical to use the name *automatic titrator* for the second type of instrument and to call the first ones simply *recorders*.

Of course, an instrument stopping the flow of reactant automatically at the equivalence point is already a complete automatic titrator, and in fact, the first automatic titrator described by ZIEGEL[2] was an apparatus of this kind.

By adding other parts it is, in principle, possible to extend the automatic functions to include for example, sampling, heating or cooling to a pre-determined temperature, recording of results, rejecting the analysed sample, cleaning, etc.

Any further addition of automatic equipment, however, results in a still higher complexity of the apparatus, a greater fragility, a greater probability of trouble and a much higher initial cost which is not always compensated for by the advantages gained.

A titrator that performs automatically only the chemical operation leaving to the operator (or possibly to other independent automatic equipment) the other functions of sampling, preparation, reading of results, rejecting, cleaning, etc., is still perhaps the most practical and economical solution of the problem of automatic analysis.

In practice, electrochemical methods of detecting the end-point of an analytical reaction are restricted to: potentiometry, amperometry (classical and with polarized electrodes, *i.e.*, the dead stop method) and conductometry. All these methods are well known, so that it is unnecessary here to record their advantages and disadvantages. Automatic titrations can be based on any one of these four methods, the last three through their direct functions of current intensity–volume of reactant. Potentiometry can be utilized either by means of the function of electric tension*–volume of reactant, or through one of its derivatives[4].

Conductometric titration is not much used in practice except in H.F. methods. Further for many cases for which conventional conductometry is suitable, either potentiometry or amperometry give equally good results, so that conductometry will no longer be taken into consideration here.

A good automatic titrator should satisfy the following conditions:

(1) it must have the maximum flexibility, so that it can be employed for the greatest possible number of methods, electrochemical reactions, and electrode combinations;

(2) it must stop the flow of titrant at the equivalence point of the analytical reaction with precision, accuracy and reproducibility of results not less than those obtained by a good well-trained analyst;

(3) it must be trouble-free over long periods of constant use.

As a consequence of the first condition, the wiring of the titrator has to be designed in such a way that both potentiometry and amperometry can be employed with the same apparatus and switching from one method to the other is both rapid and simple. The second condition requires that the instrument must be provided with a means of detecting false equivalence points (due to slow analytical reactions, see below) and with provision for reducing the flow of titrant near the equivalence point in order to avoid an overshoot as a result of a velocity of addition greater than the velocity of response of the electrodes.

Other desirable characteristics not strictly necessary, but very useful for improving the versatility of a titrator are:

(4) the apparatus should not be *blind*, *i.e.*, it should permit the monitoring at any moment, by means of a suitably connected meter, of the course of the reaction;

(5) it should be possible to disconnect the automatic part and to carry out any titration partially or completely manually;

* The C.I.T.C.E. nomenclature for electrochemical quantities is employed here. The most recent nomenclature report has been published in this periodical[3].

(6) it should be possible to control the whole apparatus, including the correct functioning of the automatic part, by simple and rapid means without employing a chemical reaction and without dismounting or opening the apparatus;

(7) it should be possible to pre-select any arbitrary point, chosen by the operator, for the stopping of the automatic titration.

The fourth condition allows one to follow an analytical reaction during its course and together with the fifth condition to use the same apparatus to obtain the whole of a titration diagram needed initially for choosing and establishing the operational conditions of the subsequent automatic analysis. The need for a supplementary manual instrument for this preliminary operation is thus avoided. The usefulness of condition (6) is obvious and condition (7) will be discussed below.

The immediate function of electrical quantity–volume of reactant must be chosen, if it is desired to use the titrator both in conventional potentiometry (with zero-current intensity) and in amperometry, so that the automatism can operate at the zero value for potentiometry or at the value of residual current intensity for amperometry.

Potentiometry carried out on the basis of the electrically obtained second derivative of the electric tension with respect to the volume has the advantage of always giving the equivalence point when $d^2U/dV^2 = 0$ so that previous knowledge of the electric tension of the galvanic cell at this point is not needed. As the inflexion point of the titration diagram is always taken as the equivalence point, the value of the second derivative is always zero at this point for any analytical reaction.

It must be pointed out, however, that this method, besides its sensitiveness to spurious signals, gives results which become less accurate with decreasing rapidity of reaction. Besides involving a greater electronic complexity it would also exclude the use of the same amplifier for potentiometry and amperometry and thus considerably reduce the versatility of the titrator and also exclude the possibility of introducing a timing circuit (see below).

The potentiometric method is therefore used in such a way as to ensure that the input electric signal is always equal to zero at the equivalence point. This is obtained either (i) by conventional potentiometry, *i.e.*, by connecting in opposition to the electric tension of the galvanic cell, an electric tension (taken from a precision voltage divider) whose value is equal to the value of the electric tension of the galvanic cell at the equivalence point, or (ii) by connecting, as comparison electrode, an electrode whose composition, or electric tension[5], is equal to that of the working indicator electrode at the equivalence point. In this second case, called *direct potentiometry*, the electric tension of the galvanic element at the equivalence point is equal to zero, so that no other electric tension in opposition is needed to detect the end-point of the analytical reaction.

Amperometric methods, including those with polarized electrodes (the so-called *dead stop method*), employ a current as the relevant electrical quantity[6]. This current passing through a resistance, creates an electrical tension that is utilized as input, as in the case of potentiometry, to the same amplifier.

An automatic titrator* has been constructed which meets with all the requirements discussed above. The block diagram and the titrating circuits are given in Figs.

* This apparatus has been patented by the Paternò-Foundation and is manufactured and distributed by AMEL, Milan (Italy).

1 and 2. The instrument is based on the following operational principle. The electric signal, coming from the measuring cell, either in potentiometry or amperometry, is always fed to the same amplifier. The output of the amplifier is connected to a meter for the reading and to an electronic relay, operated by the same electric tension actuating the meter. When the pointer comes to the value corresponding to the electric signal at the end-point of the reaction, the output of the amplifier operates through the electronic relay the automatic part, thus stopping the flow of reactant and activating the waiting circuit.

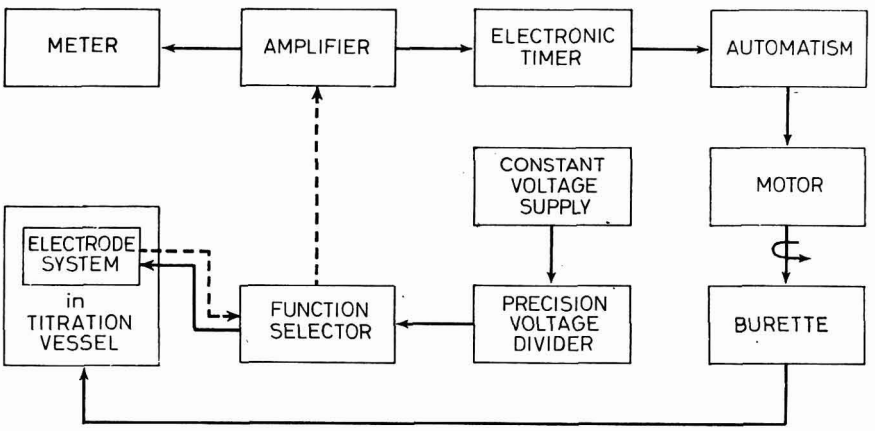

Fig. 1. Block diagram of the titrator.

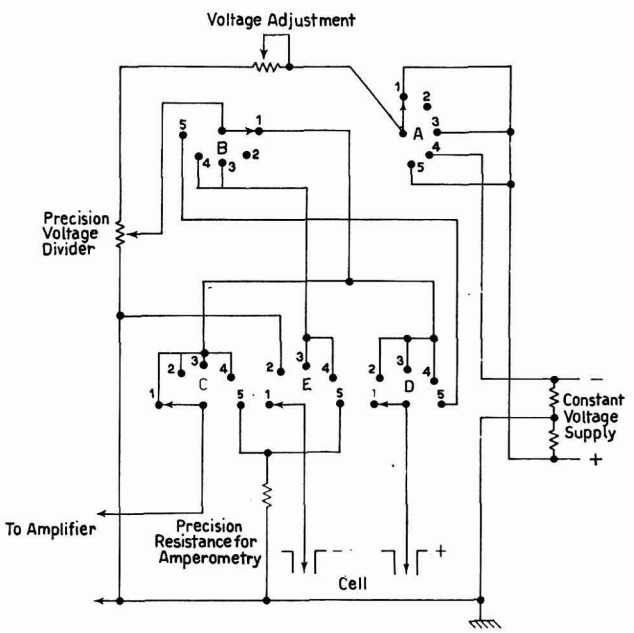

Fig. 2. Titrating circuits of the titrator: 1. control; 2, direct potentiometry; 3 and 4, classical potentiometry with the high-impedance electrode negative or positive respectively; 5, amperometry.

It has been found possible by wiring design to reduce controls to a minimum (see Fig. 3): a multiple selector-switch (7) to choose the particular circuit for the desired operation; the voltage divider (5); a key-switch (9) for the refilling of the burette; a push-button (10) for exact zeroing of the burette and, when desired, for manual titrations; a push-button (8) to start each operation; a key switch (1) to select the

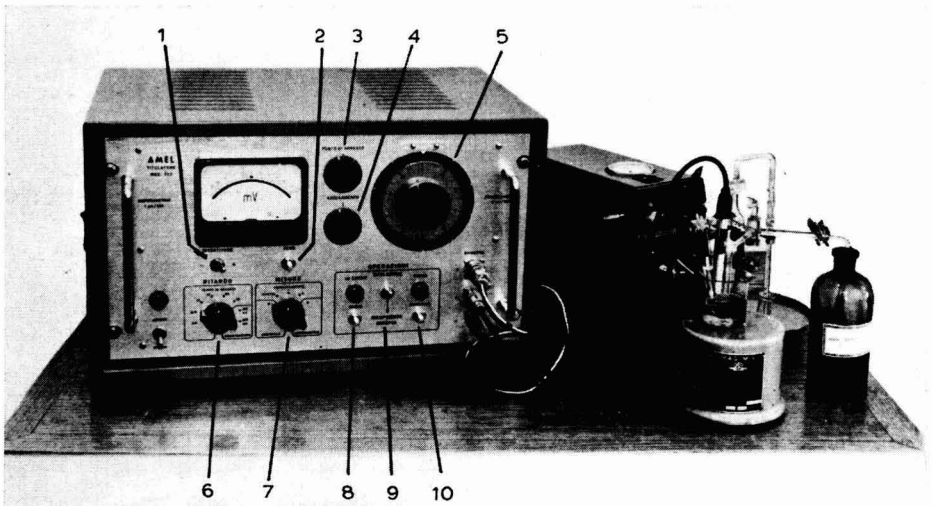

Fig. 3. Titrator assembled: (1), key switch for rising or falling electric signal; (2), push-button to control zero and to stop titration; (3), button to shift operational point of the automatism; (4), zero regulating button; (5), precision voltage divider; (6), timing selector; (7), operation selector; (8), push-button to start automatic titration; (9), key switch titration-refill; (10), push-button for manual titration and burette zeroing.

operation of the automatism for either rising or falling values of the electric signal; a selector (6) for the timing circuit; a button (4) to shift electrically the zero of the reading instrument to an arbitrary point of the scale; a button (3) to shift the operational point of the automatism from the zero-value of the input to the amplifier (the most common value) to another value chosen by the operator; and finally, a push-button (2) to control the zero and to stop the titration manually.

Each position of the selector-switch (7) corresponds to an operation. This selector bears a number of contacts mounted on various plates, all operated by the same spindle, so that only the connections strictly necessary for the chosen operation are made and all others disconnected. In this way errors of electrical connection by the operator are avoided.

The key-switch (9) activates alternatively the automatic titration circuit, or the rapid refilling of the burette, in either of the two positions it connects only the necessary circuits, disconnecting all others.

The zeroing push-button (10), used also for the manual titration, enables the motor of the burette (see below) to be directly connected (excluding the automatism) in the direction of the titration so that it is possible to adjust the burette exactly to zero before starting the titration, or to perform a completely manual titration by

reading on the meter the value of the electric quantity after each manual addition of titrant.

At the end of each titration after the elapse of the selected waiting time, the electric feeding necessary for the flow of reactant is automatically disconnected thus leaving the corresponding circuit open during the preparatory operations of the next titration, during which the electric input signals can be of very different magnitudes and sign. At the end of the preparatory operations, the operator starts the automatic titration each time by pushing the button (8).

Because for both potentiometry and amperometry, two cases of end-point approach are possible, (*i.e.*, for rising or for falling values of the relevant electric quantity) a suitable switch (1) is provided to operate the automatism to approach the selected point from lower or higher values.

To avoid errors arising from slow analytical reactions, a special timing circuit has been designed. When the electric input signal given by the electrode system equals the value corresponding to the equivalence point, the titrator stops the reactant flow and sets itself in a waiting position, for a length of time chosen by the operator and fixed on the selector (7) for all titrations of the same type. If before this waiting time has elapsed, the analytical reaction consumes the slight excess of titrant momentarily present because of the slowness of the analytical reaction and matter to be titrated still remains (*i.e.*, if the end-point indicated by the electric signal is a false equivalence point) the titrator releases again the flow of titrant and the timing circuit returns to its initial condition. If however, the electric signal remains constant until the end of the pre-selected waiting time, the timing circuit at the end of its pre-set value disconnects finally the electrical feeding to the burette and returns again to its initial condition. All is then ready for the next titration but this cannot begin until the operator reactivates the feeding circuit by pushing the starting-button (8).

To avoid errors arising in potentiometry from a too slow response of the electrodes, an auxiliary circuit is activated, with a certain anticipation in respect of the end-point, by means of which the flow of titrant is considerably slowed down in the neighbourhood of the end-point.

The burette chosen for this titrator is of the syringe type with the plunger driven by an electric motor. It has the advantage of avoiding any kind of valve; a valve is always a possible source of positive errors because of the so-called dead volume, and various other troubles like inefficient closing, sticking of the plunger, cleaning difficulties, etc. In addition, the titrant flow can be slowed near the equivalence point and the burette can be rapidly refilled.

The burette has been made with precision bore tubing* and a Teflon plunger. Table 1 shows the precision of two different burettes obtained by weighing the mercury expelled. The burette (see Fig. 4) is also equipped with two automatic end stops to avoid breakage.

The release point of the automatic action can be prefixed at any arbitrary point at the will of the operator (condition 7), within a sufficiently wide interval, by shifting both the zero of the measuring instrument and the point of activation of the automatism to coincide with the value of the electrical quantity at the end of the analytical reaction. This is also useful in those cases where the electric signal at the

* So-called KPG tube manufactured by Schott u.Gen., Mainz (Germany).

TABLE 1

VOLUMETRIC ERRORS OF THE BURETTES

The sections *a*–*d* are in micrometer divisions.

Burette 1				*Burette 2*			
a 0–500	*b* 500–1000	*c* 1000–1500	*d* 1500–2000	*a* 0–500	*b* 500–1000	*c* 1000–1500	*d* 1500–2000
6.7727	6.7655	6.7654	6.7882	6.7798	6.7852	6.7702	6.7785
6.7700	6.7660	6.7688	6.7566	6.7763	6.7213	6.7723	6.7592
6.7655	6.7670	6.7658	6.7571	6.7602	6.7769	6.7682	6.7591
6.7683	6.7650	6.7700	6.7768	6.7613	6.7763	6.7691	6.7691
6.7720	6.7630	6.7710	6.7633	6.7518	6.7853	6.7673	6.7702

Mean values

Sect. *a*. 6.7697 g Hg = 0.50034 cm³	6.7659 g Hg = 0.50007 cm³
Sect. *b*. 6.7653 g Hg = 0.50000 cm³	6.7690 g Hg = 0.50029 cm³
Sect. *c*. 6.7682 g Hg = 0.50023 cm³	6.7694 g Hg = 0.50032 cm³
Sect. *d*. 6.7682 g Hg = 0.50023 cm³	6.7672 g Hg = 0.50016 cm³

Theoretical value of each section

0.50000 cm³	0.50000 cm³

Systematic error (theor. volume — measured volume) (%)

a = + 0.068	+ 0.014
b = 0.000	+ 0.058
c = + 0.046	+ 0.064
d = + 0.046	+ 0.032

Accidental error (%)

a = ± 0.01	± 0.015
b = ± 0.02	± 0.096
c = ± 0.02	± 0.020
d = ± 0.06	± 0.020

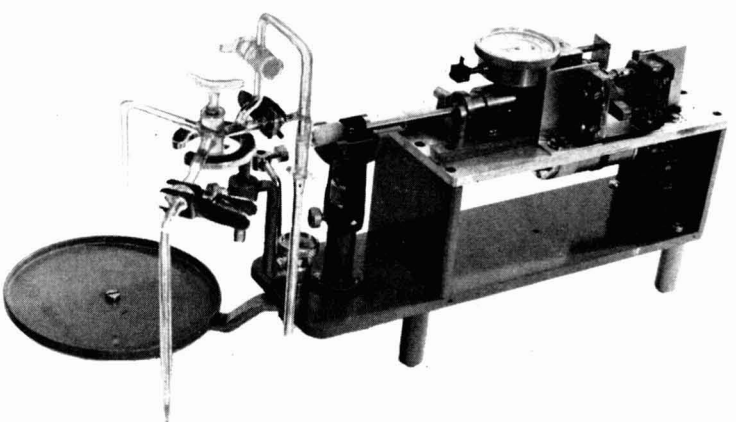

Fig. 4. Burette.

equivalence point does not correspond to the zero value of the measured quantity as in amperometry, for the titrator can still be employed by determining from a preliminary analysis the point at which the automatism must be released.

This titrator can also be employed for coulometric titrations by connecting the titrator output (usually connected with the burette motor) with a coulometric generator which produces the reactant electrolytically inside the titration cell by means of two auxiliary electrodes. The equivalence point must always be detected however, either potentiometrically or amperometrically.

Other useful features of this titrator are:

(1) The circuit is designed so that it is possible to compare the electric tension, taken from the precision voltage divider (5) with that of a standard cell and, if necessary, to bring it to the exact value ($\pm$ 2 mV) indicated on the dial.

(2) It is possible to operate all automatic parts by manual electrical control *i.e.*, to control completely the operations of the titrator, from outside without inserting any chemical reaction or dismounting or opening the titrator, simply by connecting directly, at a particular position (5) of the multiple selector, the electric tension from the divider to the input of the amplifier and bringing it gradually to zero.

The description so far given shows that this titrator can be employed also as a pH-meter, or as a manual polarograph. Finally it must be mentioned that for a special position of the timing selector, the automatism is excluded and the output of the amplifier connected with a recorder.

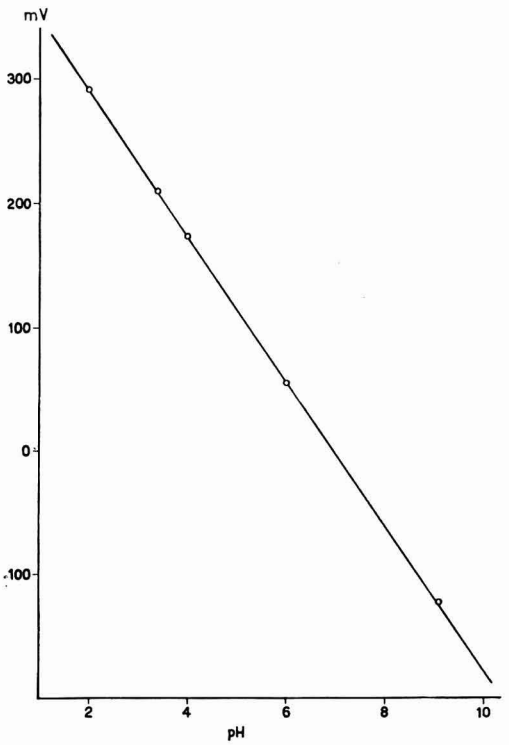

Fig. 5. Response diagram as pH-meter.

To test the performance of this apparatus some typical titrations have been carried out. They are illustrated in the following figures and diagrams.

Figure 5 gives the linearity of response as a pH-meter. It shows that the values of the electric tension at pH 4 and pH 8.5 for the particular glass electrode employed, corresponding to the methylorange end-point titration of a strong acid and to the phenolphthalein end-point titration of a weak acid, are equal to + 175 and − 90 mV respectively.

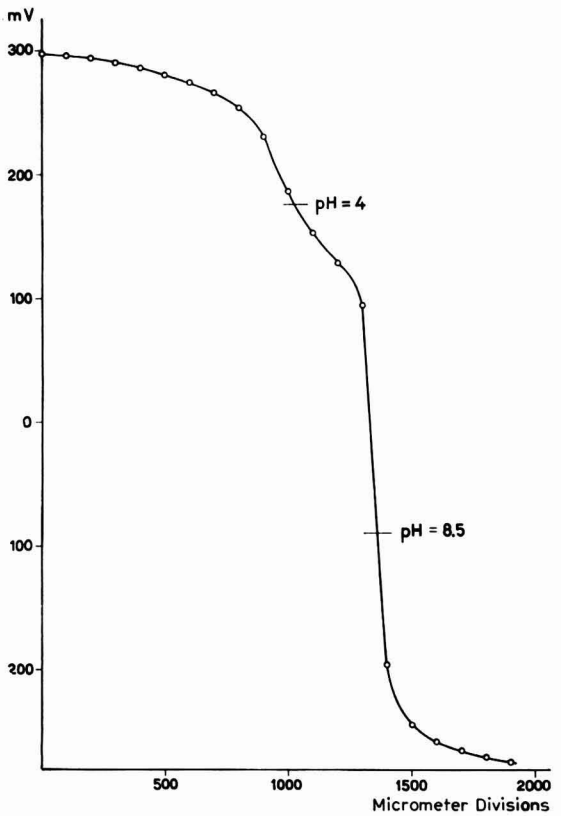

Fig. 6. Manual potentiometric double titration of strong and weak acids.

The diagram of a double potentiometric titration is given in Fig. 6 (strong + weak acids) measured point by point in order to control the values of the electric tension corresponding to the end of each of the two successive neutralizations. It is clear that the two inflexion points corresponding to the two successive neutralizations are located at + 175 mV (pH = 4) and − 90 mV (pH = 8.5). Table 2 gives the results of a number of automatic titrations on a mixture of sulphuric and acetic acids based on the above values of the electric tension of the cell at pH 4 and pH 8.5. When only one acid is titrated the result should be better or at least equally as good. The double titration, because of its greater difficulty, has been chosen in order to illustrate

TABLE 2

TITRATION WITH NaOH OF A MIXTURE OF ACETIC AND SULFURIC ACIDS

No.	H_2SO_4 ~ 0.1 N taken (g of solution)	NaOH 1 N consumed (micrometer divisions)		Deviation from mean value	CH_3COOH ~ 0.1 N taken (g of solution)	NaOH 1 N consumed (micrometer divisions)		Deviation from mean value
		actually	for 10.0000 g			actually	for 10.0000 g	
1	4.9514	582	1175.4	1.2	4.9436	547	1106.4	2.0
2	4.9408	579	1171.9	2.3	5.1081	560	1096.3	8.1
3	4.9528	582	1175.0	0.8	4.9606	550	1108.7	4.3
4	4.9939	582	1167.4	6.8	4.9661	549	1105.4	1.0
5	4.9498	584	1179.8	5.6	4.9486	544	1099.2	5.2
6	4.9518	584	1179.4	5.2	4.9646	550	1107.8	3.4
7	4.9399	580	1174.1	0.1	4.9688	551	1108.9	4.5
8	4.9475	580	1172.3	1.9	4.9466	544	1099.7	4.7
9	4.9502	580	1171.7	2.5	4.9430	545	1102.6	1.8
10	4.9377	580	1174.6	0.4	4.9600	550	1108.8	4.4
		1174.2		*Mean values*		1104.4		
		0.3		*Relative standard deviation (%)*		0.4		
		1174.6		*Theor. equivalents NaOH per 10.000 g*		1104.6		
		0.4		*Theor. — consumed equivalents NaOH*		0.2		
		0.034		*Systematic error (%)*		0.018		

the performance of this titrator. In this titration and in the following titrations also, the solutions to be automatically titrated have been weighed in order to separate sampling errors from the error of the apparatus itself.

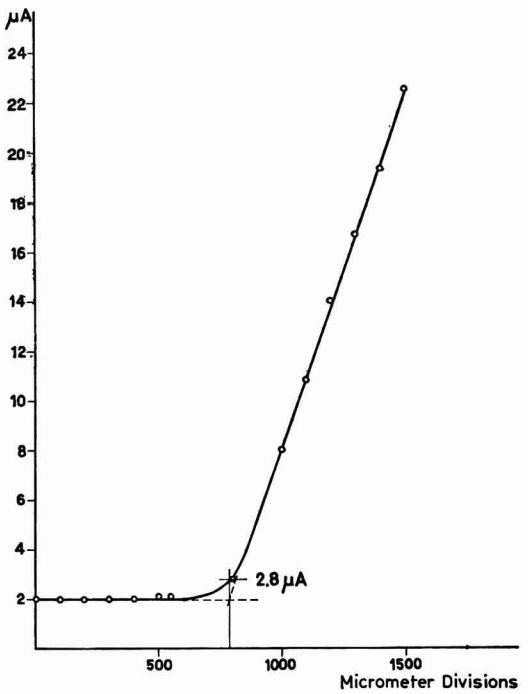

Fig. 7. Manual amperometric titration of SO_4^{2-} with Pb^{2+} with dropping mercury electrode as indicator electrode.

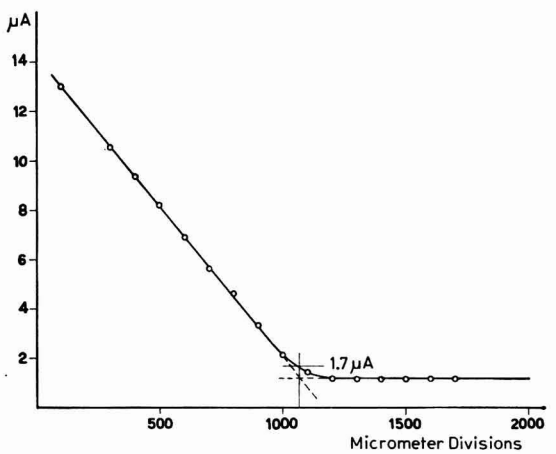

Fig. 8. Manual amperometric titration of Pb^{2+} with SO_4^{2-} with dropping mercury electrode as indicator electrode.

RESULTS OF SOME TYPICAL POTENTIOMETRIC

TABLE

Titration	*Method*	*Titrant*	*Indicator electrode*
I^-, 0.1 N [2]	potentiom.	$AgNO_3$, 1 N	Ag
Cl^-, 0.1 N [2]	potentiom.	$AgNO_3$, 1 N	Ag
Mn^{2+}, 0.01 N	potentiom.	MnO_4^-, 0.095 N	Pt
Pb^{2+}, 0.01 N [3]	amperom.	SO_4^{2-}, 0.1 N	D.M.E.[4]
SO_4^{2-}, 0.01 N [3]	amperom.	Pb^{2+}, 0.1 N	D.M.E.

[1] Mean values of 10 individual titrations
[2] Double titration of iodides and chlorides in the same solutions
[3] Concentration of the solution after dilution = 0.002 N
[4] Dropping mercury electrode

Figures 7 and 8 illustrate the course of two possible amperometric titrations with values of the current intensity:

(a) initially minimum and constant until the end of the analytical reaction (SO_4^{2-} titrated with Pb^{2+});

(b) initially maximum decreasing to the final minimum constant value (Pb^{2+} titrated with SO_4^{2-}).

On these two amperometric diagrams, measured point by point, the end-point value of the current intensity for the automatic operation has been assessed, taking into account the rounding of the diagram in the neighbourhood of the end-point. The results of these amperometric automatic titrations are given in Table 3 together with results of some other potentiometric titrations.

Table 4 shows the relevant operational data of this apparatus.

TABLE 4

OPERATIONAL DATA OF THE TITRATOR

Measuring range of the electric tension (V)	-2 to 0 or 0 to $+2$
Input impedance	1000 MΩ
Measuring range of the current intensity	0–12 μA
Resolution in electric tension	± 2 mV
Resolution in current intensity	0.2 μA
Relative standard deviation in titration	± 0.3 %
Error as pH-meter	± 0.03 pH-units
Waiting time (t)	$5 \leqslant t \leqslant 90$ sec
Mean duration of single titration	2 min
Time required for refilling burette	10 sec

SUMMARY

An electrochemical titrator is described which is suitable for automatic potentiometric, amperometric and coulometric analyses. Its two most prominent features are versatility for various kinds of electrochemical analyses, and the ability to reveal false end-points arising from slowness of the analytical reaction near the end-point. The revealing of these false end-points has been obtained by introducing special timing circuits to put

AND AMPEROMETRIC AUTOMATIC TITRATIONS

3

Volume referred to 10.0000 g solution (micrometer divisions[1])			*Relative standard deviation (%)*	*Systematic error (%)*
theoretical	*consumed*	*theor. — consum.*		
992.06	992.66	+0.60	0.2	+0.06
918.04	918.57	+0.53	0.4	+0.05
1099.3	1099.9	+0.6	0.36	+0.05
1053.0	1052.7	−0.3	0.36	−0.028
1037.9	1037.6	−0.3	0.43	−0.029

the apparatus in a waiting position between the apparent end of the analytical reaction and the reading signal. The results which have been obtained with this apparatus are shown in several diagrams and tables.

REFERENCES

1 For general considerations about automatic titrations see, for example: P. DELAHAY, *Instrumental Analysis*, Macmillan, New York, 1957; J. J. LINGANE, *Electroanalytical Chemistry*, Interscience Publisher's Inc., New York, 2nd. ed., 1958; J. P. PHILIPPS, *Automatic Titrators*, Academic Press, New York, 1959.

2 H. ZIEGEL, *Z. Anal. Chem.*, 53 (1914) 755.

3 P. VAN RYSSELBERGHE, with the collaboration of R. DEFAY, E. LANGE, G, MILAZZO and G. VALENSI, *J. Electroanal. Chem.*, 2 (1961) 265.

4 Some instruments utilizing derivatives of the function electric tension–volume are described by: E. N. WISE, *Anal. Chem.*, 23 (1951) 1479; M. KATZ AND R. A. GLENN, *Anal. Chem.*, 24 (1952) 1157; L. JENŠOVSKÝ, *Chem. Listy*, 47 (1953) 334; H. V. MALMSTADT AND E. R. FETT, *Anal. Chem.*, 26 (1954) 1348; S. TAKAGI AND Y. MAEKAWA, *Japan Analyst*, 3 (1954) 478; Y. MAEKAWA, *Japan Analyst*, 3 (1954) 482, 484, 488; *Pharm. Bull. Tokyo*, 4 (1956) 321.

5 H. LANZ, *Die Anwendung der Umschlagselektrode bei der potentiometrischen Massanalyse*, Dissertation, Dresden, 1929; in G. MILAZZO, *Electrochemistry*, Elsevier, Amsterdam, 1963, pp. 311, 312.

6 I. M. KOLTHOFF AND J. J. LINGANE, *Polarography*, Interscience Publishing Co. Inc., New York, 2nd ed., 1952, p. 887; G. W. C. MILNER, *Principles and Applications of Polarography*, Longmans Green, London, 1957, p. 633; G. CHARLOT, J. BADOZ LAMBLING AND B. TRÉMILLON, *Les Réactions Electrochimiques*, Masson, Paris, 1959, p. 186.

THE DESCRIPTION OF ADSORPTION AT ELECTRODES*

ROGER PARSONS

Department of Physical Chemistry, University of Bristol (England)

(Received October 22nd, 1963)

1. TYPES OF ADSORPTION ISOTHERM

Although a few studies of poly-molecular layers have been made, most work in this field has been concerned with conditions under which it is reasonable to suppose that the adsorbed species forms a mono-molecular layer immediately adjacent to the electrode surface. Since the electrolyte is at least a two-component system, this is strictly a problem in mixed adsorption. When a series of mixed solvents is studied throughout the composition range, it is essential to consider explicitly the adsorption of both components. However, in the adsorption of many strongly adsorbed species from dilute solution it is a reasonable approximation to treat the solvent as a continuum.

When the surface concentration of the adsorbed particles is very small, the adsorption would be expected to obey Henry's law, corresponding to a surface layer in which the free energy of the adsorbed particles is proportional to $RT \cdot \ln m$, where m is their surface concentration. In practice, particularly with adsorbed ions, it is difficult to reach this ideal dilute state; consequently the model of the adsorbed layer must take account of the interactions between the adsorbed particles. For all systems it is necessary to take account of the size of the particles. Two simple methods have been used for this. One, which is more appropriate for solid adsorbents uses a model in which particles are adsorbed on a definite number of discrete sites on the surface. This leads to the well known Langmuir[1] isotherm which may be expressed by the surface equation of state:

$$\Phi = -kT\Gamma_s \ln (1 - \Gamma/\Gamma_s) \qquad 1(1)$$

where Φ is the surface pressure, Γ is the number of sites occupied by adsorbed particles and Γ_s is the total number of sites.

The other method treats the adsorption force as non-localized so that the adsorbed particle is free to move across the surface in an essentially uniform force field. Thus the adsorbed film behaves as a two-dimensional fluid of rigid particles. The isotherm proposed by VOLMER[2] is an example deriving from this type of model. The associated equation of state may be written:

$$\Phi = kT\Gamma/(1 - B'\Gamma) \qquad 1(2)$$

* Presented at the 14th Meeting of C.I.T.C.E., Moscow, August 1963.

where B' is a constant usually taken as twice the area of a spherical adsorbed particle. VOLMER's equation is not so exact an expression of the model because the equation of state of a rigid particle fluid is more complex than that representing the distribution of particles among a fixed number of equal sites; in fact there is at present no exact solution. Equation 1(2) is probably correct at fairly low coverages because it leads to a correct value of the two-dimensional second virial coefficient if the denominator is expanded as a series. The two types of model seem to differ very little at low surface coverages; at high coverages there seems to be an essential difference in that the space between the particles in the Langmuir model must occur in units of the order of the size of the particles, *i.e.*, vacant sites may not be distributed in smaller divisions throughout the adsorbed layer, while in the fluid film model the space may be distributed in any way.

Although the Volmer equation is a correct expression for the equation of state of a two-dimensional hard sphere gas at low densities, it is clearly incorrect at high densities because if B' is twice the molecular area the equation predicts a limit of adsorption at about 55% of the close-packed density. A more realistic equation of state for a two-dimensional hard sphere fluid has been proposed recently by HELFAND, FRISCH AND LEBOWITZ[3]:

$$\Phi = kT\Gamma/(1 - B\Gamma)^2 \qquad 1(3)$$

in which B is the molecular area. Expansion of the denominator shows that this equation is in agreement with the Volmer equation at low values of Γ.

Since most of the species adsorbed at electrodes are polar, if not ionic, it seems likely that allowance merely for the size of the particles will be inadequate. A modification which allows for longer range interaction was proposed by FRUMKIN[4] who added a term in Γ^2 to the Langmuir equation of state. A similar correction to VOLMER's equation converts it into the two-dimensional analogue of VAN DER WAALS equation. From the latter it is clear that the introduction of the term in Γ^2 amounts to a modification of the second virial coefficient of the two-dimensional gas. As the coefficient of the Γ^2 term may be positive or negative, repulsive or attractive forces may be accounted for. A similar modification may be made to the HFL equation to obtain a two-parameter equation which is likely to give a reasonable representation of a two-dimensional fluid over a wide range of densities. Such a procedure has been used succesfully by HILL[5] with TONKS'[6] hard-sphere equation of state. Other additional terms have been proposed[7] in which the power to which Γ is raised is 3/2 or 5/2. When the adsorption occurs in the double layer between two conducting phases, it seems probable that the quadratic term is the leading term, since image interactions must always occur to modify ion–ion interactions.

Another approach was used by LORENZ[8] to account for attractive forces with a model involving clusters of adsorbed particles on a Langmuir surface. FRUMKIN AND DAMASKIN[9] have pointed out that this model cannot include a description of repulsive interactions although it gives a satisfactory account when attractive forces predominate.

It may be concluded, therefore, that the most useful equations of state will be: that due to Frumkin:

$$\Phi = -kT\Gamma_s \ln (1 - \Gamma/\Gamma_s) + A'\Gamma^2 + \ldots \qquad 1(4)$$

and a modified HFL equation:

$$\Phi = kT\Gamma/(1 - B\Gamma)^2 + A'\Gamma^2 + \ldots \qquad 1(5)$$

Further terms may be added to modify the third and subsequent virial coefficients, but in view of present experimental accuracy two parameters (Γ_s and A' or B and A') should be sufficient to represent the results obtained.

2. THE ELECTRICAL VARIABLE

The adsorption isotherm specifies the relation between the amount adsorbed and the activity of the adsorbate in the bulk phase at constant temperature and composition of the other components. In an electrochemical system there is another variable since the amount of adsorption at constant temperature and bulk concentration depends on the potential of the electrode. Consequently, in determining the form of the isotherm it is necessary to keep an electrical variable constant. The electrical variable which was chosen first, by STERN[10], was the potential (ϕ_1) at the site where an ion is adsorbed. This model was later clarified by GRAHAME[11] who made it clear that ϕ_1 included the electrostatic interactions of the adsorbed particle with its neighboring particles (GRAHAME's ψ^v) as well as the electrostatic interactions with the electrode (GRAHAME's ψ^{02}). Thus, when ϕ_1 is held constant and the adsorption isotherm determined, the interaction of the particle with the electrode is not constant but varies in a complementary way with the particle–particle interaction potential. This means that the interaction parameters in the isotherm so determined include not only contributions from the particle–particle interaction as they should, but also some of the particle–electrode interaction which is more properly included in the standard free energy of adsorption.

A similar proposal was made by FRUMKIN[4] for the adsorption of neutral molecules which was considered at constant metal–solution potential difference. If the potential-distance profile across the interface is independent of surface coverage, then this amounts to constancy of the potential at the adsorbed site. It seems unlikely that this condition is generally valid as a result of the so-called *discreteness of charge effect*, although it is more likely to be correct for neutral molecules.

An alternative suggestion was made[12] in 1955 that adsorption should be considered at constant charge on the electrode. Under such conditions the electrode–particle interaction should be approximately constant so that the interaction parameters derived from the isotherm should be a true reflection of the particle–particle interaction. It is possible that even under these conditions the electrode–particle interaction could vary, for example, if the adsorption of particles changed the dielectric constant of the medium surrounding them, or as a result of an induced heterogeneity effect, as proposed by BOUDART[13]. However, in spite of some qualifications, the constant charge isotherm provides a more convenient starting point for interpretation than the constant potential isotherm. It may be noted that in the adsorption of gases on solids, constant charge isotherms are always studied, even when charge transfer occurs between the adsorbate and adsorbent, *i.e.*, the charge on the surface of the solid is kept at zero, while the potential (the surface potential) is allowed to vary.

3. METHODS OF TESTING ADSORPTION ISOTHERMS

The available experimental data is obtained in three principal forms: (i) surface pressure (or interfacial tension); (ii) surface concentration; and (iii) electrode capacity. A direct test of the adsorption isotherm (the surface concentration–bulk activity relation) can be carried out only with data of type (ii). At present such data are of insufficient accuracy to distinguish clearly between different types of isotherms. BLOMGREN AND BOCKRIS[14] for example suggest that the error on the radio-active method is about 10% of a monolayer. The surface concentration may be calculated from data of types (i) and (iii) with the aid of Gibbs' equation, but the errors introduced by the differentiation again make the distinction between isotherms uncertain.

More satisfactory distinctions can be made by comparing experimental and theoretical surface pressure–bulk activity relations. Accuracies of between 0.1 and 1% in the surface pressure can be achieved using data of types (i) and (iii) or preferably a combination of both. A method of testing isotherms by plotting the logarithm of the surface pressure against the logarithm of the bulk activity at constant charge has been developed previously[15]. This method has the advantage that the shape and

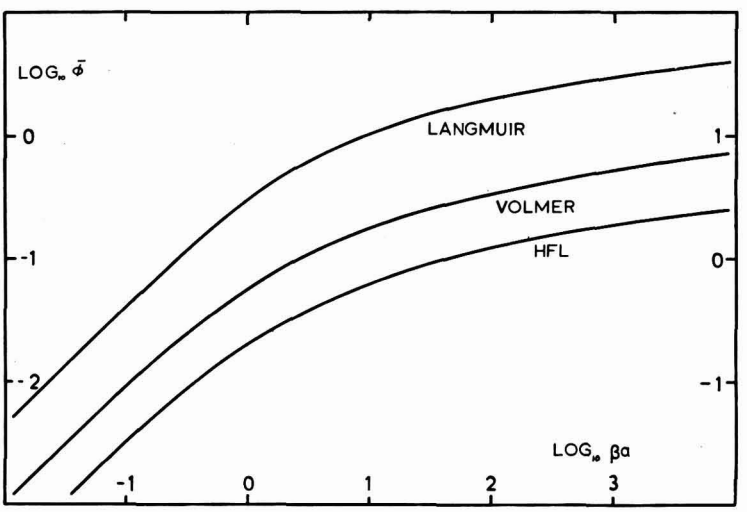

Fig. 1. Log-plot of surface pressure against bulk activity for the Langmuir, Volmer and Helfand, Frisch and Lebowitz hard sphere isotherms. The left-hand scale is for the Langmuir and the right-hand for the other two isotherms.

position of the curve depend on the values of the isotherm constants and the free energy of adsorption at the chosen charge only. This simplifies the analysis considerably. On the other hand the surface pressure–bulk activity relation is not particularly sensitive to the differences between isotherms or to changes in the interaction parameter. Several surface pressure curves based on one-parameter equations of state are shown in Fig. 1. While the high accuracy of the experimental results will permit a decision as to which of these provides the best fit, introduction of an additional parameter makes the distinction between equations like 1(4) and 1(5) very difficult, if not impossible.

The corresponding isotherms are plotted in Fig. 2, and it is evident that the difference in the shape of the curves is more marked. This suggests that even more difference would be observed if the curves were differentiated once more, *i.e.*, that the capacity would provide the most sensitive route to the distinction between isotherms.

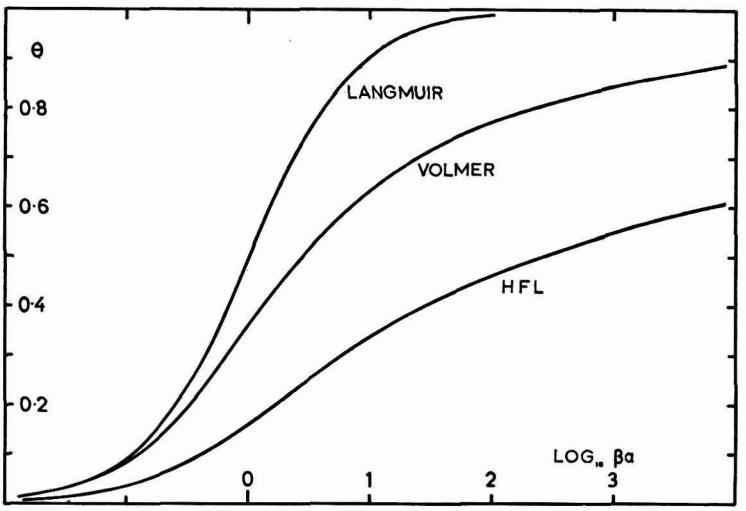

Fig. 2. Surface coverage against log of bulk activity for the Langmuir, Volmer and HFL isotherms.

On the other hand, the capacity is a more complicated function of the isotherm parameters and the charge. Thus it was shown recently[16] that if an isotherm has the form

$$\Gamma = \Gamma(\beta a) \qquad 3(1)$$

where a is the bulk activity of the adsorbate and β is the adsorption coefficient (or

$$\beta = \exp(-\Delta G^{\ominus}/kT) \qquad 3(2)$$

where $\Delta G^{\ominus}$ is the standard free energy of adsorption) which is dependent upon the charge q while the other parameters in the function Γ are independent of q, then

$$E - E^{b} = -kT(\partial \ln \beta/\partial q)\Gamma \qquad 3(3)$$

where E^{b} is the value of the potential difference (E) across the cell when $\Gamma = 0$. Hence, the capacity (C) is given by

$$\frac{1}{C} - \frac{1}{C^{b}} = -kT \frac{\partial}{\partial q}\left(\frac{\partial \ln \beta}{\partial q}\Gamma\right) \qquad 3(4)$$

or

$$\frac{1}{C} - \frac{1}{C^{b}} = -kT\left[\Gamma \frac{\partial^2 \ln \beta}{\partial q^2} + \frac{\partial \Gamma}{\partial \ln \beta}\left(\frac{\partial \ln \beta}{\partial q}\right)^2\right] \qquad 3(5)$$

where C^{b} is the value of C when $\Gamma = 0$.

It is clear that even with the possibly over-simplified assumptions of eqn. 3(1), the

capacity depends not only on the isotherm parameters at the given value of q but also on the first and second derivatives with respect to q of the free energy of adsorption.

The form of the capacity–charge (or potential) curve has been investigated[17] assuming linear and quadratic variation of $\ln\beta$ with q (or E.) The theoretical curves reproduce the general form of the experimental curves and can be made to reproduce experimental results quite precisely if definite assumptions about the isotherm and its parameters are made[9]. The form of the dependence is too complicated however to deduce the nature of the isotherm from the experimental results. This work and other more detailed studies indicate that the dependence of $\ln\beta$ on q is usually close to linear or to quadratic and suggests that either one of these dependencies will be a good first approximation.

Consideration of eqn. 3(5) suggests that the concentration dependence of the capacity at constant q might lead to fruitful results. As argued previously, the interaction parameters of the isotherm are then most likely to be constant as also will be $\partial \ln\beta/\partial q$ and $\partial^2 \ln\beta/\partial q^2$. The problem then consists in using the theoretically calculated values of Γ and $\partial\Gamma/\partial \ln\beta$ together with the experimental ($1/C$—$\ln a$) curve to obtain the nature of the isotherm, its parameters and their charge dependence.

4. CAPACITY–ACTIVITY RELATION WITH ISOTHERM HAVING A STANDARD FREE ENERGY LINEAR IN THE CHARGE

If the free energy of adsorption is a precisely linear function of charge then $\partial^2 \ln\beta/\partial q^2 = 0$ and eqn. 3(5) may be written

$$\frac{1}{C} - \frac{1}{C^b} = -kT \frac{\partial\Gamma}{\partial \ln\beta}\left(\frac{\partial \ln\beta}{\partial q}\right)^2 \qquad 4(1)$$

It is convenient to write this in terms of the fractional coverage θ:

$$\frac{1}{C} - \frac{1}{C^b} = -\frac{kT}{\Gamma_s}\frac{\partial\theta}{\partial \ln\beta}\left(\frac{\partial \ln\beta}{\partial q}\right)^2 \qquad 4(2)$$

Similarly, the isotherms related to eqns. 1(4) and 1(5) may be written:

$$\ln\frac{\theta}{1-\theta} + A\theta = \ln(\Gamma_s\beta a) \qquad 4(3)$$

and*

$$\ln\frac{\theta}{1-\theta} + \frac{1}{1-\theta} + \frac{1}{(1-\theta)^2} + A\theta = \ln(\beta a \cdot 0.907/B) + 2, \qquad 4(4)$$

if it is assumed that the saturation coverage Γ_s in the HFL model is $0.907/B$, *i.e.*, a close-packed layer. It follows from the Frumkin isotherm that

$$\frac{\partial\theta}{\partial \ln\beta} = \left\{\frac{1}{\theta(1-\theta)} + A\right\}^{-1} \qquad 4(5)$$

and from the modified HFL isotherm that

$$\frac{\partial\theta}{\partial \ln\beta} = \left\{\frac{1+\theta}{(1-\theta)^3\theta} + A\right\}^{-1} \qquad 4(6)$$

* I am grateful to Dr. B. B. DAMASKIN for pointing out a simplification in eqn. 4(4).

It may be noted that, just as the Frumkin equation leads to a Langmuir capacity term $\theta(1-\theta)$ *in series* with the constant capacity $1/A$ as observed by CONWAY AND GILEADI[18], so the modified HFL equation leads to an HFL capacity $(1-\theta)^3 \times \theta/(1+\theta)$ *in series* with the constant capacity $1/A$.

Both equations lead to values of $\partial\theta/\partial \ln \beta$ which are small at both small and large coverages, but which rise to a maximum value at intermediate coverage a type of behaviour which must be common to all isotherms not involving a phase transition. Some values of $\partial\theta/\partial \ln\beta$ obtained using the Frumkin isotherm are shown in Fig. 3.

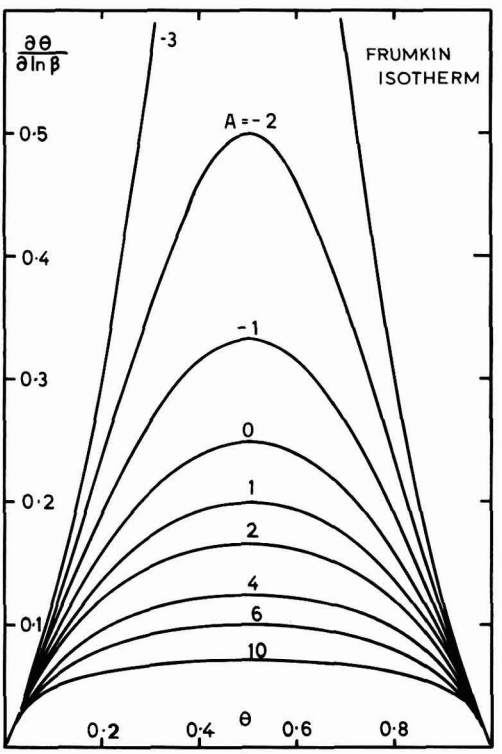

Fig. 3. Plot of eqn. 4(5) for various values of the interaction constant A.

The curves are symmetrical and the maximum occurs at $\theta = \frac{1}{2}$. The corresponding curves from the modified HFL isotherm are shown in Fig. 4; they are markedly asymmetrical and have a maximum at $\Gamma B = 0.215$. Since close-packing occurs at $\Gamma = 0.907/B$, the peak in Fig. 4 corresponds to a fractional coverage of 0.237. The value of the coverage at which the maximum occurs is independent of the value of A. Thus a plot of $(1/C - 1/C^b)$ against fractional coverage would provide an immediate distinction between the two types of isotherm, both from the symmetry and from the position of the maximum. Values of Γ obtained by integration of the capacity curves followed by graphical differentiation would be sufficiently accurate for this

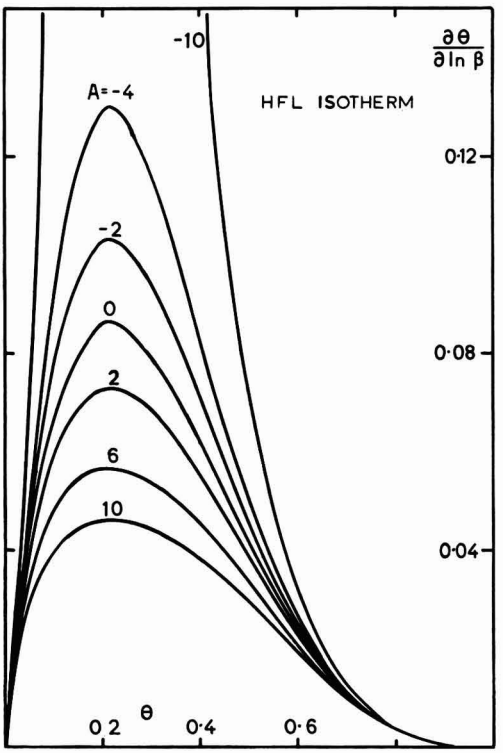

Fig. 4. Plot of eqn. 4(6) for various values of the interaction constant A.

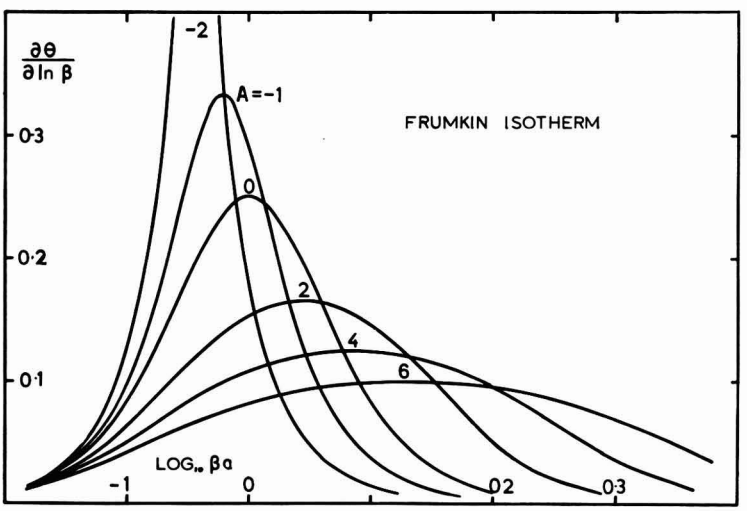

Fig. 5. Plot of $\partial\theta/\partial \ln \beta$, eqn. 4(5), against $\log_{10}\beta a$, eqn. 4(3), for various values of the interaction constant A.

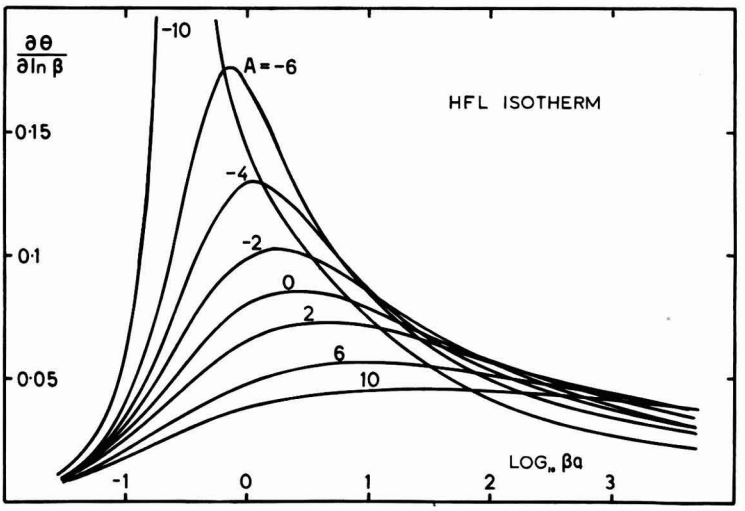

Fig. 6. Plot of $\partial\theta/\partial \ln \beta$, eqn. 4(6), against $\log_{10}\beta a$, eqn. 4(4), for various values of the interaction constant A.

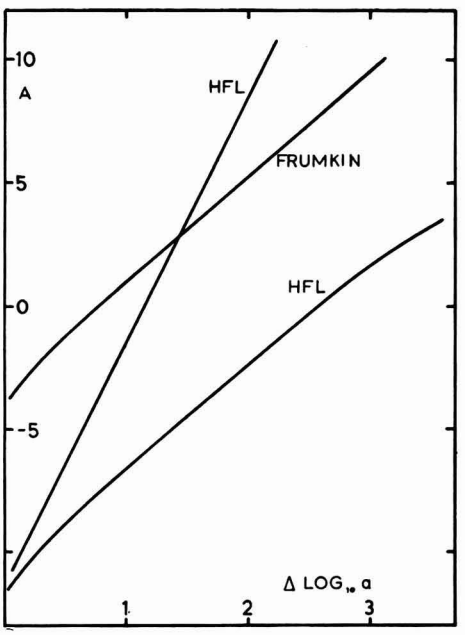

Fig. 7. Half-peak width according to the Frumkin and HFL isotherm. $\Delta\log_{10}a$ is the change in the log of the activity between the peak in $\partial\theta/\partial \ln \beta$ and the point where $\partial\theta/\partial \ln \beta$ has half its peak value. The upper curve labelled HFL refers to the low coverage side of the peak and the lower curve to the higher coverage side. Only one curve is shown for the Frumkin isotherm because the peak is symmetrical in this case (see Fig. 5).

purpose. Since this procedure still requires two integration constants it is worthwhile to investigate whether the capacity curves may be used in a more direct way.

Equations 4(2)–4(6) permit the calculation of the relation between $(1/C - 1/C^b)$ and $\log \beta a$; such curves are shown in Fig. 5 for the Frumkin isotherm and in Fig. 6 for the modified HFL isotherm. First, it is important to note that the symmetry properties of the plots against θ are retained in the plots against $\log \beta a$. Consequently the experimental plot of $(1/C - 1/C^b)$ against $\log a$ at constant q may be used to distinguish between the Frumkin and the HFL isotherms, the former being symmetrical, the latter not. Second, it is evident from Figs. 5 and 6 that the width of these curves is strongly dependent upon the value of A and it is this property which may be used to obtain the value of A from the experimental curves. The width of the curve may be characterized by the diameter of the peak at any selected fraction of the total peak: height, for example the half-height width. This quantity is plotted in Fig. 7 against A for both isotherms (or rather, the half-diameter, which is different for the two halves of the curve for the HFL isotherm); it is almost linear in A so that the value of A may readily be obtained from the experimental curves. The only difficulty which may occur when A is large and positive is that of obtaining experimental results over a sufficiently wide concentration range.

Once the value of A is known eqns. 4(3) — or 4(4) — and 4(5) — or 4(6) — may be used to compute $\log(\Gamma_s \beta a)$ and $\partial \theta / \partial \ln \beta$ as a function of θ. The position of the peak provides one point on the $[\partial \theta / \partial \ln \beta - \ln(\Gamma_s \beta a)]$ curve, hence each experimental point may be assigned a value of θ and of $\partial \theta / \partial \ln \beta$. A plot of $-1/C$ against $\partial \theta / \partial \ln \beta$ may then be constructed; this has a slope of $(kT/\Gamma_s)(\partial \ln \beta / \partial q)^2$ and an intercept of $1/C^b$, so that the capacity in the absence of the adsorbate may be determined if is not known already (this is important in the case of ionic adsorption from a pure solution of a single salt; this case is further considered below). A second plot of E against θ may also be constructed; from eqn. 3(3) this has a slope of $-(kT/\Gamma_s) \times (\partial \ln \beta / \partial q)$ which combined with the slope of the previous plot permits the evaluation of $(\partial \ln \beta / \partial q)$ and Γ_s. It is now possible to calculate the values of Γ and also the standard free energy of adsorption at each value of q.

The calculation procedure described above involves the implicit assumption that the adsorbed substance is present only in the inner layer and causes no change in the structure of the remainder of the double layer. This is reasonably correct for the adsorption of a neutral dipolar substance like thiourea from a solution containing ions which are not specifically adsorbed; at constant charge on the metal the structure of the diffuse layer remains constant. It is not correct for the adsorption of ions, especially from a solution of a single salt, since increase of, say, negative charge on the inner layer must be balanced by an equal increase of the positive charge on the diffuse layer. This leads to a varying contribution to the measured capacity from the diffuse layer. To allow for this, two alternative modifications to the above procedure may be used.

(i) The measured capacity may be used directly as described and the values of Γ obtained regarded as first approximations from which the diffuse-layer contribution to the total capacity is found. The latter is then corrected for the diffuse-layer contribution and the whole sequence repeated using the first approximation to the inner-layer capacity. Further iteration may be necessary.

(ii) The capacity curves are integrated and then differentiated graphically to obtain

approximate values of Γ for calculation of the diffuse-layer capacity. The inner-layer capacity is then calculated and used in the above procedure. This alternative may be the more rapid method, but it does require a second integration constant from interfacial tension measurements or from diffuse-layer theory.

5. CAPACITY–ACTIVITY RELATION WITH ISOTHERM HAVING A STANDARD FREE ENERGY QUADRATIC IN THE CHARGE

The analysis of isotherms of this type is more difficult because of the presence now of the term in $\partial^2 \ln \beta/\partial q^2$ and the fact that $\partial \ln \beta/\partial q$ is now linearly dependent on the charge. The strictly quadratic dependence may be written

$$\ln \beta = \ln \beta_{\max} - (b/2)\delta^2 \qquad 5(1)$$

where $\beta_{\max}$ is the maximum value of β which occurs at a value of the charge $q_{\max}$ and $\delta = q - q_{\max}$. Then eqn. 3(3) becomes

$$E - E^b = (kT/\Gamma_s) b\,\delta\theta \qquad 5(2)$$

and eqn. 3(5):

$$\frac{1}{C} - \frac{1}{C^b} = \frac{kT}{\Gamma_s}\left\{b\theta - (b\delta)^2 \frac{\partial\theta}{\partial \ln \beta}\right\} \qquad 5(3)$$

It follows that the greatest lowering of $-(1/C)$ occurs at $q_{\max}$ ($\delta = 0$) and $E_{\max}$ at all concentrations. Thus, this point may be determined directly from the measured capacity curves.

With the definition

$$\Delta = E - E_{\max} \qquad 5(4)$$

eqn. 5(2) may be written

$$\Delta - \Delta^b = (kT/\Gamma_s) b\,\delta\theta$$

or

$$\frac{\Delta}{\delta} - \frac{\Delta^b}{\delta} = (kT/\Gamma_s) b\theta \qquad 5(5)$$

The quantity δ/Δ is an integral capacity K, measured not from $q = 0$ but from $\delta = 0$. Hence eqn. 5(5) may also be written

$$\frac{1}{K} - \frac{1}{K^b} = (kT/\Gamma_s) b\theta \qquad 5(6)$$

When $\delta = 0$, the integral capacity K is equal to the differential capacity C as may be seen by comparing eqn. 5(3) with eqn. 5(6). Further, eqn. 5(6) is in fact the first term on the right-hand side of eqn. 5(3) so that

$$\left(\frac{1}{C} - \frac{1}{C^b}\right) - \left(\frac{1}{K} - \frac{1}{K^b}\right) = -\frac{kT}{\Gamma_s}(b\delta)^2 \frac{\delta\theta}{\partial \ln \beta} \qquad 5(7)$$

Thus calculation of the left-hand side of eqn. 5(7) from experimental results provides a quantity which at constant q is proportional to $\partial\theta/\partial \ln \beta$ and consequently may be

used in the same way that $(1/C - 1/C^b)$ was used in the previous section to determine the nature of the isotherm and its constants. Once A is known from the peak width, plots can be made of the left-hand side of eqn. 5(6) against θ and of the left-hand side of eqn. 5(7) against $\partial\theta/\partial \ln \beta$. The quantities b and Γ_s are readily found from the slopes of these lines.

6. USE OF THE PEAK-HEIGHT–ACTIVITY RELATION FOR DISTINGUISHING ISOTHERMS

It has already been pointed out[17] that the condition for a peak in $-1/C$ when eqn. 5(1) is valid is

$$b\delta_p^2 = \frac{3(\partial\Gamma/\partial \ln \beta)}{\partial^2\Gamma/(\partial \ln \beta)^2} \qquad 6(1)$$

An alternative form of this condition is

$$b\delta_p^2 = 3\Big/\frac{\delta}{\partial\Gamma}\Big(\frac{\partial\Gamma}{\partial \ln\beta}\Big) \qquad 6(2)$$

The activity (or concentration) dependence of the charge (δ_p) at which the peak occurs may then be obtained by substituting eqn. 5(1) into the appropriate isotherm and solving the resulting equation with eqn. 6(2) for δ_p as a function of $\ln a$. Although these equations cannot be solved analytically it is easy to obtain a graphical solution. The simplest method is to plot the right-hand side of eqn. 6(2) against Γ and on the same graph, $\log \beta a$ as a function of Γ calculated from the isotherm equation. The set of intersections corresponding to different values of δ_p and $\log a$ is the set of required solutions.

The curve of the right-hand side of eqn. 6(2) for any isotherm is asymptotic to a value of Γ which depends on the nature of the isotherm. This may be understood by considering the shape of the curve of $\partial\Gamma/\partial \ln \beta$. It was pointed out above that this always passes through a maximum at some intermediate value of Γ (*cf.* Figs. 3 and 4). The denominator of the right-hand side of eqn. 6(2) is the slope of $\partial\Gamma/\partial \ln \beta$; hence the asymptote is the value of Γ at which $\partial\Gamma/\partial \ln \beta$ has a maximum. As the bulk activity increases, the intersection of the two curves in the above graphical solution becomes closer and closer to the asymptotic value of Γ which may be called Γ_a. Thus, at high bulk activities the isotherm equation may be written

$$\text{const.} = \ln \beta_{\max} \cdot a - (b/2)\delta_p^2 \qquad 6(3)$$

where the constant on the left-hand side is the isotherm function with $\Gamma = \Gamma_a$. It follows from eqn. 6(3) that the linear relation between δ_p^2 and $\log a$ first deduced by LORENZ AND MÖCKEL[19] is independent of any assumption about the detailed form of the adsorption isotherm. It depends only on the assumption of eqn. 3(1) and the quadratic dependence of $\ln \beta$.

Now at the peak, under these conditions of high bulk activity, eqn. 5(3) may be written

$$\frac{1}{C_p} - \frac{1}{C^b} = \frac{kT}{\Gamma_a}\Big\{b\theta_a - (b\delta_p)^2\Big(\frac{\partial\theta}{\partial \ln \beta}\Big)_a\Big\} \qquad 6(4)$$

while at q_{max} ($\delta = 0$)

$$\frac{1}{C_{max}} - \frac{1}{C^b} = \frac{kT}{\Gamma_s} b\,\theta_{max} \qquad 6(5)$$

Consequently

$$\frac{\frac{1}{C_p} - \frac{1}{C^b}}{\frac{1}{C_{max}} - \frac{1}{C^b}} = \frac{\theta_a}{\theta_{max}} - \frac{b\delta_p^2}{\theta_{max}} \left(\frac{\partial\theta}{\partial \ln\beta}\right)_a \qquad 6(6)$$

Under these conditions the ratio on the left-hand side of eqn. 6(6) will be a linear function of δ_p^2 and the intercept at $\delta_p = 0$ will be θ_a/θ_{max}. Since θ_{max} at high bulk activity is very close to unity, this intercept is equal to the fractional coverage at the maximum in the $\partial\theta/\partial \ln\beta$ curve and provides a method of distinguishing isotherms like that of FRUMKIN from that of HELFAND, FRISCH AND LEBOWITZ.

7. DISCUSSION

Figure 8 shows the change in the reciprocal capacity of the inner layer plotted against the amount of specifically adsorbed anion for the system mercury–aqueous sodium benzene disulphonate[20]. It is clear from this figure that the curves are asymmetric

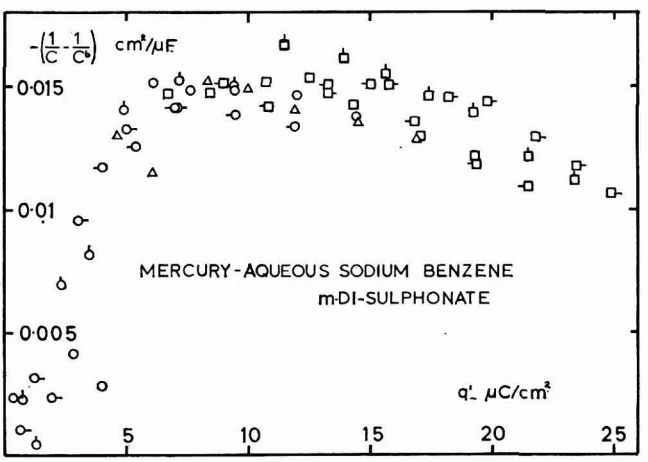

Fig. 8. Plot of the change in reciprocal capacity of the mercury–aqueous solution interface caused by the adsorption of the benzene-*m*-disulphonate ion at 20° as a function of the specifically adsorbed charge. Data of PARRY AND PARSONS[20]. Charge on the mercury surface (in μC/cm²): ⊙, −8; ◑, −6; ⊖, −4; ○, −2; △, 0; □, 2; ⊟, 4; ⊞, 6; ⊡, 8.

which suggests that the HFL isotherm will describe this system better than the Frumkin isotherm. The peak in the curve occurs at about 9 μC/cm²; a value which would give a coverage at close-packing of 38 μC/cm². This is higher than the value previously estimated (27 μC/cm²) using a Temkin isotherm, but is in reasonable

agreement with that calculated from the size of the anion assuming that it is adsorbed flat and rotates freely (34.5 μC/cm^2). The lower saturation value obtained previously is evidently due to the very slow approach to saturation of a fluid monolayer (see Fig. 2).

It may also be observed in Fig. 8 that the height of the peak varies somewhat with the charge. This might be due to the rather unreliable values for the capacity of the inner layer in the absence of specifically adsorbed ions. Correction for the latter can be made more reliably in the case of halide ion adsorption since the fluoride ion provides a reasonable reference ion which is not specifically adsorbed. The difference between the reciprocals of the inner-layer capacities of mercury in contact with aqueous KI and KF is shown in Fig. 9 using GRAHAME's data[11]. Again the curves

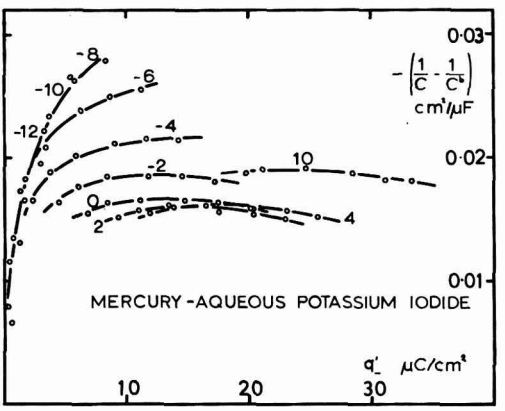

Fig. 9. Plot of the change in reciprocal capacity of the mercury–aqueous solution interface caused by the adsorption of the iodide ion at 25° as a function of the specifically adsorbed charge. Data of GRAHAME[11]. The charge on the mercury surface in μC/cm^2 is indicated by each line.

appear to be asymmetrical but the height goes through a well-defined minimum value at a charge of about +2 μC/cm^2. There is also some evidence of a trend in the position of the peak from about 15 μC/cm^2 at the more negative charges to about 25 μC/cm^2 at the more positive charges. Assuming an HFL isotherm, this would correspond to saturation coverages ranging from 63–105 μC/cm^2. The latter agrees with the close-packed coverage calculated assuming the crystal radius of the iodide ion.

Similar changes in the height of the peak are found with the adsorption of thiourea on mercury from an aqueous potassium nitrate solution. The change in reciprocal capacity for this system is shown in Fig. 10 as a function of log concentration[21]. The curves here are much more symmetrical which suggests that the Frumkin isotherm is a better description of this system than the HFL isotherm. It is possible that this is due to the formation of a chemical bond between the sulphur of the thiourea and a mercury atom. Thus definite adsorption sites exist for thiourea adsorption but apparently not for the adsorption of benzene disulphonate or for iodide. For a liquid surface it is possible in this way to distinguish between chemisorption and physical adsorption.

The fact that similar changes in peak height are found in the two dissimilar systems of Figs. 9 and 10 suggests that they have a common origin in the $(\partial \ln \beta/\partial q)^2$ factor of eqn. 4(2). A minimum in this quantity is in agreement with the earlier findings for thiourea adsorption[15] and corresponds to a peak in the effective dielectric

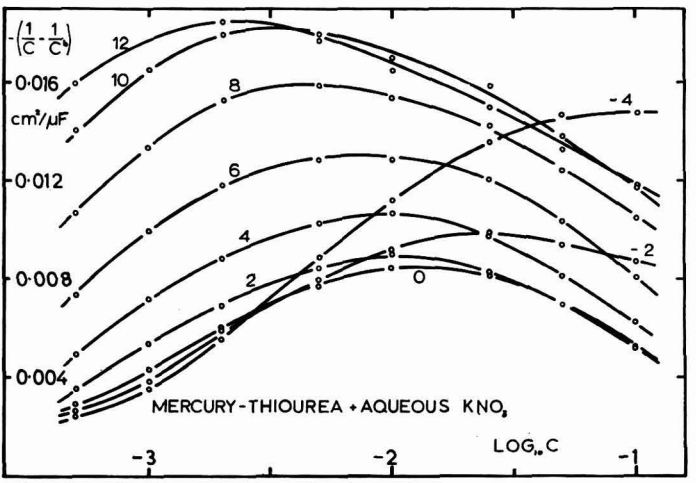

Fig. 10. Plot of the change in reciprocal capacity of the mercury–aqueous KNO_3 interface caused by the adsorption of thiourea at 25° as a function of the bulk concentration of the latter. Data of PARSONS AND SYMONS[21]. The charge on the mercury surface in $\mu C/cm^2$ is indicated by each line.

constant of the inner layer at zero charge or at a small positive charge. On the other hand, if $(\partial \ln \beta/\partial q)$ does change with q, it is not strictly correct to interpret the curves assuming a linear variation of free energy with charge. It is possible that errors in the analysis arising from this simplifying assumption may be small, but this must be verified by a more thorough analysis.

One result of the non-linear dependence of $\ln \beta$ on q is to change the value of the coverage at which the peak in the reciprocal capacity is observed. If $\partial^2 \ln \beta/\partial q^2$ has the same sign as $\partial \ln \beta/\partial q$, the peak occurs at larger coverages and *vice versa*. Although this could be the explanation for the shifts of the peak apparent in Fig. 9, this does not seem to be in good agreement with the changes observed in the peak height. The interpretation must remain rather uncertain at present partly because the results cover only a small concentration range so that only a small segment of the curve is available for each value of the charge.

No completely suitable measurements are at present available for illustrating the analysis for a substance having $\ln \beta$ quadratic in q. With the technique described in Section 5, the results of BREITER AND DELAHAY[22] seem to indicate that the HFL isotherm is preferable for describing the adsorption of *n*-amyl alcohol, but again the concentration range is inadequate for a conclusive demonstration. The technique of Section 6 applied to the results of DAMASKIN[9] for *tert.*-amyl alcohol at high concentrations gives a negative value of θ_a. It is possible that this is due to the variation

of the interaction parameter with charge as suggested by DAMASKIN. If this is correct the relation between peak height and the square of the charge must be fortuitous.

The fact that deviations from the simple ($\ln \beta - q$) laws can lead to asymmetric capacity curves, means that it may be possible to be led to incorrect conclusions about the nature of the isotherm obeyed by the adsorbed substance. It is difficult to estimate how important a restriction this may be. In the case of curves like those of Fig. 8 where the peak appears to occur at almost the same coverage at different values of q, it is probably unimportant.

Another possible cause of asymmetry in $\partial\theta/\partial \ln \beta$ is the existence of other powers of Γ in the first correction term of the Langmuir or HFL isotherm. As pointed out by CONWAY *et al.*[23], the higher the power to which Γ is raised the lower is the value of the coverage at the peak. It was suggested in Section 1 that the square term is the most probable first correction term. However, further terms in the virial series might lead to a change in the peak position.

Although these qualifications must be borne in mind, it seems likely that the technique of studying the concentration dependence of the capacity at constant charge will provide useful results, particularly for solid metals because interfacial tension measurements are unnecessary.

SUMMARY

A number of different isotherms has been used to describe the adsorption of ions and molecules at metal electrodes. These are discussed critically with the object of assessing their usefulness for this purpose. The problem of the electrical variable is discussed and it is concluded that isotherms at constant charge provide parameters with the simpler interpretation.

Methods of fitting isotherms to experimental results are considered. While the surface pressure–concentration curve combines reliability of the experimental results with simplicity of interpretation, it is much less sensitive than the capacity to the detailed nature of the isotherm; in particular it is doubtful whether the distinction between localized and non-localized adsorption can be made using the results in this form. On the other hand, the capacity is more difficult to interpret because it is a more complicated function of the isotherm and of the standard free energy of adsorption. The most promising technique appears to be the analysis of capacity–concentration curves at constant charge. Analysis of experimental results in this way suggests that adsorption on mercury is probably non-localized. An isotherm developed from the equation of state of a two-dimensional hard sphere gas in suggested which should be of wide applicability. The predictions of this isotherm are compared with those of previously used equations.

REFERENCES

1 I. LANGMUIR, *J. Am. Chem. Soc.*, 40 (1918) 1369.
2 M. VOLMER, *Z. Physik. Chem.*, 115 (1925) 253.
3 E. HELFAND, H. L. FRISCH AND J. L. LEBOWITZ, *J. Chem., Phys.* 34 (1961) 1037; F. H. STILLINGER, A.C.S. meeting, Atlantic City, September 1962; F. P. BUFF AND F. H. STILLINGER, *J. Chem. Phys.*, 39 (1963) 1911.
4 A. N. FRUMKIN, *Z. Physik.*, 35 (1926) 792.
5 T. L. HILL, *J. Chem. Phys.*, 20 (1952) 141.
6 L. TONKS, *Phys. Rev.*, 50 (1936) 955.
7 E. BLOMGREN AND J. O'M. BOCKRIS, *J. Phys. Chem.*, 63 (1959) 1475.

8 W. LORENZ, *Z. Eletrochem.*, 62 (1958) 193.
9 A. N. FRUMKIN AND B. B. DAMASKIN, *Modern Aspects of Electrochemistry*, Vol. 3, edited by J. O'M. BOCKRIS, Butterworths, London, 1964.
10 O. STERN, *Z. Elektrochem.*, 30 (1924) 508.
11 D. C. GRAHAME, *J. Am. Chem. Soc.*, 80 (1958) 4201.
12 R. PARSONS, *Trans. Faraday Soc.*, 51 (1955) 1518.
13 M. BOUDART, *J. Am. Chem. Soc.*, 74 (1962) 3556.
14 E. BLOMGREN AND J. O'M. BOCKRIS, *Nature*, 186 (19060) 305.
15 R. PARSONS, *Proc. Roy. Soc. (London)*, A261 (1961) 79.
16 R. PARSONS, *Trans. Faraday Soc.*, 55 (1959) 999.
17 R. PARSONS, *J. Electroanal. Chem.*, 5 (1963) 397.
18 B. E. CONWAY AND E. GILEADI, *Trans. Faraday Soc.*, 58 (1962) 2493.
19 W. LORENZ AND W. MÖCKEL, *Z. Electrochem.*, 60 (1956) 507.
20 J. M PARRY AND R. PARSONS, *Trans. Faraday Soc.*, 59 (1963) 241.
21 R. PARSONS AND P. C. SYMONS, unpublished results.
22 M. W. BREITER AND P. DELAHAY, *J. Am. Chem. Soc.*, 81 (1959) 2938.
23 B. E. CONWAY, E. GILEADI AND M. DZIECIUCH, *Electrochim. Acta*, 8 (1963) 143.

J. Electroanal. Chem., 7 (1964) 136–152

A note on the paper "The description of adsorption at electrodes" by R. Parsons*

PARSONS[1] criticizes the application of Langmuir's isotherm to adsorption at the surface of solutions, as having been deduced for localized adsorption, and suggests the use of an equation of state proposed by HELFAND, FRISCH AND LEBOWITZ (HFL)[2], which expresses the two-dimensional pressure of an adsorbed layer of solid spheres, assuming the adsorption to be non-localized. In my opinion this criticism is not justified. I shall try to prove it by two methods:

(a) The decrease in the surface tension is an analogue of the osmotic pressure of concentrated solutions, rather than of the two-dimensional pressure of a compressed gas. In illustration, let us separate the solution from the pure solvent by a semi-permeable membrane of width l and area S, which crosses the liquid surface. Evidently, the force which has to be applied upon the membrane in the direction of the solution to maintain the system in equilibrium is equal to $PS + l(\sigma_A - \sigma)$, where P is the osmotic pressure of the solution and $(\sigma_A - \sigma)$ is the decrease in surface tension. From the molecular point of view, the second term should be considered as the excess of the osmotic pressure of adsorbed molecules P_s over that of the solution layer of the same thickness in the absence of adsorption, multiplied by the thickness of the surface layer, δ:

$$\sigma_A - \sigma = (P_s - P)\delta \qquad (1)$$

All adsorption is assumed to occur in the monomolecular layer, so that the osmotic pressure can be referred to a definite concentration of adsorbed molecules.

Let us introduce the values of mole fractions of the solvent and of the adsorbate in the surface layer, x_A' and x_B'. For this purpose, let us draw the Gibbs dividing surface in such a way that it cuts off the mono-layer from the bulk of the solution. If θ is the coverage and x_{OA}' and x_{OB}' the limiting amounts of the solvent and of the

* Contribution to the 14th Meeting of C.I.T.C.E., Moscow, August 1963.

solute respectively in the monolayer then obviously

$$x_A' = \frac{(1 - \theta)\, x_{OA}'}{(1 - \theta)\, x_{OA}' + \theta x_{OB}'}$$

and

$$x_B' = \frac{\theta x_{OB}'}{(1 - \theta)\, x_{OA}' + \theta x_{OB}'}$$

We shall confine ourselves to the simplest case when $x_{OA}' = x_{OB}' = 1/S$. Then $x_A' = 1 - \theta$ and $x_B' = \theta$. The quantity $S\delta$ expresses the molecular volume of the solute or of the solvent V. It follows from thermodynamical considerations[3] that the osmotic pressure of an ideal concentrated solution is

$$P = -\frac{RT}{V} \ln(1 - x_B),$$

where V is the molecular volume of the solvent and x_B the mole fraction of the solute (van-Laar's equation). By using this equation for the surface layer, we obtain

$$\sigma_A - \sigma = (P_S - P)\delta = -\frac{RT}{S} \ln \frac{1 - x_B'}{1 - x_B} \tag{2}$$

In the case of high enough adsorptivity the concentration of component B in the bulk can be considered to be small in comparison with the surface concentration for a dilute solution and

$$\sigma_A - \sigma = -\frac{RT}{S} \ln(1 - x_B') \tag{3}$$

Thus, we obtain an equation of state corresponding to Langmuir's isotherm. The connection between van-Laar's equation for the osmotic pressure and Langmuir's adsorption isotherm was pointed out by me many years ago[4], but as far as I know, this question has not been considered since.

(b) BUTLER[5], SCHUCHOWITZKY[6], BELTON AND EVANS[7] and GUGGENHEIM[8] developed the statistical theory of the surface tension of binary mixtures, assuming the surface layer to be monomolecular*. Some of the results obtained will be quoted here. In the simplest case, when the solution can be considered to be ideal both in the bulk and in the surface layer and $x_{OA}' = x_{OB}' = 1/S$, there is a relationship between the surface tension of the solution σ and that of the components σ_A and σ_B which can be expressed for example as follows[8]:

$$\exp(-\sigma S/RT) = x_A \exp(-\sigma_A S/RT) + x_B \exp(-\sigma_B S/RT) \tag{4}$$

where x_A and x_B are mole fractions in the bulk of the solution.

It follows from eqn. (4) that

$$\Delta\sigma = \sigma_A - \sigma = \frac{RT}{S} \ln[1 + x_B(C - 1)] \tag{5}$$

i.e., Shishkovsky's equation[5,6], where $C = \exp(\sigma_A - \sigma_B)\, S/RT$.

* A more rigorous treatment has been given by ONO AND KONDO[9].

From eqn. (5), by using Gibb's adsorption formula

$$d\sigma = -\frac{RT}{S}\left(\frac{x_A'}{x_A}\,dx_A + \frac{x_B'}{x_B}\,dx_B\right)$$

and taking into account that $x_A' + x_B' = 1$, we obtain

$$x_B' = \frac{Cx_B}{1 + x_B(C - 1)} \tag{6}$$

i.e., Langmuir's adsorption isotherm[5,6]. It follows from eqns. (5) and (6) that

$$\Delta\sigma = -\frac{RT}{S}\ln\frac{1 - x_B'}{1 - x_B} \tag{7}$$

is in accordance with eqn. (2). Equation (7) was first deduced by BUTLER[5]. From eqns. (5) and (6) the following equation of state can be obtained:

$$\Delta\sigma = -\frac{RT}{S}\ln\left(1 - \frac{C - 1}{C}x_B'\right) \tag{8}$$

which coincides with eqn. (3) at $C \gg 1$*.

Thus, it appears that there can be no doubt concerning the applicability of Langmuir's formula in the case of adsorption from solutions, when the systems are ideal and the areas per molecule of the solvent and of the solute are equal. It could not be otherwise, since the stoichiometry of the elementary act of adsorption from solution under given assumptions is the same as in the case of localized adsorption of a gas at the surface of a solid body, *i.e.*, in the case of localized adsorption, one free site in the surface layer disappears as a result of adsorption and there appears an occupied site, which can be considered as a hole in the initial surface layer. The same occurs in the case of adsorption at the surface of a solution, but here the role of the free site is played by a molecule of the solvent.

The arguments advanced cannot serve, of course, as a sufficient theoretical basis for the application of Langmuir's equation to real systems for which the above assumptions do not hold. Whether this is permissible can be decided only by experiment, but it seems to me that these arguments can help when choosing the direction for the further development of the theory of adsorption at the surface of solutions.

Finally, I should like to point out that for the case of regular solutions GUGGENHEIM[8] obtained in the zero'th approximation an expression which under the conditions $x_B \ll 1$ and $x_B'/x_B \gg 1$ becomes

$$\Delta\sigma = -\frac{RT}{S}\ln(1 - x_B') - \text{const.}\,(x_B')^2$$

* If we introduce into eqn. (8), instead of the surface concentration x_B', the Gibbs adsorption Γ_B, calculated under the assumption that the adsorption of the solvent equals zero, the equation of state takes the usual form

$$\Delta\sigma = -\frac{RT}{S}\ln\left(1 - \Gamma_B/x_{OB}'\right) \tag{9}$$

irrespective of the value of C.

Equation (9) is identical to the equation of state proposed by FRUMKIN[4], which was apparently unknown to GUGGENHEIM.

Institute of Electrochemistry,
Academy of Sciences,
Moscow (U.S.S.R.)

A. N. FRUMKIN

1 R. PARSONS, *J. Electroanal. Chem.*, 7 (1964) 136.
2 E. HELFAND, H. L. FRISCH AND J. L. LEBOWITZ, *J. Chem. Phys.*, 34 (1961) 1037.
3 E. GUGGENHEIM, *Modern Thermodynamics by the Methods of Willard Gibbs*, Methuen, London, 1933, p. 96.
4 A. FRUMKIN, *Z. Physik. Chem.*, 116 (1925) 466.
5 J. A. V. BUTLER, *Proc. Roy. Soc. (London), Ser. A.*, 135 (1932) 348.
6 A. SCHUCHOWITZKY, *Acta Physicochim. URSS*, 19 (1944) 176; *Zh. Fiz. Khim.*, 17 (1943) 313; 18 (1944) 214.
7 J. BELTON AND M. EVANS, *Trans. Faraday Soc.*, 41 (1945) 1.
8 E. GUGGENHEIM, *Trans. Faraday Soc.*, 41 (1945) 150.
9 S. ONO AND S. KONDO, *Molecular Theory of Surface Tension in Liquids, Handbuch der Physik*, Vol. 10, edited by S. FLÜGGE, Springer, Berlin, 1960.

J. Electroanal. Chem., 7 (1964) 152–155

Discussion on the choice of the electrical variable in the study of the adsorption isotherms of organic compounds and on the form of the adsorption isotherm

According to PARSONS[1], in the study of the adsorption isotherm, the charge rather than the electrode potential should be chosen as the electrical variable. The validity of this viewpoint in the case of adsorption of neutral molecules from solutions with a high concentration of the supporting electrolyte appears to us, however, to be questionable.

Let us assume the dependence of the electrode charge, q, on the coverage of the surface with the organic substance, θ, to be expressed by the relation[2]:

$$q = q_0(1 - \theta) + q'\theta \tag{1}$$

which has been well confirmed by the experiments for the case of adsorption of aliphatic compounds on mercury[2,3] (q_0 and q' are the values of q at $\theta = 0$ and $\theta = 1$, respectively). Equation (1) may be re-written as:

$$q = q_m + [C_0(1 - \theta) + C'\theta]\,(E - E_m) \tag{1a}$$

where E_m is the potential of maximum adsorption, q_m the value of q at $E = E_m$ and C_0 and C', the double-layer capacities at $\theta = 0$ and $\theta = 1$, respectively. The thermodynamical transformations show that when eqn. (1) is satisfied and if $C_0 =$ constant and $C' =$ constant, the adsorption isotherm of the organic substance can be written as:

$$\begin{aligned} f(\theta) = Bc &= B_m c \exp\,[-\alpha(E - E_m)^2] \\ &= B_m c \exp\{-\alpha(q - q_m)^2/\,[C_0(1 - \theta) + C'\theta]^2\} \end{aligned} \tag{2}$$

where $f(\theta)$ is a function of θ independent of E and determined by the choice of the

equation of state of the surface layer, and B_m and α are constants ($\alpha = (C_0 - C')/2A$, where $A = RT\Gamma_m$).

From eqn. (2) we obtain the equation of the adsorption isotherm in the dimensionless form:
at E = const.,

$$y_E \equiv (c/c_{\theta=0.5})_E = f(\theta)/f(0.5) \tag{3}$$

and at q = const.,

$$y_q \equiv (c/c_{\theta=0.5})_q$$

$$= \frac{f(\theta)}{f(0.5)} \exp\{\alpha(q - q_m)^2 [1/[C_0(1 - \theta) + C'\theta]^2 - 4/(C_0 + C')^2]\} \tag{4}$$

It is clear from eqn. (3) that to the first approximation, when eqn. (1) is satisfied, the form of the adsorption isotherm at a constant potential does not depend on the potential. At the same time, it follows from eqn. (4) that when any function $f(\theta)$ not depending on q is chosen, the form of the adsorption isotherm at a constant electrode charge will depend on the magnitude of the charge. The exception to this is the case when $C_0 = C'$, which, however, is not realized for the adsorption of most organic compounds. Consequently, it is preferable to study the adsorption isotherm of organic substances at a constant potential and not at a constant electrode charge.

Let us illustrate this conclusion for the case of adsorption of *tert.*-amyl alcohol on mercury[4]. Figure 1 shows the experimental adsorption isotherms of *tert.*-amyl alcohol at constant electrode charges:

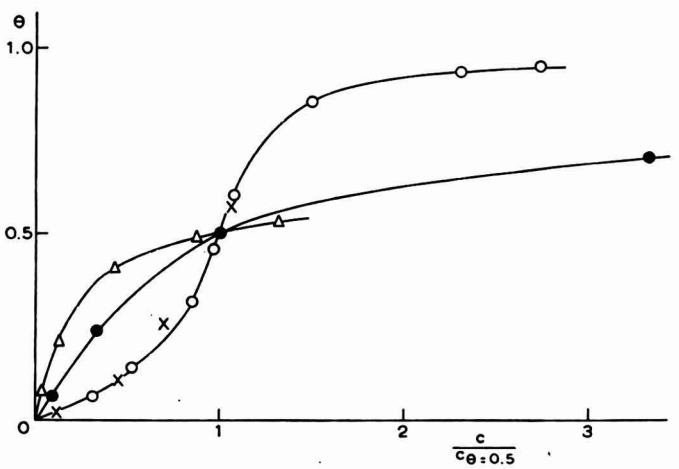

Fig. 1. Dimensionless adsorption isotherms of *tert.*-$C_5H_{11}OH$ on mercury from 0.9 N NaF solution: ⊙–⊙, $q = q_m = -1.65$ μC/cm^2 ($E = -0.55$ *vs.* N.C.E.); ●–●, $q = -6.0$ μC/cm^2; △–△, $q = -9.0$ μC/cm^2; ×–×, $E = -1.23$ *vs.* N.C.E.

$q_m = -1.65$, $q = -6.0$ and $q = -9.0$ μC/cm^2. It is clear from the figure that the form of the dimensionless adsorption isotherm changes sharply with a change in the charge. At the same time, over a corresponding potential range (-0.55 to -1.23 *vs.*

N.C.E.) the form of the dimensionless adsorption isotherm at E = constant changes negligibly; the small change observed is due to the change in the function $f(\theta)$ with the potential[4].

The increase in $|q|$ corresponds, as it were, to the occurrence of repulsive forces between the adsorbed molecules of *tert.*-amyl alcohol. Thus, from a comparison of the experimental isotherms with the equation of the Frumkin isotherm[2],

$$c/c_{\theta=0.5} = \frac{\theta}{1-\theta} \exp[a_{\mathrm{eff}}(1-2\theta)] \tag{5}$$

where a_{eff} is a certain effective value of the attraction constant, we may conclude that at electrode charges equal to -1.65, -6.0 and -9.0 μC/cm^2 the form of the dimensionless isotherms is well reproduced by eqn. (5) at values of a_{eff} equal to 1.6, 0.3 and -1.9 respectively. The positive values of the attraction constant are known[5] to correspond to the predominance of attractive forces between the adsorbed particles, whereas the negative values correspond to the predominance of repulsive forces.

The real reason for the change in the adsorption isotherm with an increase in $|q|$, however, is the fact that away from q_m, the strength of the field in the double-layer does not remain constant at a constant charge, but changes (increases) with increasing concentration. Therefore, the "repulsion" observed is fictitious; the dependence of a_{eff} on q obtained can be determined theoretically. In fact, by using Frumkin's isotherm (5), we obtain from eqn. (4):

$$y_q = \frac{\theta}{1-\theta} \exp[a(1-2\theta)] \exp\{\alpha(q-q_m)^2[1/[C_0(1-\theta)+C'\theta]^2 - 4/(C_0+C')^2]\} \tag{4a}$$

whence

$$dy_q/d\theta = \exp[a(1-2\theta)] \exp\{\alpha(q-q_m)^2[1/[C_0(1-\theta)+C'\theta]^2 - 4/(C_0+C')^2]\} \left\{\frac{1-2a\theta(1-\theta)}{(1-\theta)^2} + \frac{\theta}{1-\theta}\frac{2\alpha(q-q_m)^2(C_0-C')}{[C_0(1-\theta)+C'\theta]^3}\right\} \tag{6}$$

At $\theta = 0.5$,

$$(dy_q/d\theta)_{\theta=0.5} = (4-2a) + 8(C_0-C')^2(q-q_m)^2/A(C_0+C')^3 \tag{6a}$$

By equating this value with the slope of the equivalent isotherm (5) equal to $(4-2a_{\mathrm{eff}})$, we obtain for the effective value a_{eff}:

$$a_{\mathrm{eff}} = a - 4(C_0-C')^2(q-q_m)^2/A(C_0+C')^3 \tag{7}$$

According to ref. 4, for *tert.*-amyl alcohol, $a = 1.6$, $A = 1$, $q_m = -1.65$, $C' = 4.4$ and the mean value of C_0 over the potential range under consideration is equal to 16.8. Therefore,

$$a_{\mathrm{eff}} = 1.6 - 0.0646\,(q+1.65)^2 \tag{7a}$$

In Fig. 2, the values of a_{eff} calculated by means of this equation are compared with the experimental values, it can be seen that there is a good agreement between the calculated and the experimental values at q = constant. This points once more to the fictitious character of the repulsive forces and to the inexpediency of choosing the electrode charge as the electrical variable in the case of adsorption of neutral molecules on mercury. In the case of solid electrodes, only the isotherms determined at a constant potential can be found experimentally, since the determination of the

charge is not accurate enough to permit the fulfilment of the condition q = constant to be controlled.

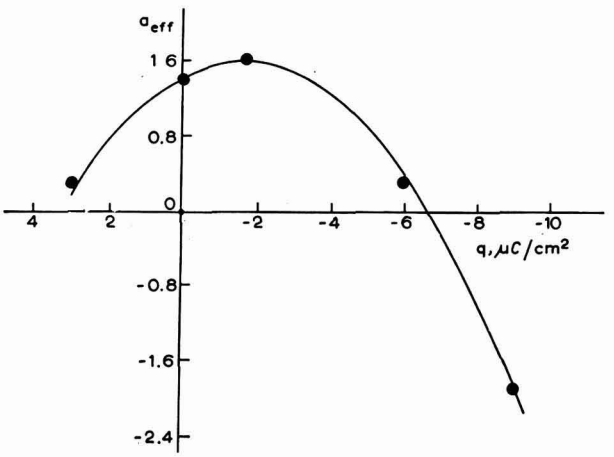

Fig. 2. Dependence of the effective value of the attraction constant on the electrode charge: solid line, calculated by means of eqn. (7a); dots, values of a_{eff} obtained by the comparison of the experimental adsorption isotherms of *tert.*-$C_5H_{11}OH$ at q = const. with eqn. (5).

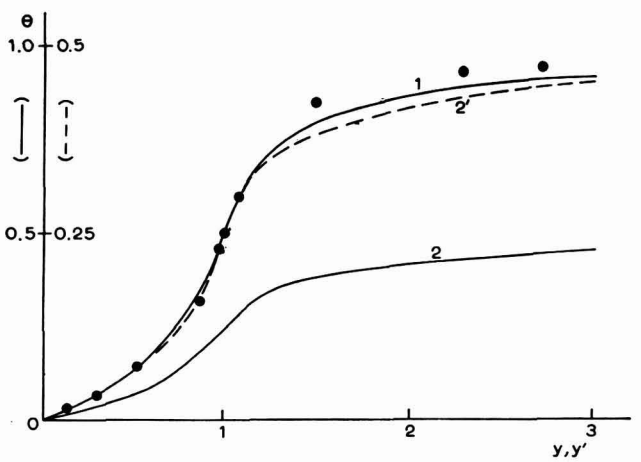

Fig. 3. Dimensionless adsorption isotherms: (1), calculated by means of eqn. (5) at a = 1.6; (2), calculated by means of eqn. (8) at a' = 4.82; (2'), curve (2) plotted with the scale of the ordinate axis doubled; dots, experimental values for *tert.*-$C_5H_{11}OH$ (according to LORENZ AND MÜLLER[7]).

A few words should be said about the form of the adsorption isotherm resulting from the equation of state of HELFAND, FRISCH AND LEBOWITZ[6] used by PARSONS[1]

in his paper. The equation of this isotherm can be written in the dimensionless form as:

$$y' \equiv (c/c_{\theta=0.25}) = 3 \exp(-28/9) \frac{\theta}{1-\theta} \exp[(2-\theta)/(1-\theta)^2] \exp[a'(0.5-2\theta)] \quad (8)$$

where a' is the new attraction constant. In Fig. 3 the calculation by means of this equation with $a' = 4.82$ (which corresponds to the experimental slope of the adsorption isotherm of *tert.*-amyl alcohol), is compared with the calculation by means of Frumkin's equation (5) at $a = 1.6$ (ref. 5.), as well as with the experimental data of LORENZ AND MÜLLER[7] for *tert.*-amyl alcohol. The figure shows that the experimental data are well described by Frumkin's isotherm and are not in agreement with eqn. (8). If the scale of the ordinate axis for the Parsons' isotherm (8) is doubled, the form of the two isotherms over a certain concentration range will practically coincide, but if we try to bring about an agreement of Parsons' isotherm with the experimental data for *tert.*-amyl alcohol in this way we must assume that:

(1) the equation

$$C = C_0(1-\theta) + C'\theta \quad (9)$$

from which the experimental values of θ are deduced[7] at the potential of maximum adsorption, gives an error in the value of θ equal to 100 %;

(2) the coverage $\theta = 0.7$ can be attained only at a concentration of *tert.*-amyl alcohol equal to 65.2 M, whereas the concentration of pure *tert.*-amyl alcohol equals 11.3 M. Both these assumptions are hardly acceptable and therefore the use of Parsons' isotherm (8) to describe the adsorption of *tert.*-amyl alcohol is questionable.

Chemistry Faculty,
Moscow State University,
Moscow (U.S.S.R.)

B. B. DAMASKIN

1 R. PARSONS, *J. Electroanal. Chem.*, 7 (1964) 136.
2 A. FRUMKIN, *Z. Physik*, 35 (1926) 792.
3 B. B. DAMASKIN, *Electrochim. Acta*, (in press).
4 B. B. DAMASKIN AND N. B. GRIGORJEV, *Dokl. Akad. Nauk SSSR*, 147 (1962) 135.
5 B. B. DAMASKIN, *Dokl. Akad. Nauk SSSR*, 144 (1962) 1073.
6 E. HELFAND, H. L. FRISCH AND J. L. LEBOWITZ, *J. Chem. Phys.*, 34 (1961) 1037.
7 W. LORENZ AND W. MÜLLER, *Z. Physik. Chem. (Frankfurt)*, 25 (1960) 161.

Book Reviews

Electron-Probe Micro-Analysis, by L. S. BIRKS, Wiley and Sons, Interscience Division, London and New York, 1963, 264 pages, 70s.

Electron-probe micro-analysis has been an accepted analytical technique for two or three years. During this time it has attracted much attention and the number of instruments in use is increasing rapidly. There is therefore need of an up-to-date text-book on the subject for the guidance of those contemplating using this method of analysis.

In this book by L. S. BIRKS, a short historical background is followed by a chapter on electron optics which describes (i) the types of probe-forming lenses used in various commercial and other instruments, (ii) the aberrations of these lenses and (iii) the procedure for the alignment of these electron optical systems.

A chapter on specimen observation deals with visual optics and the scanning methods for viewing with X-rays or electrons. This chapter is not particularly well-balanced. For instance, the discussion of X-ray viewing is confined to images formed from d.c. amplified X-ray signals, this is a recent approach which has been by no means universally adopted. The concepts of contrast and brightness are different with the many instruments that have only a.c. amplifiers. There follows a very useful chapter on specimen types and specimen preparation.

The author then turns to the X-ray aspects of the technique and this section of the book is well done. He discusses the various spectrometer systems in use, the resulting efficiencies of the reflecting crystals and the characteristics of detectors, including their use for non-dispersive analysis. He deals boldly with the relation between X-ray intensity and sample composition, discussing in an easily readable fashion the various factors involved, and deriving correction procedures for absorption, fluorescence and atomic number effects. It is a pity there is a noticeable and repeated misprint of accelerating voltage in referring to CASTAING's experimental excitation data. These procedures are then applied to quantitative problems. A good indication of the scope of electron-probe micro-analysis is provided by the 23 pages devoted to more general applications. There is a final brief chapter on related topics and future trends.

The appendices constitute 70 of the 250 pages of this volume and they include a useful collection of data for analyser operators. There are tables for the correction of observed X-ray intensities at each of several electron-accelerating voltages; 36 pages are devoted to absorption coefficients, and there are also tables of excitation energies and wave-lengths for K, L and M series lines.

This book goes a long way towards meeting the present need. There is, however, one criticism that can be made. Although the author acknowledges the limited accuracy obtained in quantitative electron-probe work, he has given little recognition to the amount of theoretical work still going on which is aimed at a more complete understanding of the problems of this micro-analytical technique. With this reservation the book is one to be recommended.

Thermodynamische Elektrochemie, by E. LANGE AND H. GÖHR, Alfred Huthig Verlag, Heidelberg, 1962, 429 pages, D.M. 39.

This book, written by Prof. E. LANGE and Dr. H. GÖHR, is designed as a systematic treatise on electrochemistry, beginning at the simplest single phase in the absence of any net current and proceeding through all the different aspects and phenomena to more complex systems.

It has an exceedingly rigorous approach, particularly from a thermodynamic standpoint. Kinetics are also used in some sections of the book.

In addition, certain topics not usually to be found in text-books on electrochemistry, have been considered, *e.g.*, the non-isothermal single phase, Peltier heats, etc. The construction of the book, although undoubtedly logical, is sometimes much too formal and this does not always make for easy reading.

The quality of the printing and the presentation are good.

G. MILAZZO, Istituto Superiore di Sanità, Rome

Treatise on Analytical Chemistry, I. M. KOLTHOFF, P. J. ELVING AND E. B. SANDELL Part II, Vol. 7, Interscience Publishers Inc., New York and London, 1963, xxi + 556 pages, 150 s.

This new volume of the well-known treatise on analytical chemistry by KOLTHOFF, ELVING AND SANDELL deals with a number of rather rare elements. The analytical chemistry of those elements (except bismuth, vanadium and chromium) is somewhat difficult in itself and what little published work there is on the subject *i.e.*, the rare earths and platinum metals, is scattered throughout many scientific periodicals.

As in the preceding volumes, many specialists have been asked to write the individual chapters of this volume. M. M. WOYSKI AND R. E. HARRIS (West Chicago Research Laboratory, American Potash and Chemical Corporation), have written the first chapter on the rare earths (146 pages); J. S. FRITZ (Institute for Atomic Research and Department of Chemistry, Iowa State University) the chapter on bismuth (30 pages); H. R. Grady (Research Center Division Vanadium Corporation of America) the chapter on vanadium (96 pages); W. H. HARTFORD (Solvay Process, Allied Chemical Corporation) the chapter on chromium (106 pages), and finally T. J. WALSH AND E. A. HAUSMANN (Research and Development Division, Engelhard Industries Inc.) have written the last chapter on the platinum metals (144 pages). The general lay-out of this volume is similar to that of the previous volumes of this series, *i.e.*, general properties, identification, separation, classical gravimetric and volumetric methods of determination and finally physico-chemical methods of analysis.

Of particular value are the methods that have been selected or recommended as a result of the authors' practical experience and their application to the analysis of certain classes of materials.

The material, is set out very clearly although of course in a condensed form, but there are many bibliographical references to help supplement the text.

G. MILAZZO, Istituto Superiore di Sanità, Rome

Progress in Infrared Spectroscopy, Vol. 1, *Proceedings of the Fifth Annual Meeting of the Infrared Spectroscopy Institute*, held at Canisius College, Buffalo, New York, August 14–18th, 1961, Plenum Press, New York, 446 pages.

This book is a collection of the Proceedings of the Fifth Annual Meeting of the Infrared Spectroscopy Institute held at the Canisius College in 1961 and includes twenty-one chapters on several topics in spectroscopy, mainly infrared. There is also an Appendix containing answers to many questions that have been asked by students.

The book sets out to offer to chemists working in chemical industries or in applied spectroscopy laboratories, a comprehensive survey of the techniques and methods used in qualitative and quantitative spectroscopic analysis. Thus, special emphasis is given to instrumentation and its related problems, such as sample handling, intensity measurements and analytical methods. Nine chapters are devoted to these topics which are discussed on a very practical and simple level. This is probably the first serious attempt to collect together the essentially practical problems in spectroscopy without insistence on the theoretical aspects, and the editor is to be congratulated on this part of the book. However, some chapters, like the one on group theory, do not quite fit into this pattern and are therefore out of line with the rest of the book.

Four chapters deal with far infrared spectroscopy with various techniques and applications according to the most recent developments in this field. Again the matter seems overemphasized for far infrared spectroscopy has not advanced much beyond the research stage as yet. On the other hand very little space is devoted to one of the most important aspects of applied spectroscopical analysis, *i.e.*, the interpretation of high polymer spectra, which is confined to a very short chapter. Apart from these criticisms the book follows the original pattern very well.

Three chapters are devoted to the problem of intensity measurements and their application to quantitative analysis. One chapter deals with the sampling of KBr discs, two chapters with the problem of infrared instrumentation and two short chapters with some of the methods used in vibrational assignments, such as analysis of the rotational band envelope and spectral correlation tables.

There are four chapters on the analytical applications of other spectroscopic techniques, such as Raman spectroscopy, nuclear magnetic resonance and ultraviolet spectroscopy. A useful collection of references, completes that part of the book which is of a more direct interest for industrial laboratories.

In addition, there are three other chapters, one on group theory and two on the infrared spectra of inorganic molecules which, as stated before, do not seem in line with the purpose of the book. The chapter on group theory and on its application to molecular vibration is especially recommended for graduate students approaching the matter, since it is presented very clearly. The two chapters on infrared spectra of inorganic molecules and ions, give a concise and useful survey of the subject.

In conclusion this book is an excellent aid for applied spectroscopy laboratories where it will certainly find favourable acceptance.

S. CALIFANO, Università di Napoli

Polyanions et Polycations, by M. P. SOUCHAY, Ed. Gauthier-Villars, Paris, 1963, 247 pages, Fr. 42.

Professor SOUCHAY has produced a comprehensive monograph dealing with the descriptive chemistry of condensed acid and base systems. The implication in the title that the subject of the book is ionic species is slightly misleading, since neutral and even non-ionizable systems such as the phosphonitrilic compounds are presented as being no less deserving of the reader's attention. The treatment is conventional, dealing largely with the constitution of iso- and heteropoly ions, acids, and salts with little attention to physical properties other than structures. This perhaps reflects the fact that physical studies of such systems are still few in number. However, the author describes physical techniques such as ultra-centrifugation, diffusion, and light scattering which have been used for the elucidation of polyion constitution.

The analytical chemist will find little of immediate technical value in this book and in the reviewer's opinion, its author has failed to impress us with the frequency with which hetero-polyion formation interferes in the analytical chemistry of niobium, zirconium, etc. There is little doubt that the rare-metal analyst would benefit by a reading of the appropriate sections of SOUCHAY's book providing he is prepared to translate the significant points into analytical terms.

Although the book provides an excellent survey of the types of inorganic substance which undergo condensation polymerization, the treatment of the more familiar ones such as tungstic and molybdic acids is not exhaustive. There are 299 references listed in the bibliography. A person who is entering upon research into the nature of dissolved constituents will find this work an easy means whereby he may orient himself. Those already established may find the book rather too general and broad in character to be of great assistance to them.

A. D. WESTLAND, University of Ottawa

J. Electroanal. Chem., 7 (1964) 163

Announcements

15TH MEETING OF THE COMITÉ INTERNATIONAL DE THERMODYNAMIQUE ET DE CINÉTIQUE ELECTROCHIMIQUES (LONDON AND CAMBRIDGE) SEPTEMBER, 1964

The 15th Meeting of CITCE will be held in London and Cambridge (Great Britain), September 21st–26th, 1964. There will be two general themes for this meeting: the first, *Measurements in fused salt electrolytes*, and the second, *Instrumental methods in electrochemistry*. Sessions of the following Commissions will be held during this meeting:

Commission 2, *Electrochemical Nomenclature and Definitions*;
Commission 3, *Experimental Methods in Electrochemistry*;
Commission 4, *Batteries*;

Commission 5, *Corrosion*;
Commission 6, *Electrochemical Kinetics*;
Commission 8, *Electrochemistry of High Temperatures*.

In addition there will be two general discussions on topics associated with the general themes: the first, *The proof of the existence of specific entities in fused salts and in fused salt solutions*, and the second, *The derivation and interpretation of the rate constants of fast electrode reactions and of fast reactions in solution*.

Correspondence regarding attendance or presentation of papers at this meeting should be addressed to Dr. M. FLEISCHMANN, Secretary General of CITCE, Department of Physical Chemistry, University of Newcastle upon Tyne, Newcastle upon Tyne 1, Great Britain; or to Dr. T. P. HOAR, Department of Metallurgy, University of Cambridge, Pembroke Street, Cambridge, Great Britain.

Summaries of papers should be received before May 1st, 1964 and the full texts before June 15th, 1964. Participation forms may be obtained from Dr. FLEISCHMANN from January, 1964.

ELWELL AWARD, 1964

The object of this award is to encourage young Midland scientists in the profession of analytical chemistry.

Entries are invited for the annual competition for the Elwell Award from any scientist, including those engaged in full-time post-graduate studies under the age of 30, working or residing in the area covered by the Midlands Section of the Society for Analytical Chemistry; *i.e.* South of, but including, Stoke-on-Trent and North of, but excluding Carmarthen.

The Award, consisting of a silver trophy, will be retained for one year by the candidate deemed by a panel of referees to have submitted the best paper dealing with some aspect of analytical chemistry. In addition, the successful candidate will receive a gift of scientific books of his own choice to the value of 10 guineas; the runner-up will receive scientific books to the value of 3 guineas.

Papers submitted should describe, in a form suitable for presentation at a local Section Meeting, work in which he or she has been actively associated, though not necessarily entirely responsible.

The basic requirement is that the contribution should advance, even in a small way, existing knowledge of analytical chemistry.

Selected papers will be presented at a Meeting of the Section during September, 1964, and the name of the successful candidate will be announced on the same evening. The closing date for entries is 8th June, 1964, and the latest date for submission of papers is the 29th June, 1964.

Entry forms and other particulars may be obtained from: M. L. Richardson, A.R.I.C., A.C.T. (Birm.), Honorary Secretary, Midlands Section of the Society for Analytical Chemistry, c/o John & E. Sturge Ltd., Lifford Chemical Works, Lifford Lane, Kings Norton, Birmingham, 30.

CONTENTS

ELSEVIER PUBLISHING COMPANY, AMSTERDAM

Printed in The Netherlands by

NEDERLANDSE BOEKDRUK INRICHTING N.V., 'S-HERTOGENBOSCH